

The Creation of a Hantavirus Vaccine
Using Reverse Genetics and Its Evaluation in the Lethal
Syrian Hamster Model

by

Kyle Brown

B.Sc. (Microbiology), University of Manitoba 2003

A thesis submitted to the Faculty of Graduate Studies of
the University of Manitoba
in partial fulfillment of the requirements for the degree of

Doctor of Philosophy

Department of Medical Microbiology

University of Manitoba

Winnipeg, Manitoba

© 2012 by Kyle Brown

TABLE OF CONTENTS

ACKNOWLEDGEMENTS	vi
DEDICATION	vii
ABSTRACT	viii
LIST OF TABLES	x
LIST OF FIGURES	xi
LIST OF COPYRIGHTED MATERIAL	xiii
LIST OF ABBREVIATIONS	xiv
1.0 INTRODUCTION	1
1.1 Emergence and Epidemics of Hantaviruses	1
1.1.1 Emergence and Viral Transmission of Old World Hantaviruses	1
1.1.2 Emergence and Viral Transmission of New World Hantaviruses	3
1.2 Natural Reservoir of Hantaviruses	4
1.3 Biology of Hantaviruses	8
1.4 Viral Life Cycle	9
1.4.1 Virus Entry	9
1.4.2 Viral Transcription	12
1.4.3 Translation and Processing of Viral Proteins	15
1.4.4 Viral Replication	16
1.4.5 Assembly and Egress	17
1.5 Hantavirus Infection of Humans	19
1.5.1 Clinical Signs of Disease	19
1.5.2 Pathogenesis and Pathology	21
1.5.3 Immune Evasion	23
1.5.4 Diagnosis	24
1.5.5 Treatment and Prevention	25
1.5.5.1 Old World Hantavirus Vaccines	26
1.5.5.2 New World Hantavirus Vaccines	27
1.6 Rationale: Reverse Genetics Systems	28
1.7 Rationale: Use of Recombinant VSV as a Vaccine Platform	35
1.8 Hypothesis and Objectives	36

2.0 MATERIALS AND METHODS	40
2.1 Cells and Viruses	40
2.2 Antibodies and Primers	41
2.3 Molecular Biology Techniques	42
2.3.1 RNA Extractions	42
2.3.2 Polymerase Chain Reaction (PCR)	43
2.3.3 Reverse Transcription-Polymerase Chain Reaction (RT-PCR)	45
2.3.4 Amplicon Analysis	46
2.3.5 Quantitative Real-Time RT-PCR (qRT-PCR)	47
2.4 Molecular Cloning Techniques	49
2.4.1 DNA Digestion	49
2.4.2 DNA Ligation	50
2.4.3 DNA Plasmid Transformation	50
2.4.4 Screening and Verification of the Constructs by Restriction Digest	51
2.5 Cloning Strategy – Creation of ANDV N Expression Constructs	52
2.6 Cloning Strategy – Creation of ANDV Glycoprotein Expression Constructs	52
2.7 Cloning Strategy – Creation of ANDV L Expression Constructs	56
2.8 Cloning Strategy – Creation of Minigenome Constructs	58
2.9 Cloning Strategy – Creation of Recombinant VSV Constructs	59
2.10 Transfection	64
2.11 Detection of Protein Expression by Immunostaining Techniques	65
2.11.1 Sodium Dodecyl Sulphate Polyacrylamide Gel Electrophoresis (SDS-PAGE) Gels and Wet Transfer	65
2.11.2 Western Blot	66
2.11.3 Immunofluorescent Assay (IFA)	67
2.12 Minigenome Rescue	68
2.13 Detection of Minigenome Reporter Signal	68
2.13.1 Chloramphenicol Acetyl Transferase (CAT) Assay and Thin-Layer Chromatography (TLC)	69
2.13.2 Luciferase (LUC) Assay	70
2.14 Rescue of Recombinant VSV	70
2.15 Infectivity Assays	74
2.15.1 Plaque Forming Assay	74
2.15.2 Focus Forming Assay	75
2.15.3 50% Tissue Culture Infectious Dose	76
2.16 Transmission Electron Microscopy (TEM) of VSV	78
2.17 Growth Kinetic Analysis of VSV	80
2.18 Immunization and Challenge of Syrian Hamster Lethal Disease Model	80
2.19 Hamster Serological Assays	81
2.19.1 Neutralization Assays	82
2.19.2 N-Specific Indirect Enzyme Linked Immunosorbent Assay (ELISA)	83
2.20 qRT-PCR Hamster Cytokine Assay	84

3.0 RESULTS	85
3.1 Cloning and Expression of ANDV Proteins in Mammalian Expression Constructs	85
3.1.1 ANDV N Constructs	85
3.1.2 ANDV Glycoprotein Constructs	86
3.1.3 ANDV L Constructs	86
3.1.4 Confirmation of Protein Expression	92
3.2 Cloning and Rescue of Minigenome Constructs	95
3.3 Cloning and Rescue of Recombinant VSV	98
3.4 <i>In Vitro</i> Characterization of Recombinant VSV Vaccine	104
3.4.1 TEM Imaging of VSV	104
3.4.2 Growth Kinetic Analysis of VSV	108
3.5 <i>In Vivo</i> Protection Studies	110
3.5.1 Vaccine Efficacy Against Lethal ANDV Challenge	110
3.5.2 Detection and Quantification of ANDV Replication	113
3.5.2.1 ANDV RNA	113
3.5.2.2 N Protein-Specific Seroconversion	113
3.5.3 Measurement of Immune Response	115
3.5.3.1 Humoral Response – Neutralizing Antibodies	115
3.5.3.2 Validation of Assay	118
3.6 Time to Protection and Post-Exposure Vaccine Efficacy	120
3.6.1 Time to Protection Survival Study	120
3.6.2 Post-Exposure Survival Study	122
3.6.3 Time to Protection – Measurement of Immune Response	124
3.6.3.1 Time to Protection – ANDV Replication	124
3.6.3.2 Time to Protection – ANDV Glycoprotein Neutralizing Antibodies	126
3.6.3.3 Time to Protection – Stimulation of Innate Immune System	126
4.0 DISCUSSION	131
4.1 Cloning and Expression of ANDV Proteins <i>In Vitro</i>	131
4.2 Cloning and Rescue of Minigenome Constructs	134
4.3 Cloning and Rescue of Recombinant VSV Constructs	136
4.4 <i>In Vivo</i> Protection Studies	139
4.4.1 Efficacy of VSV Δ G/ANDVGPC as a Vaccine Platform	139
4.4.2 Immune Response	141
4.5 Time to Protection and Post-Exposure Vaccine Efficacy	144
4.5.1 Time to Protection Efficacy	144
4.5.2 Post-Exposure Efficacy	145
4.5.3 Time to Protection – Adaptive Immune Response	147
4.5.4 Time to Protection – Innate Immune Response	149

5.0 CONCLUSIONS	152
6.0 REFERENCES	155
7.0 APPENDICES	177
Appendix 1 – Buffer Recipes	177
Appendix 2 – List of Primary and Secondary Antibodies	180
Appendix 3 – List of Primers	181
Appendix 4 – DNA and Protein Ladders	184
Appendix 5 – Minigenome Rescue Conditions	185

ACKNOWLEDGEMENTS

First of all, I would like to thank my supervisor Heinz Feldmann for all of the support that he's given me throughout the years. Despite all of the difficulties that were encountered throughout this study, Heinz has ensured that I would be able to come to Montana on many occasions to complete this work, and would continue to be financially supported while I remained in Winnipeg. His belief in my work as a student has provided the ultimate encouragement for me throughout the years. Additionally, I would like to thank Gary Kobinger for supporting me in Winnipeg through funding and the provision of lab space so that this work could continue in Heinz's absence.

Thank you to the Department of Medical Microbiology for the support over the years, and especially to Angela Nelson who was always quick to answer any necessary questions. Thank you also to my committee members Steven Pind and Kevin Coombs for all of the helpful suggestions they've provided for the project and ultimately for reading my thesis.

I would also like to thank all of the various members of the Special Pathogens program at the National Microbiology Laboratory that I have shared lab space with, become close friends with, and who have helped to improve my techniques, scientific understanding, and helped provide fun outside the lab. Without them, these years would have been much less eventful.

I also have to thank the members of the Rocky Mountain Laboratory in Montana who have proved to be absolutely essential in completing this work. Specifically, thank you to David Safronetz, Andrea Marzi, Marko Zivcec, Hideki Ebihara, Yoshimi Tsuda and Jessica Levine Spengler for all of their direct involvement in the different experiments throughout this study. In addition, I would like to acknowledge the people involved in animal care for the hamster experiments, as well as Beth Fisher and David Dorward in the EM department for their help in imaging the VSV particles. Finally thank you so much to Kay Menk and Joyce Walczynski who did so much of the behind the scenes work in getting me down to Montana every time, and letting me in and out of the building on a daily basis!

I must also thank the people that have provided reagents towards this work. Thank you to Jack Rose for the VSV reverse genetics system and rescue plasmids, Connie Schmaljohn for the ANDV stock, and to Robbin Lindsay and Antonia Dibernardo for the recombinant SNV N antigen and ELISA plates.

Finally, thank you to the Canadian Institutes of Health Research (CIHR) for funding towards portions of this project.

DEDICATION

This thesis is dedicated to my parents who have been a constant encouragement to me throughout all of my years. They have pushed me to achieve, to be successful and have supported me when I've stumbled.

It is also dedicated to my loving wife Alanna, who has been by my side throughout this entire lengthy process and never questioned why I was doing something so ridiculous. She also provided me with our wonderful son Nathaniel, who has served as a good distraction during my thesis writing and with whom I hope to spend much more time with now that my work is finally complete.

Finally, it is also dedicated to my close friends and family members that have always had time to go out and have a good time when the work has become overwhelming.

ABSTRACT

Andes virus (ANDV) is a highly pathogenic New World hantavirus found in Chile and Argentina that causes Hantavirus Pulmonary Syndrome (HPS). A significantly high case fatality rate, the potential for human-to-human transmission, and the lack of licensed vaccines or effective treatments for the disease suggest an urgent need for the development of such measures. Many vaccine platforms have been recently described using reverse genetics systems to generate attenuated virus strains, as well as recombinant viruses expressing foreign proteins. This study attempted to generate and characterize vaccines based on an ANDV infectious clone system, as well as a recombinant vesicular stomatitis virus (VSV) vector expressing the ANDV glycoprotein precursor (VSV Δ G/ANDVGPC), to test their efficacy in the only lethal disease animal model of HPS. Although an ANDV infectious clone system was not successfully established, precluding its use as a possible vaccine candidate, the first New World hantavirus minigenome system was described. In addition, Syrian hamsters immunized with a single dose of the recombinant VSV Δ G/ANDVGPC vaccine were fully protected against disease when challenged at 28, 14, 7, or 3 days post-immunization with a lethal dose of ANDV; however, the mechanism of protection seems to differ, depending on the time point of immunization. At 28 days post-immunization, a lack of detectable ANDV RNA in tissue samples as well as a lack of seroconversion against the ANDV nucleoprotein (N) in nearly all hamsters suggested mostly sterile immunity. The vaccine was able to generate high levels of neutralizing anti-ANDV G_N/G_C antibodies that seem to play a role as a mechanism of vaccine protection. Administration of the vaccine at 7

and 3 days before challenge also resulted in full protection, but the lack of a neutralizing humoral immune response and the up-regulation of hamster cytokines involved in innate pathways suggested a possible role of innate responses in protection. The role of innate immunity was supported by the fact that administration of the vaccine 24 hours post-challenge was successful in protecting 90% of hamsters. Overall, the data suggests the potential for the use of the VSV platform as a fast-acting and effective prophylaxis/post-exposure treatment against lethal hantavirus infections.

LIST OF TABLES

Table 1: General Cycling Conditions for PfuTurbo Polymerase PCR	44
Table 2: General Cycling Conditions for iProof Polymerase PCR	44
Table 3: General Cycling Conditions for RobusT RT-PCR	46
Table 4: General Incubation Conditions for Superscript III RT-PCR	46
Table 5: General Cycling Conditions for QuantiTect qRT-PCR	48
Table 6: General Cycling Conditions for Rotor-Gene qRT-PCR	48
Table 7: Recombinant VSV Constructs	64
Table 8: DNA Transfection Amounts for VSV Rescue	71
Table 9: VSV titres	101
Table 10: Comparison of VSV Δ G/ANDVGPC and ANDV Neutralization Titres	119

LIST OF FIGURES

Figure 1: Geographical Distribution of Hantaviruses	5
Figure 2: Transmission Cycle of Hantavirus Infection	7
Figure 3: Hantavirus Structure and Organization	10
Figure 4: Hantavirus Life Cycle	11
Figure 5: Prime & Realign Model of Virus Transcription and Replication	18
Figure 6: Minigenome Reverse Genetic System	31
Figure 7: Full-Length Infectious Clone Reverse Genetic System	34
Figure 8: Sub-cloning Vectors	53
Figure 9: Expression Vectors	54
Figure 10: Cloning Strategy – Minigenome	60
Figure 11: Cloning Strategy – Minigenome Insertion	61
Figure 12: Cloning Strategy – Recombinant VSV	63
Figure 13: Rescue Strategy – Recombinant VSV	73
Figure 14: Restriction Enzyme Digest Confirmation – N Constructs	87
Figure 15: Restriction Enzyme Digest Confirmation – Glycoprotein Constructs	88
Figure 16: Restriction Enzyme Digest Confirmation – L Constructs	90
Figure 17: Western Blot – N and GPC Expression Constructs	91
Figure 18: IFA – N, GPC and L Expression Constructs	94
Figure 19: Rescue of CAT Minigenomes	97
Figure 20: Restriction Enzyme Digest Confirmation – VSV Full Length Constructs	100

Figure 21: Western Blot – Rescue of Recombinant VSV	102
Figure 22: RT-PCR – Rescue of Recombinant VSV	103
Figure 23: TEM – Recombinant VSV Infected Cell Monolayer	105
Figure 24: TEM – Purified Recombinant VSV	106
Figure 25: Western Blot – Purified Recombinant VSV	107
Figure 26: Recombinant VSV Growth Kinetic Study	109
Figure 27: Vaccine Protection Study	112
Figure 28: Detection of ANDV RNA	114
Figure 29: N Protein-Specific Seroconversion	116
Figure 30: ANDV Glycoprotein Neutralizing Antibodies	117
Figure 31: Time to Protection Study	121
Figure 32: Post-Exposure Study	123
Figure 33: Time to Protection N Protein-Specific Seroconversion	125
Figure 34: Time to Protection ANDV Glycoprotein Neutralizing Antibodies	127
Figure 35: Hamster Real-Time Cytokine Assay	129

LIST OF COPYRIGHTED MATERIAL

- Figure 5: Prime & Realign Model of Virus Transcription and Replication (Adapted from Figure 6, Journal of Virology, volume 69, issue 9, pp. 5754-5762, reproduced with permission from American Society for Microbiology) 18
- Results: (Adapted from Journal of Virology, volume 85, issue 23, pp. 12781-12791, reproduced with permission from American Society for Microbiology) 85

LIST OF ABBREVIATIONS

aa	Amino acids
Ad5	Human Adenovirus 5
ANDV	Andes virus
BHK-21	Baby Hamster Kidney cell line
BSA	Bovine serum albumin
BSL	Biosafety Level
CAG	Chicken β -actin
CAT	Chloramphenicol Acetyl Transferase
cDNA	Complementary DNA
COS-7	African Green Monkey Kidney cell line
CFR	Case Fatality Rate
CMV	Cytomegalovirus
CPE	Cytopathic effect
cRNA	Complementary RNA
C _T	Cycle Threshold
DMEM	Dulbecco's Modified Eagle's Medium
dNTP	Deoxynucleotide Triphosphate
ELISA	Enzyme-Linked Immunosorbent Assay
FBS	Fetal Bovine Serum
FFU	Focus Forming Unit

FRNT ₈₀	80% Focus Reduction Neutralization Titre
G(P)	Glycoprotein
G _C	Carboxy-terminal Glycoprotein
GFP	Green Fluorescent Protein
G _N	Amino-terminal Glycoprotein
GPC	Glycoprotein Precursor
H(C)PS	Hantavirus (Cardio-) Pulmonary Syndrome
HEK 293T	Human Embryonic Kidney cell line
HFRS	Hemorrhagic Fever with Renal Syndrome
HRP	Horseradish Peroxidase
hrs	hours
HTNV	<i>Hantaan Virus</i>
i.p.	Intra-peritoneal
IFA	Immunofluorescent Assay
IFN(- γ)	Interferon (-gamma)
IRF-1	Interferon Regulatory Factor-1
kDa	kiloDalton
L	RNA-dependent RNA polymerase
LB	Luria-Bertani
LD ₅₀	50% Lethal Dose
L-glut	L-glutamine
LUC	Luciferase

M	Matrix Protein
MCS	Multiple Cloning Site
min	minutes
MOI	Multiplicity of Infection
mRNA	Messenger RNA
Mx-2	Myxovirus Resistance Protein-2
N	Nucleoprotein
NCRs	Non-coding Regions
NHP	Non-Human Primate
NSs	Non-structural S-segment Protein
nt	Nucleotides
ORFs	Open Reading Frames
P	Phosphoprotein
P/S	Penicillin/Streptomycin
PBS(T)	Phosphate Buffered Saline (with 0.1% Tween-20)
PCR	Polymerase Chain Reaction
PFA	Paraformaldehyde
PFU	Plaque Forming Unit
Pol I	Human RNA Polymerase I
Pol II	RNA Polymerase II
PRNT ₈₀	80% Plaque Reduction Neutralization Titre
PUUV	Puumala virus

qRT-PCR	Quantitative Real-Time RT-PCR
RNP	Ribonucleoprotein
RPL18	Ribosomal Protein L18
RT-PCR	Reverse Transcription-Polymerase Chain Reaction
sec	seconds
SEOV	Seoul virus
SNV	Sin Nombre virus
STAT-1	Signal Transducer and Activator of Transcription-1
SV40	Simian virus 40
T7	T7 phage RNA Polymerase
TCID ₅₀	50% Tissue Culture Infectious Dose
TEM	Transmission Electron Microscopy
TULV	Tula virus
VeroE6	African Green Monkey Kidney cell line
vRNA	Viral RNA
VSV	Vesicular stomatitis virus
ZEBOV	Zaire Ebola virus

1.0 Introduction

Hantavirus represents a genus within the family *Bunyaviridae*. The genus contains a large number of species that are grouped together based on their geographical distribution and disease pathology. “Old World” hantaviruses are found primarily in Europe and Asia and cause a disease known as Hemorrhagic Fever with Renal Syndrome (HFRS). “New World” hantaviruses are found primarily in North and South America and cause a disease known as Hantavirus (Cardio-) Pulmonary Syndrome (HPS or HCPS). Hantaviruses are usually transmitted from their rodent hosts to humans via the inhalation of aerosolized urine and feces from infected animals, although human-to-human transmission has been documented in a few cases. Pathogenic hantaviruses are typically considered a biosafety level (BSL)-3 containment virus due to the possibility of life-threatening disease with no available prophylactic or therapeutic treatments. Experimental infection of animals requires the use of BSL-4 due to the increased risk of transmission from the infected animals. Non-pathogenic hantaviruses such as Prospect Hill virus (PHV) may be worked with at the lower BSL-2 level, with additional BSL-3 containment used for animal work.

1.1 Emergence and Epidemics of Hantaviruses

1.1.1 Emergence and Viral Transmission of Old World Hantaviruses

During their deployment in the Korean War in the early 1950s, more than 3200 United Nations troops contracted an acute febrile illness, with close to 33% expressing hemorrhagic manifestations. Overall, a mortality rate of between 5 and 10% was

Introduction

observed over a 3 year period. The disease attracted worldwide attention and was given the name Korean Hemorrhagic Fever (116, 202). The etiological agent was identified in 1976 from *Apodemus agrarius* field mice (118), isolated from human patient sera in 1978 (120), and was finally propagated in a human cell culture in 1981 (47). The virus was named Hantaan virus (HTNV), after the river that runs between North and South Korea, near where the first cases were identified. Close examination of the HTNV antigenic features, genetic composition and structural morphology as seen by electron microscopy suggested that the virus should be a new genus of *Bunyaviridae*, termed *Hantavirus*, with HTNV as its prototypical member (189, 191, 220). Although the virus was placed in the *Bunyaviridae* family, it was unique in that it represented the first member of the group to be carried by a rodent rather than arthropod host (193). The virus transmission was believed to occur predominantly through the inhalation of aerosolized, contaminated urine and feces from infected rodents (21, 94). The disease was also quickly defined as a “place” disease and not a contagious one, based on the lack of human-to-human transmission of the virus (202). The disease manifestations of Korean Hemorrhagic Fever were very similar to earlier cases of Epidemic Hemorrhagic Fever seen in regions of China, Japan and the former Soviet Union, as well as milder cases of Nephropathia Epidemica seen in Scandinavia (22, 116, 121, 122, 124, 210). A close etiological relationship was established between these different diseases, and the World Health Organization working group on HFRS recommended in 1982 that all of these diseases be classified as HFRS (115). Although the first cases of HFRS in Korea were identified in rural areas, it soon became clear that these infections were also

occurring frequently in urban areas. HFRS cases identified in the urban centers of Korea, Japan and China were soon associated with Seoul virus, carried by *Rattus norvegicus* and *Rattus rattus* (113, 207). Additional studies showed that HTNV reacted with convalescent serum obtained from patients with Nephropathia Epidemica in Scandinavia, quickly leading to the discovery of Puumala virus (PUUV), carried by the bank vole (*Clethrionomys glareolus*) (160). Many other hantaviruses were quickly discovered once it was determined that many rodents carried their own specific hantavirus. Although Old World hantaviruses are mostly found in Europe and Asia, hantaviruses such as Sangassou virus have also been recently identified in Africa (99). To date, there have been no documented human cases of infection; therefore, its pathogenicity is currently unknown. Currently, there are close to 200,000 cases of HFRS annually, with a case fatality rate (CFR) of between 0.1-15% (138, 198).

1.1.2 Emergence and Viral Transmission of New World Hantaviruses

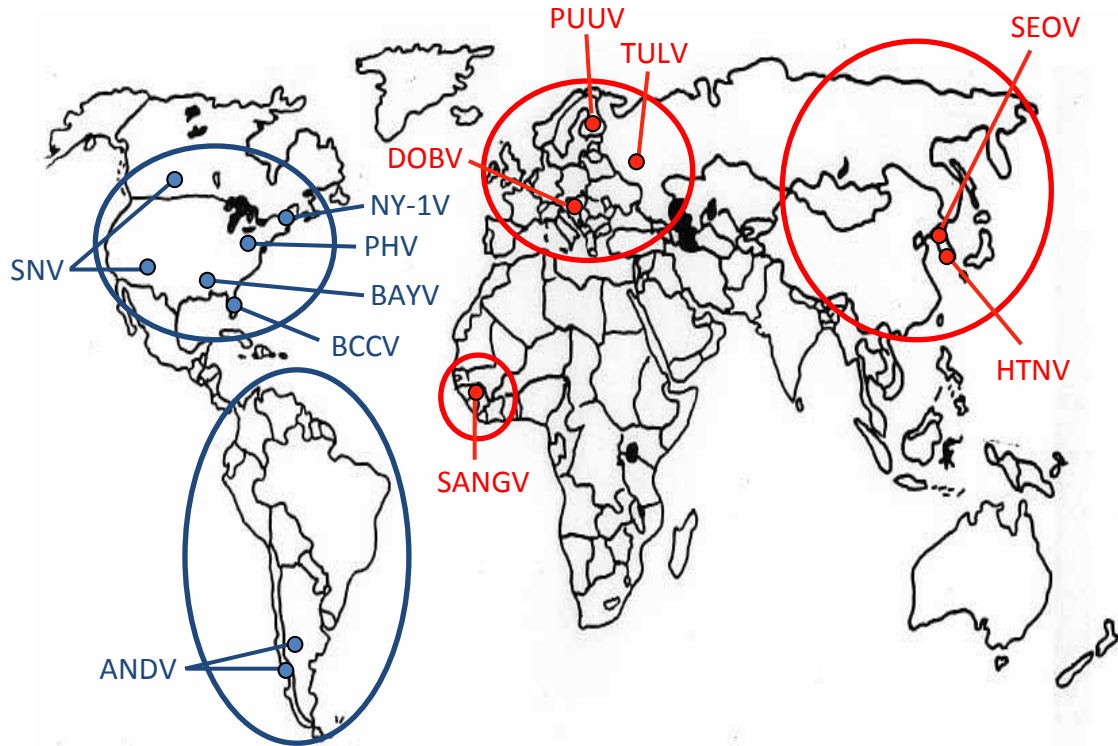
In 1993, a cluster of cases in the Four Corners region of the United States emerged with patients demonstrating a vascular leakage syndrome characterized by massive pulmonary edema followed by shock. Death was observed between 2-10 days after onset of illness in close to 50% of the cases. Within a few weeks of the outbreak, the agent responsible was identified as a hantavirus, and the disease was given the name HPS (96, 159). The newly identified virus was given the name Sin Nombre Virus (SNV), and its rodent host was quickly identified as the common deer mouse, *Peromyscus maniculatus* (23, 159). A series of outbreaks in Argentina and Chile a few

years later in 1995 led to the discovery of Andes virus (ANDV), carried by the long-tailed pygmy rice rat, *Oligoryzomys longicaudatus* (127, 131). Unlike previous HPS and HFRS cases that are limited to the rodent-human transmission paradigm, there is evidence suggesting that human-to-human transmission of ANDV does occur, although it remains a rare event (36, 112, 141, 165, 213). Within a few more years, HPS was shown to occur all across North and South America, caused by at least 10 different hantaviruses, all with different rodent hosts. This search for both HPS and HFRS-causing hantaviruses also led to the discovery of a large number of hantaviruses not associated with human illness (193). Currently, there are approximately 200 cases of HPS annually; a rate much lower than what is seen for HFRS, albeit with a CFR that is much higher, ranging from between 30 to 50% (9, 89, 138). The distribution of Old and New World hantaviruses is shown in Figure 1.

1.2 Natural Reservoir of Hantaviruses

Hantaviruses are typically carried by a specific host rodent species (193), although recent studies have identified hantaviruses that are carried by shrews (20, 98), challenging the dogma that hantaviruses are limited to only rodent species. Each different hantavirus appears to be carried by a different host reservoir species, acting as an identifier between viruses, although the differentiation between hantavirus species and strains remains unclear. The Eighth Report of the International Congress on

“Old World” Hantaviruses



“New World” Hantaviruses

Figure 1. Geographical Distribution of Hantaviruses. New World hantaviruses are located in North and South America and are typically associated with HPS. Old World hantaviruses are primarily located in Europe and Asia, with viruses recently being identified in Africa. These hantaviruses are typically associated with HFRS. SNV = Sin Nombre virus, ANDV = Andes virus, NY-1V = New York-1 virus, PHV = Prospect Hill virus, BAYV = Bayou virus, BCCV = Black Creek Canal virus, DOBV = Dobrava virus, TULV = Tula virus, PUUV = Puumala virus, SEOV = Seoul virus, HTNV = Hantaan virus, SANGV = Sangassou virus

Introduction

Taxonomy of Viruses (ICTV) lists 22 different hantavirus species that are identified as part of the *Hantavirus* genus, each with a different natural reservoir host (158). Old World hantaviruses are typically associated with two sub-families of rodents; *Murinae* (HTNV, Dobrava virus and Seoul virus) and *Arvicolinae* (PUUV). New World hantaviruses are usually associated with sub-family *Sigmodontinae* (SNV, ANDV, Black Creek Canal virus) (94, 193). Hantaviruses appear to have co-evolved with their host reservoir species, so that a hantavirus infection in the natural host species typically produces no overt signs of disease, combined with a long period of persistence that may last from months to years (33, 117, 157). The infection is typically spread laterally throughout a group of rodents through inhalation of infected aerosols, as well as aggressive behaviour such as scratching and biting. There appears to be no vertical transmission from infected rodent to offspring, and maternal antibodies are protective against both vertical transmission and subsequent challenge (13, 31, 119). Humans are typically dead-end hosts for the virus and are infected when exposed to aerosols from the excreta of infected rodents. The cycle of transmission is illustrated in Figure 2. Experimentally infected rodents reach a peak of viremia approximately 2 weeks post-infection, with peak shedding of the virus in urine and feces (and possibly saliva) between 2 and 10 weeks (117, 157). Virus primarily targets endothelial cells, and is typically found in large amounts in both lungs and kidneys of infected animals (154). The reduction of viremia is correlated to the development of serum neutralizing antibodies; however, the virus is never completely cleared and continues to persist and be shed for the lifetime of the animal.

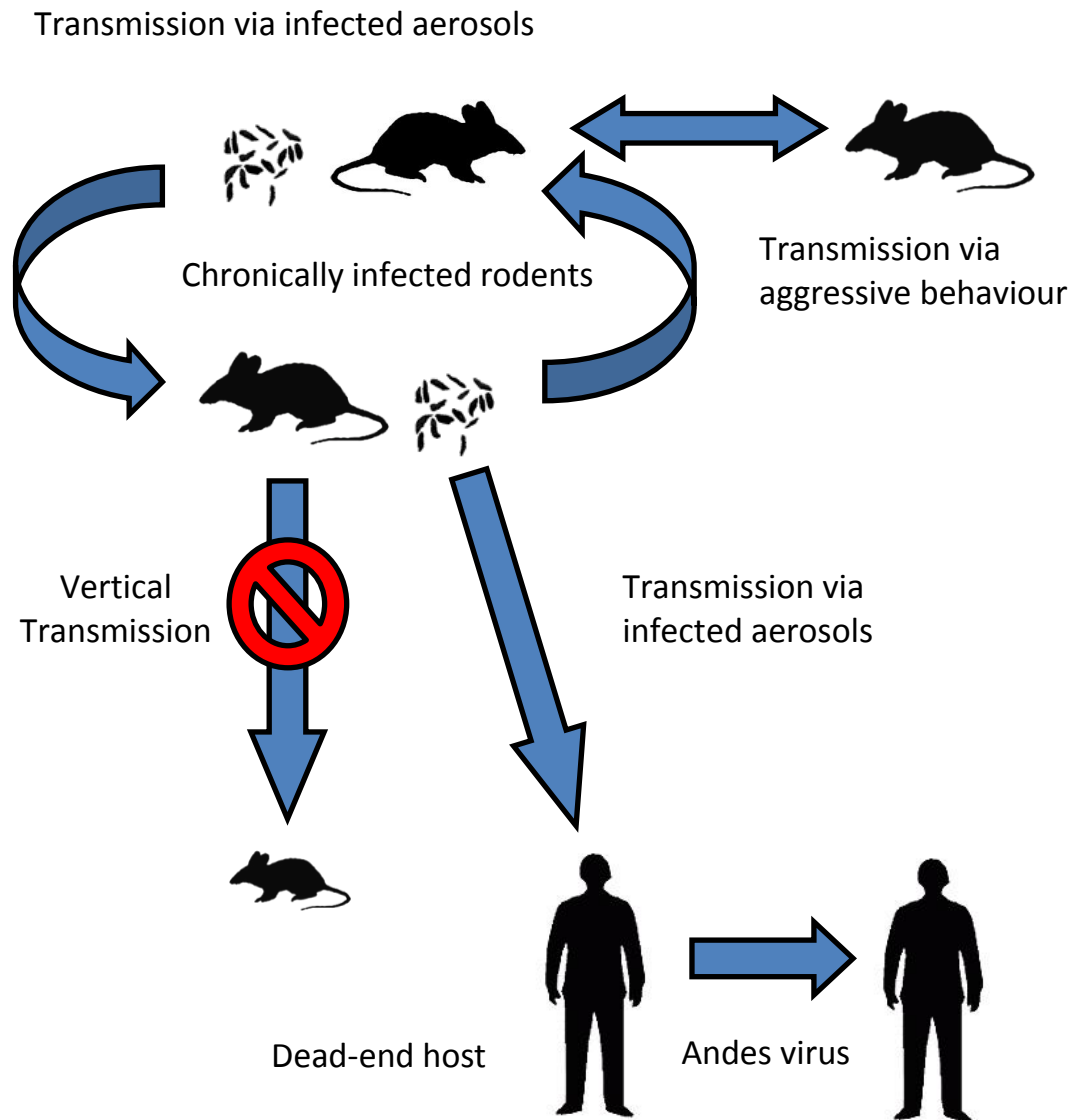


Figure 2. Transmission Cycle of Hantavirus Infection. Hantaviruses are maintained through persistence of the virus in chronically infected rodent reservoirs. The virus is typically shed through the urine and feces of infected animals, and is therefore transmitted to other rodents through the inhalation of the infected excreta. Some transmission may also occur through aggressive behaviour such as scratching and biting. There is no evidence of vertical transmission of the virus from mother to offspring. Humans are also typically infected through the inhalation of the infected aerosols. Humans usually represent a dead-end host for the virus; however, Andes virus has been shown to rarely infect through a person-to-person mode of transmission.

1.3 Biology of Hantaviruses

Hantaviruses are roughly spherical, enveloped particles between 80-120nm in diameter with glycoprotein spikes projecting between 5-10nm from the virus envelope. They contain, like other members of *Bunyaviridae*, a tri-segmented, single-stranded, negative-sense RNA genome (193). The three RNA genomic segments, labelled small (S, ~1.9 kilobases (kb) in length), medium (M, ~3.7kb in length) and large (L, ~6.5kb in length) based on their size, have the same conserved nucleotide region at their 3' and 5' termini (consensus sequence AUCAUCAUCUG-) (193). Base pairing of these regions is predicted to cause stable panhandle structures and non-covalently closed circular RNA structures (73). At least one of each genomic nucleocapsid is required in each virus particle for infectivity, however, they may not always be present in equimolar ratios (82). The 3 segments encode for 4 different proteins. The S segment encodes for the nucleocapsid protein (N), which interacts with viral RNA (vRNA) and plays a role in the encapsidation of each genome segment (151). The specific interaction of N with the RNA panhandle structures results in the formation of S, M and L ribonucleocapsids. The M segment encodes the glycoprotein precursor (GPC) that is co-translationally cleaved into two components; G_N (the N-terminal portion of GPC, formerly G1) and G_C (the C-terminal portion of GPC, formerly G2). The glycoprotein spikes on the surface of the virus envelope consist of a G_N and G_C heterodimer that are responsible for viral attachment/entry (193). The hantavirus glycoproteins are typical class I transmembrane proteins, with the amino-terminus on the surface and the carboxy-terminus anchored in the membrane of the virus particle. The L segment encodes for the RNA-dependent

RNA polymerase (L protein), responsible for viral transcription and replication (193). The L and N proteins together form the ribonucleoprotein (RNP) complex which contains all of the factors necessary for viral transcription and replication of genome products and genome. A diagrammatic representation of the virus particle and genome is shown in Figure 3.

1.4 Viral Life Cycle

Although many aspects of the hantavirus life cycle have been elucidated, much of the currently known information has been inferred from experimental data collected from other members of the large *Bunyaviridae* family. A diagrammatic representation of the viral life cycle is represented in Figure 4.

1.4.1 Virus Entry

The attachment of the hantavirus to the target cell involves an interaction between the viral glycoproteins G_N and G_C and a specific cellular receptor. The presence of neutralizing sites on each glycoprotein suggests that both proteins may be required in this early entry step (5). Unlike most other bunyaviruses, a cellular receptor for hantaviruses has been identified, with β 3 integrins being identified for pathogenic hantaviruses, and β 1 integrins for non-pathogenic hantaviruses. These may, however, not be the sole receptors for hantavirus entry, as experiments blocking decay-accelerating factor (DAF/CD55) prevented entry of Old World hantaviruses, suggesting its possible role as an important co-factor (105). Hantaviruses preferentially target

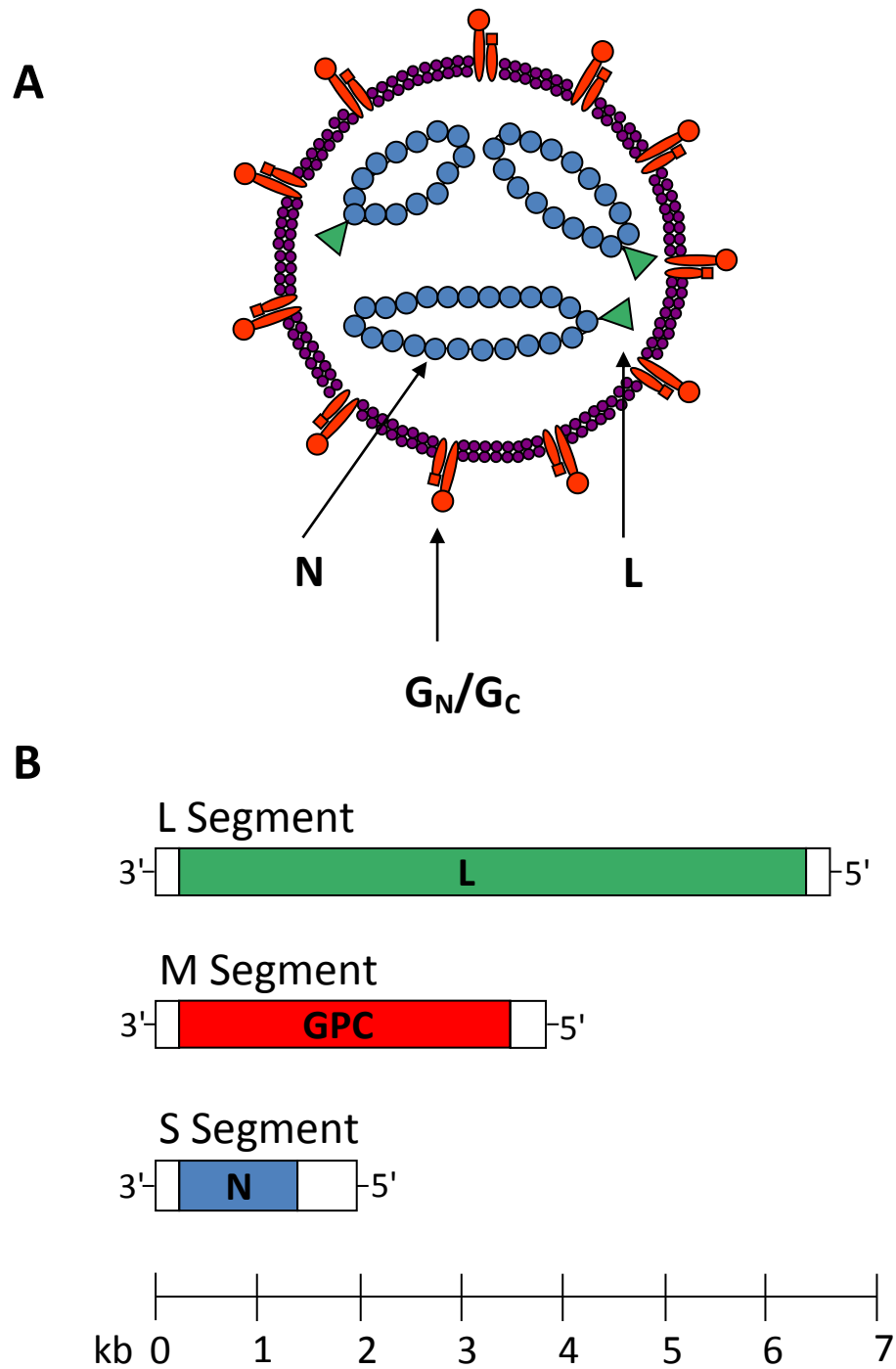


Figure 3. Hantavirus Structure and Organization. (A) Illustration representing the enveloped hantavirus virion structure and organization. (B) A diagrammatical representation of the hantavirus tri-segmented, single-stranded, negative-sense RNA genome. N = Nucleocapsid protein, GPC = Glycoprotein precursor (cleaved to G_N/G_C glycoproteins), L = RNA dependent RNA polymerase

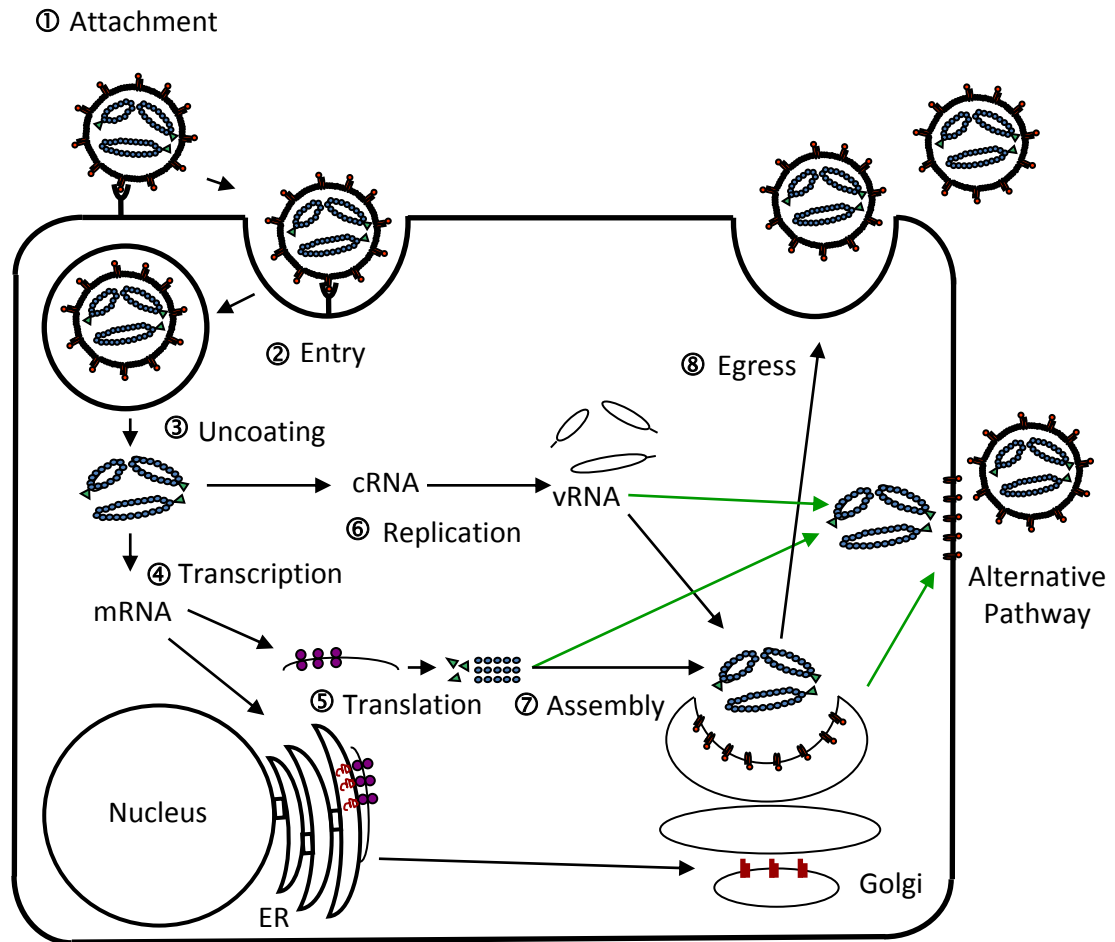


Figure 4. Hantavirus Life Cycle. (1) Attachment. Hantaviruses bind the $\beta 1$ or $\beta 3$ integrin host cellular receptor. (2) Entry. Viral entry occurs through endocytosis via clathrin-coated pits. (3) Uncoating. Conformational changes of glycoproteins in acidified vesicles allow fusion with membranes and entry to cytoplasm, exposing viral genetic material. (4) Transcription. Viral messenger RNA (mRNA) is transcribed by the viral ribonucleoprotein (RNP) complex. (5) Translation. N and L protein transcripts are translated on free ribosomes whereas the glycoproteins are translated on membrane-bound ribosomes of the endoplasmic reticulum (ER). GPC is cleaved during translation by signal peptidase while the protein is in the ER. (6) Replication. An unknown mechanism triggers virus to switch to full-length genome production through the production of full-length complementary RNA (cRNA) (7) Assembly. G_N , G_C , N and L proteins are transported to the Golgi membranes. Viral RNA (vRNA) is encapsidated by N protein. (8) Egress. Virus buds from the Golgi membranes where it leaves the cell via the exocytosis pathway. An alternative pathway has been proposed for some hantaviruses that bypasses the Golgi and buds at the plasma membrane. This pathway has not been experimentally demonstrated, but has been included (shown with green lines) to illustrate the differences.

endothelial cells (54, 168), but have also been shown to be capable of infecting macrophage/monocytes as well as dendritic cells (174, 211). After attachment, hantaviruses have been shown to enter the cell by endocytosis via clathrin-coated pits (85). After endocytosis, virus particles are required to enter acidified vesicles in order to become infectious. This acidification results in a conformational change in the glycoproteins, allowing fusion and entry into the cell cytoplasm. Many experimental studies have proposed that the G_C glycoprotein mediates fusion, with evidence that supports this (212). Computational analysis studies have shown that this protein contains a number of characteristics similar to class II fusion proteins identified in other virus families (53). However, other studies have shown that G_N and G_C are required to be expressed together to achieve successful expression on the cell surface as well as cell fusion, suggesting that although G_C may be the primary player in cell fusion, it may need to be expressed with G_N to achieve its correct conformation (164).

1.4.2 Viral Transcription

All members of *Bunyaviridae* encode their structural proteins in the complementary RNA (cRNA) orientation, but many also encode non-structural proteins that may be in either the cRNA or vRNA orientation, requiring the use of an ambisense coding strategy. Most hantaviruses, unlike other members of the family, do not encode for any non-structural proteins and therefore only use a negative-sense coding strategy (193). However, some New World hantaviruses as well as the PUUV and Tula virus (TULV) Old World hantaviruses contain putative NSs ORFs in an overlapping reading

frame of the N protein coding region, similar to the orthobunyaviruses (88). The production of this protein has been demonstrated for PUUV and TULV, and is thought to play a role in interferon (IFN) antagonism (90). Transcription of vRNA into messenger RNA (mRNA) occurs through an interaction of the RNA-dependent RNA polymerase L, the nucleocapsid protein N and the viral ribonucleocapsids. L and N appear to be the only protein requirements for RNA synthesis, and their localization near the perinuclear region and association with perinuclear membranes of the infected cells suggests that RNA synthesis is membrane-associated (109). The 3' and 5' non-coding regions (NCRs) of each ribonucleocapsid contain the signals necessary for mRNA and anti-genome production, and therefore act as the genome promoters. Although the minimum number of nucleotides and exact sequence complementarity requirement has been demonstrated for Rift Valley Fever, Uukuniemi and Bunyawerma viruses through the use of reverse genetic systems, the requirements for hantaviruses have yet to be fully elucidated (43, 101, 171). These experiments all seem to support the theory that the RNA panhandle structure formed via the complementary 3' and 5' ends of each segment seems to be more important than the actual nucleotide sequence itself. However, this only seems to apply *in vitro*, as experiments done with the full length infectious clone of BUNV show a requirement for non-conserved, non-complementary regions for successful virus production (132). There is also a great deal of variability in the length of the NCRs of each genomic segment, and deletions in these regions cause fewer replication-competent genomes to be produced. This leads to an overall down-regulation of virus replication, in some cases leading to viral persistence (147). The NCRs of the S

segment are larger than the M segment, which in turn are larger than the L segment of ANDV, which may explain the difference in relative abundance of the viral proteins, with the highest amount of protein being expressed from the segment with the fewest deletions in these regions (166).

Although hantavirus transcription and replication occurs exclusively in the cytoplasm and not in the nucleus, they have been shown to use an orthomyxovirus-like cap-snatching mechanism that generates mRNAs with 5' m7G caps derived from host cytoplasmic mRNAs through an endonuclease activity of the L protein (52, 82). To produce mRNA transcripts, hantaviruses are proposed to use a concept termed “prime and realign” (52). In this model, capped host primers with a terminal G residue would align with the third nucleotide (C) of the vRNA template. After the synthesis of a few oligonucleotides, the RNA would slip back two nucleotide positions on the repeated terminal section (AUCAUCAUC) so that the G would no longer be part of the 5'-templated extension. Deletions of one of the triplet repeats are occasionally seen in this terminal region, suggesting that the priming may sometimes occur at the second triplet instead of the first. This theory is supported by the fact that almost all mRNAs have a G at the -1 position of the transcript, despite a general heterogeneity of the remainder of the capped primer (52). Although most negative-sense RNA viruses use a poly-U stretch to terminate transcription and generate a poly-A tail at the 3' end of the mRNA, most viruses in *Bunyaviridae* do not follow this method of termination (193). Examination of the 3' terminus of SNV mRNA suggested that the viral polymerase uses a different mechanism of termination with each genomic segment (82). The S segment mRNA

terminated at CCC-rich motifs downstream of a conserved CCCACCC motif. The L segment mRNA did not terminate before the end of the genomic template, unlike what is seen in other segmented RNA viruses, meaning the 3' ends of the mRNA transcripts represent the entire vRNA template. This mechanism of termination may be partially due to the relatively short length of the 5' NCR of the vRNA. Neither the S nor L segments showed any signs of poly-adenylation. However, the M segment mRNA terminated in a region containing a stretch of 8 uridines, generating a poly-A tail. These termination signals in the different segments appear to be conserved across most hantavirus species (82).

1.4.3 Translation and Processing of Viral Proteins

Viral proteins are synthesized almost immediately after infection and transcription occur, with S and L mRNAs being translated on free ribosomes and M mRNAs using membrane-bound ribosomes located on the endoplasmic reticulum (193). The hantavirus N proteins are predicted to have a coiled-coil structure which trigger trimerization of the proteins (1). These N trimers appear to preferentially interact with the 5' ends and panhandle of the vRNA (152, 200). The N protein appears to play a large role in many aspects of virus replication. It has been shown to have both chaperone activity and the ability to act as an initiator of translation by interacting with the 5' mRNA cap and essentially bypassing and replacing the host eIF4F complex (150, 151). This cap-binding ability also allows it to sequester cellular mRNA in cytoplasmic processing bodies until required for use in initiation of transcription by the L protein

(149). The viral glycoproteins G_N and G_C are translated from a single GPC mRNA transcript. The full-length GPC protein is not seen in infected cells, as the proteins are cleaved during translation by a signal peptidase at a conserved pentapeptide WAASA sequence in the middle of the ORF (136). Most hantaviruses are predicted to contain between 5-7 potential N-linked glycosylation sites, with 4 being conserved across all species (3 sites located on G_N and 1 site located on G_C) (205). The oligosaccharides are of primarily the high-mannose type, possibly resulting from incomplete processing due to their retention in the Golgi prior to budding (192) or the availability of the sites in the protein's final conformation. The L protein does not appear to have any processing or post-translational modification, and contains many features that are common to other polymerase proteins (108).

1.4.4 Virus Replication

The switch from viral transcription to replication must require some sort of host cellular or viral factor in order to switch from primed mRNA synthesis to independently initiated full-length genome production. Although it has not been shown experimentally for hantaviruses, encapsidation of the genome by the N protein for other negative-strand RNA viruses has been shown to act as an anti-termination signal (110, 135, 187). The replication of viral full-length genome has been proposed to use a similar “prime and realign” strategy as described for viral transcription (52). Instead of using a host mRNA primer, the third position of the vRNA is bound by a guanosine tri-phosphate. Extension of the genome continues until realignment occurs, with the guanosine tri-phosphate

moving to the -1 position. This nucleotide is then cleaved by the endonuclease activity of the L protein, leaving a uridine monophosphate at the starting position. This overhanging monophosphorylated uridine has been experimentally demonstrated (52). A comparison of the prime and realign model for transcription and replication is shown in Figure 5.

1.4.5 Assembly and Egress

In contrast to all other negative-strand RNA viruses, bunyaviruses usually mature in and bud through the membranes of the Golgi (193). It has been suggested that some hantaviruses, including HTNV, SNV and Black Creek Canal virus, may also use an alternative pathway of maturation with budding through the plasma membrane (163, 178). It is currently unclear why this alternative pathway may be used, and the hypothesis is based on the observation that no intracellular viral particles were observed, as well as the presence of the glycoproteins on the surface of the plasma membrane. The expression of both G_N and G_C are required in order for the proteins to leave the endoplasmic reticulum and be transported to the Golgi, as independent expression of either protein or deletions within the proteins that interfered with proper folding prevented this from occurring (185, 201). Furthermore, independent expression of G_N caused it to be polyubiquitinated, suggesting proteasomal degradation when not associated with G_C (55). Determining the exact sequence for the targeting of the proteins to the Golgi remains difficult, as there appears to be no consensus motif or conserved regions across the viruses in the family (193). N protein has been shown to accumulate

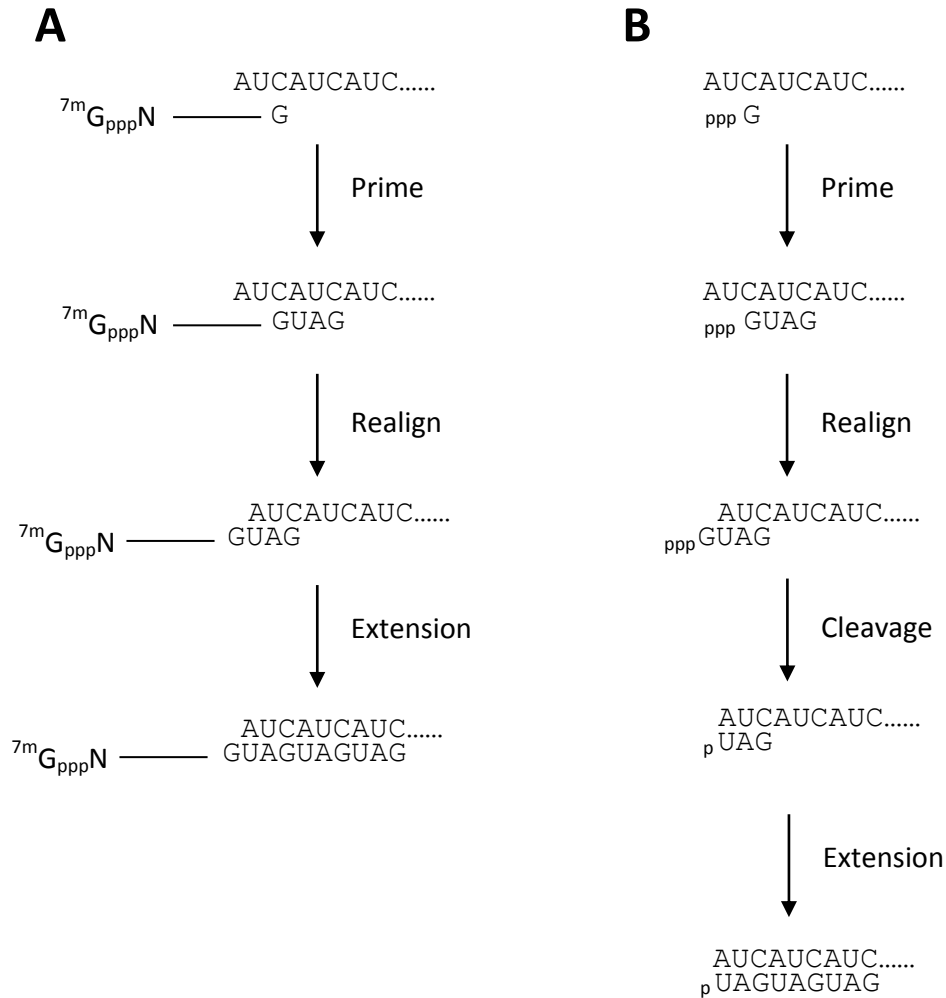


Figure 5. Prime & Realign Model of Virus Transcription and Replication.

(A) Transcription. Capped host primers with a terminal G residue ($7^m\text{G}_{\text{ppp}}\text{N---G}$) bind to the 3rd position of the template terminal repeats (C residue). This primer is extended by a few nucleotides, and then is realigned with the G moving to the -1 position. Extension then continues for the remainder of the template. (B) Replication. Instead of binding to a host primer, a guanosine triphosphate (GTP, pppG) binds the same 3rd nucleotide position. Extension and realignment occur, with the GTP moving to the -1 position. The nucleotide is then cleaved by the polymerase, leaving a monophosphorylated U (pU) residue in the +1 position. Extension then continues for the remainder of the template. (Model adapted from Garcin *et al.* (1995). *Journal of Virology*: 69:9:5754-5762, with permission from American Society for Microbiology).

quickly in the cytoplasm after infection, with most of it localizing to the Golgi region after 24 hrs (92, 177).

The HTNV N protein has been shown to traffic via microtubule dynein to the endoplasmic reticulum-Golgi-intermediate compartment (ERGIC), suggesting that both the ERGIC and Golgi complex may be important in assembly (175). Newly synthesized vRNA is quickly encapsidated by the N protein, forming the RNPs. Unlike most other negative-strand RNA viruses, hantaviruses do not contain a matrix (M) protein, and it has been theorized that the RNPs must interact with the glycoprotein spikes in order for budding to occur. Unfortunately, many questions exist as to how the RNPs are directed to the budding compartment, how they interact with the glycoprotein spikes and what the mechanisms are that drive budding (88). Many of the signals and protein interactions that drive these processes have yet to be identified in any member of the virus family. It is believed that after budding through the Golgi, the virus particles are released from the cell using the normal exocytosis pathway. A study with polarized Vero C1008 cells infected with Black Creek Canal virus showed that virus release appears to predominantly occur at the apical surface of these cells, in contrast to other members of *Bunyaviridae* (178).

1.5 Hantavirus Infection of Humans

1.5.1 Clinical Signs of Disease

Unlike infections of the host reservoir species, human infection with hantaviruses typically results in disease. Following infection, there is usually an

incubation period of between 1 to 3 weeks where no clinical signs are observed. After this, patients with either HFRS or HPS typically have an onset of flu-like symptoms, characterized by high fever, flushing and myalgia (75, 91). Clinical manifestations of HFRS usually involve bleeding disorders and haemorrhaging as well as acute renal failure. These haemorrhages may range from small petechiae to severe internal bleeding and disseminated intravascular coagulopathy. In contrast, clinical manifestations of HPS usually involve pneumonia and cardiac dysfunction. Patients also typically experience hypotension and shock during this period in both diseases that lasts anywhere from 12 to 48 hours (94). Laboratory findings typically involve a thrombocytopenia and lymphocytosis with a left shift (128). Patients with HFRS may also develop increased levels of complement and immune complexes which are not usually seen in HPS (169). Hantaviruses are not typically cytopathic in the cell types that they infect. Therefore, virus specific organ pathology most likely develops through indirect mechanisms involving up or down regulation of cytokines as well as involvement of these ICs and complement activation. The primary causes of death in patients with HFRS are complications resulting from haemorrhages and/or renal failure. In patients with HPS, death is usually a result of severe cardiopulmonary dysfunction (94). Different pathogenic hantaviruses cause varying levels of disease severity. Among the Old World hantaviruses, HTNV and Dobrava viruses typically result in the most severe infections (5-15% CFR), with Seoul virus infections generally being much milder (1-2% CFR) (97). PUUV-associated HFRS results in the least number of deaths, with a CFR of under 1%. Of the HPS-associated hantaviruses, SNV and ANDV seem to cause the most

severe infections, with a CFR of up to 50%. Although Old World hantaviruses are typically associated with HFRS and New World hantaviruses with HPS, a few cases have recently emerged that seem to challenge these definitions. PUUV infection causing pulmonary symptoms that meet the clinical definition of HPS have been recorded (19, 176), and hantaviruses such as Black Creek Canal virus, Bayou virus and ANDV have been shown to cause haemorrhaging and renal involvement (4, 74, 126), suggesting that these two diseases may be more closely related than previously believed.

1.5.2 Pathogenesis and Pathology

Although the early stages of hantavirus infection are unclear, the virus is typically brought in through the respiratory route. The virus glycoproteins also typically have a tropism for endothelial cells, due to the high levels of the hantavirus receptor being expressed on them. These cells are shown to contain high levels of hantavirus antigen in post-mortem investigations, as well as a dramatically increased permeability in fatal HFRS and HPS cases (37, 224). Although increased permeability of infected endothelium is associated with fatal hantavirus infections, it does not appear to be specifically virus related. As mentioned in the previous section, hantaviruses are usually non-cytopathic *in vitro*, and no tissue damage is seen as a direct result of hantavirus infection. Therefore, hantavirus-associated disease seems to be primarily caused by excessive stimulation of the immune system, resulting in an increase in cytokines, chemokines, immune complexes and complement activation (94). Immune complexes are only seen in HFRS, and are typically composed of both C3 complement and IgM

molecules (86). These complexes cause deposits in tissue that result in local inflammation, the release of tissue-damaging substances, and the infiltration of inflammatory cells, leading to necrosis, ischemia, and haemorrhages in the medulla of the kidney as they attempt to reabsorb lost fluids. The complement system is also usually activated in HFRS, with the degree of activation directly correlated with the severity of disease, and with the presence of activated C1 in serum coinciding with hemorrhagic syndromes, proteinuria and shock (40). HPS is usually primarily associated with changes seen in the lungs. Examination of lung tissue usually reveals mild to moderate levels of interstitial pneumonitis with congestion, edema and mononuclear cell infiltration. Extensive amounts of fluid and fibrin are also seen in the alveoli of the lungs (224). One of the major contributors to the tissue damage seen in both HPS and HFRS is thought to be hantavirus-specific CD8⁺ cytotoxic lymphocytes. These immune cells are found in large amounts in the kidneys of HFRS patients, as well as in the lungs of HPS patients, and are believed to destroy infected endothelial cells, leading to increased permeability, tissue damage and the pathology seen during infection (35). By attempting to control infection, these cytotoxic lymphocytes also produce cytokines that are implicated with collateral damage, including IFN- γ and tumor necrosis factor- α (133). However, recent animal studies where T-cells were depleted suggest that they may not be required for hantavirus pathogenesis (70). Overall, the immune system must strike a delicate balance between virus clearance and minimizing tissue damage in order for a patient to overcome infection.

1.5.3 Immune Evasion

Like most viruses, hantaviruses have a number of mechanisms that they use in order to try and modulate the host immune system responses. *In vitro* studies with pathogenic and non-pathogenic hantaviruses have shown that pathogenic hantaviruses appear to delay the induction of the type I interferon response pathways (IFN- α , IFN- β and myxovirus resistance protein A (MxA)) when compared to the non-pathogenic hantaviruses (56, 95, 104, 204). It is unclear which viral components are involved, although the glycoproteins have been implicated as the primary mediators of this antagonism. The G_N cytoplasmic tail of the New York-1 virus has been shown to inhibit the retinoic acid inducible gene I (RIG-I) and TANK-binding kinase 1 (TBK-1)-dependent IFN responses, and the glycoproteins of both ANDV and Prospect Hill virus have been shown to inhibit nuclear translocation of signal transducer and activator of transcription-1 (STAT-1) (2, 3, 204). Another study has suggested that the mechanism of antagonism may be hantavirus species-specific, as SNV was able to antagonize the IFN pathway to a greater extent through its glycoprotein in contrast to ANDV, which required expression of both its glycoprotein and N protein (125). The S segment of TULV and PUUV contains a non-structural NSs protein that has also been shown to play an important role in IFN antagonism *in vitro* (90). Although this data appears to support the role of hantavirus proteins in IFN antagonism, the effect does not always appear to be very strong, with the lack of a clear, strong human IFN antagonist like Ebola virus VP35 and VP24 (6, 181), or influenza virus NS1 (100).

1.5.4 Diagnosis

Clinical diagnosis of hantavirus infection is almost impossible due to the large number of non-specific early symptoms. Severe HFRS can easily be confused with leptospirosis, post-streptococcal glomerulonephritis, pyelonephritis and other hemorrhagic fevers. HPS is most commonly confused with influenza infection (193). Acute diagnosis of hantavirus infection is most commonly done by IgM capture ELISA using hantavirus-infected cell slurry as the antigen (107). ELISA using recombinant N protein has also been used with great success (34, 39). Cross-reactivity between related hantaviruses is frequently seen, such that inclusion of a number of representative hantavirus antigens can allow detection of virtually all hantavirus infections. Unfortunately, this cross-reactivity also makes it difficult to specifically identify the virus causing the infection. Recent studies have attempted to circumvent this through the deletion of the N-terminal immuno-dominant epitope from the recombinant N protein, reducing sensitivity, but greatly increasing the specificity of a positive result (102). Virus isolation attempts from infected tissue are almost always negative, although this is most likely due to the poor growth of hantaviruses usually seen in tissue culture. Quantitative real-time RT-PCR (qRT-PCR) assays have been shown to be very sensitive at the detection of hantaviral RNA, and can be used to compliment immunodiagnostic assays as well as allow detailed genetic comparisons (159, 167).

1.5.5 Treatment and Prevention

Although there are currently no approved vaccines or treatments available for hantavirus infections, a number of options have been examined for their effectiveness against hantaviral disease (138, 188). The main treatment for severe HPS or HFRS cases remains supportive therapy, with mechanical ventilation for HPS and extracorporeal blood purification (hemodialysis) for HFRS (138). The anti-viral drug ribavirin appears to be an effective treatment for HFRS when given intravenously early on in infection, however, its effectiveness in HPS remains unclear (89, 146, 184, 222). It has also been shown that hantaviruses are sensitive to interferon treatment prior to an established infection, but become insensitive to treatment following an established infection (206).

In the development of hantavirus vaccines, most of the efforts have been directed towards HFRS-causing viruses, as they represent the greatest burden on public health. The exact contributions of innate immunity versus adaptive immunity, as well as humoral versus cellular immunity towards protection have yet to be fully elucidated. Many studies have shown the importance of developing a strong neutralizing antibody response, whereas others have supported the role of a cellular immune response (138). The expression of the viral glycoproteins typically induces the production of neutralizing antibodies, whereas the N protein has been shown to induce both cellular, as well as humoral immune responses (138, 188). In addition, antibodies directed towards the N protein tend to be more cross-reactive, due to the more conserved nature of the protein across different species (30, 61). This cross-reactivity of the N protein has also been demonstrated with cytotoxic T-lymphocyte epitopes (137).

1.5.5.1 Old World Hantavirus Vaccines

The development of vaccines against hantaviruses causing HFRS has been severely hampered by the lack of a lethal animal model. Of the Old World hantaviruses, only PUUV has a disease model using cynomolgus macaques (*Macaca fascicularis*). Therefore, the successfulness of a vaccine must be determined by its ability to prevent infection and/or virus replication in an animal model that does not show any disease symptoms. Formalin inactivated virus-based vaccines derived from mouse brain or cell culture have been developed and tested in both animals and humans in Asia (188). A commercially available vaccine in Korea named HantavaxTM consists of inactivated HTNV derived from suckling mouse brain, and has been available for over 10 years with no demonstrated safety concerns. It showed full protection in mice, and vaccinated individuals showed high levels of seroconversion and virus specific-antibody titres. However, fewer than 50% of individuals developed neutralizing antibodies after a booster dose 12 months later (24, 203) and overall protection levels appear to be low. In contrast, a cell culture-derived bivalent inactivated vaccine against HTNV and SEOV showed an 85% neutralizing antibody response with a low (0.5%) incidence of side effects in vaccinated individuals, with the added benefit of protection from both of the most common co-circulating hantaviruses (32). Recombinant virus platforms have also been examined, with vaccinia virus expressing both HTNV glycoproteins and nucleocapsid protein making it to Phase I and II human clinical trials. Although initially appearing promising in animal studies (25, 190), very few participants with pre-existing immunity towards vaccinia virus developed neutralizing antibodies, and those without

immunity required high doses of the vaccine in order to maintain a long-term response (144). The high levels of pre-existing immunity combined with the rare occurrences of vaccinia virus-induced disease make it unlikely that this approach would ever be commercialized. Other recombinant virus platforms tested include pseudotyped vesicular stomatitis virus (VSV) vectors expressing the HTNV glycoproteins and Hepatitis B core virus-like particles expressing portions of the PUUV or HTNV nucleocapsids, both of which appear to be highly immunogenic and afford protection in mice (62, 63, 114). A third series of vaccines have been based on DNA platforms, using the full length or portions of the glycoproteins and N protein. These vaccines have shown full protection in mouse, hamster and non-human primate (NHP) animal models (77, 78, 80).

1.5.5.2 New World Hantavirus Vaccines

Like the Old World hantaviruses, most New World hantaviruses do not have a lethal animal model. Early studies in non-lethal models based on the DNA platform seemed to offer full protection (7, 8). In 2001, the Syrian Golden hamster was described as a lethal animal model for ANDV infection (81). To date, it remains the only small animal model for hantavirus infection where the disease course closely mimics what is seen in human cases in regards to disease progression and pathology (18). Since its development, most vaccine platforms have been based off ANDV and subsequently tested in the hamster model. The first vaccine platform to be extensively tested was DNA-based. Immunization of hamsters with ANDV M-segment cDNA was unable to

produce a response that afforded protection against lethal ANDV challenge (29). However, the injection of the same vaccine into NHPs or rabbits was able to generate a high neutralizing antibody response that when passively transferred into hamsters, fully protected them from lethal challenge (79). The second platform to be tested was based on recombinant human adenovirus 5 (Ad5). Ad5 expressing G_N, G_C, N, or a combination of G_N and G_C together were given to hamsters that were subsequently challenged with a lethal dose of ANDV. All constructs were fully protective against signs of illness or death, with the Ad5-G_N or Ad5-G_N and Ad5-G_C in combination almost completely preventing virus replication (186). Unlike the DNA-based vaccine, these constructs only generated very low levels of neutralizing antibodies, and the main mechanism of protection was proposed to be a strong cellular immune response (primarily CD8⁺ cytotoxic lymphocytes), as observed in BALB/c mice (186).

1.6 Rationale: Reverse Genetics Systems

For many years, the study of RNA viruses had been severely limited by the lack of efficient molecular tools required to allow genetic manipulation of the RNA. The development of reverse genetics systems allows for changes to be made to the viral genomic RNA using more easily manipulated and stable cDNA, so that the effects of these changes can be examined on the virus at the phenotypic level (217). This allows for the examination of the requirements for many different aspects of the virus life cycle, such as entry, transcription and replication, virus assembly and budding through additions, deletions, or the creation of chimeric viruses containing coding sequences

from different viruses. The ability to add additional transcriptional units to a virus offers the ability to more easily detect the virus (for example, with the addition of a fluorescent protein) or the use of the virus as a vaccine or gene therapy platform (156, 217).

The first systems were developed for the recovery of positive-strand RNA viruses such as poliovirus, whose genomes, like mRNA, can be directly translated by the host cell machinery (172). Therefore, RNA transcribed from plasmid DNA for these viruses is infectious when introduced into permissive cells and does not require any additional steps (27). The development of systems for negative-strand RNA viruses was much more difficult, as eukaryotic cells do not possess the ability to transcribe RNA from an RNA template. The solution to this problem was found by providing the viral negative-strand RNA genome as an anti-genomic cDNA with an RNA polymerase promoter and terminator that is able to drive the transcription of a full length genomic copy that is in the appropriate viral sense (vRNA). The addition of helper plasmids or virus expressing the RdRp and other viral proteins required to form the RNP complex and encapsidate the genome allows viral transcription and replication to be initiated *in vitro* (27). Early experiments used two main methods to provide the RNP complex proteins. First, cDNA expression plasmids under the control of the T7 bacteriophage RNA (T7) polymerase promoter were transfected into cells that were subsequently infected with recombinant vaccinia virus expressing the T7 polymerase protein (vTF7-3) (48). Second, T7-transcribed vRNA was transfected into cells subsequently infected with homologous helper virus, which provided all of the necessary proteins to form a biologically active complex (217).

However, the recovery of infectious virus from the systems proved to be difficult, leading to the initial production of minigenome systems, where the viral genome was replaced by a detectable reporter gene, such as green fluorescent protein (GFP), chloramphenicol acetyl transferase (CAT) or luciferase (LUC). A diagrammatic illustration of a representative minigenome system is provided in Figure 6. The first minigenome system of a negative-strand virus was produced in 1989, when a synthetic genomic segment containing the influenza virus non-translated regions and a CAT reporter gene was rescued after being complexed with the necessary RNP proteins, and a subsequent helper virus infection (134). Minigenomes are much smaller and less complex than full length genomes, and their use allowed the recognition of a number of different obstacles preventing successful rescue, and the subsequent optimization of these systems. First, in a system where the RNP complex proteins are provided by helper plasmids, the ratio of these plasmids was shown to be critical in order to provide the proper ratio of the proteins necessary for different biological reactions (transcription versus replication) (15, 28). The optimization of this ratio proved to be one of the difficult first steps, but also allowed the determination of which proteins were required to form a functional RNP complex. Another set of problems were identified using the T7 system for rescue. The wild-type T7 promoter adds three terminal G residues to the end of the viral genome; these extra residues can either decrease rescue efficiency, or eliminate rescue completely. The use of a truncated T7 promoter was shown not to add these nucleotides, providing for an appropriate viral 5' end (93). This truncated promoter was quickly combined with the hepatitis delta virus ribozyme sequence at the

opposite end, which uses exact self-cleavage at the 5' end to generate a precise viral 3' end (170). Finally, the use of recombinant vaccinia virus to deliver the T7 polymerase was shown to be associated with virus-induced cytotoxicity. A modified, replication deficient vaccinia virus expressing the T7 polymerase (MVA-T7) was shown to be more useful, as it would still produce the polymerase protein at high levels, but was unable to produce infectious virus, therefore reducing cytotoxicity and resulting in no contamination of any resulting recombinant virus (148, 209, 221). Attempts to eliminate vaccinia virus completely led to the development of expression plasmids under the control of the CMV immediate early (CMV) (46) or the chicken β -actin (CAG) (161) promoters and stable cell lines (173) that have all been used to express the T7 polymerase with varying degrees of success, unfortunately, usually with lower levels of protein expression.

Although the efficiency of the T7 system was greatly increased as a result of these studies, the search began for a better alternative. The first alternative to be described was based on RNA polymerase I (Pol I) (227). A number of advantages were identified; Pol I is expressed in the nucleus of every eukaryotic cell, and therefore does not need to be provided from an external source, it generates transcripts with exact 3' and 5' ends without the addition of any extraneous residues, and it is ideally suited for viruses that replicate in the nucleus, such as influenza virus (217). Potential disadvantages include the fact that most RNA viruses replicate in the cytoplasm, and therefore the plasmids must be transported into the nucleus for transcription to occur. However, this does not appear to be a significant problem, as a number of cytoplasmic-

replicating virus minigenomes have been rescued using the Pol I system (42, 44, 45). Second, there is a host restriction with the RNA polymerase. The development of a rescue system must therefore include the Pol I promoter from the species that matches the cell line in which rescue of the virus will be attempted. The second system to be described was based on RNA polymerase II (Pol II). Like Pol I, Pol II is also located in the nucleus and does not need to be provided from an external source, however, its promoter is not host-specific, and can thus be used in a variety of different cell types. The main disadvantage of Pol II is that it does not have a defined promoter sequence like Pol I, and therefore typically adds additional nucleotides onto the 5' end and a poly-A tail onto the 3' ends of the viral genome that must be spliced by the inclusion of hammerhead and hepatitis delta virus ribozyme sequences (139). Based on these optimization steps, a number of different minigenome systems were soon developed for viruses from many different virus families (42, 44, 45, 69, 123, 130, 153). Minigenomes are still frequently used for viruses that would otherwise require high biosafety containment (BSL3 and BSL4), as they can be typically be used in a regular BSL-2 laboratory. These advances also finally allowed for the development of full-length infectious clone reverse genetic systems and the first rescues of negative-strand RNA viruses completely from cDNA. A diagrammatic illustration of a representative infectious clone system is provided in Figure 7.

The first non-segmented negative strand RNA viruses to be rescued were rabies virus in 1994 (197), followed closely by vesicular stomatitis virus (VSV) and measles virus in 1995 (111, 173, 219). All of these systems were based on the use of the T7

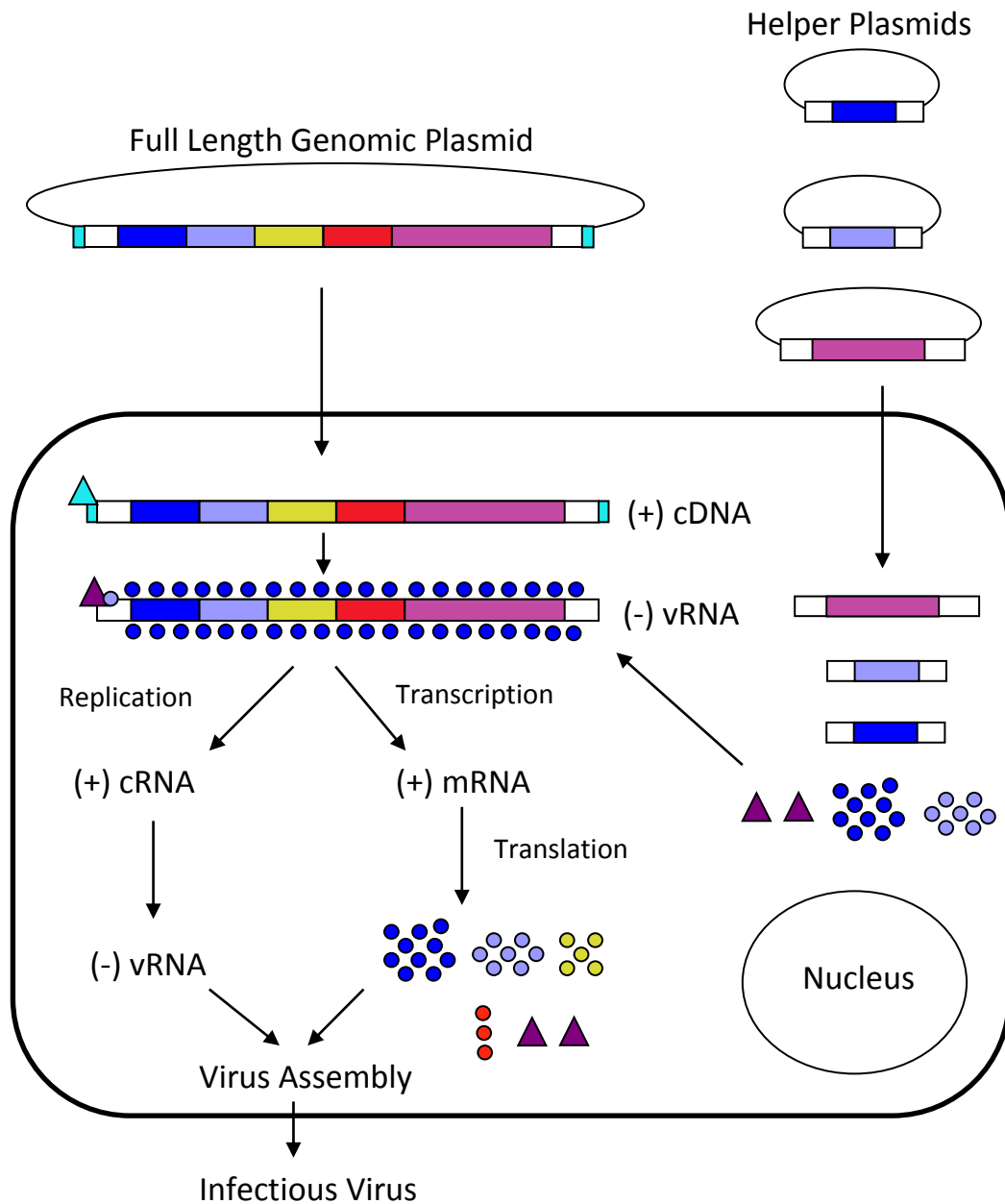


Figure 7. Full-Length Infectious Clone Reverse Genetic System. The full length genomic plasmid contains the viral genome flanked by the untranslated regions in the anti-genomic sense, flanked by promoter and termination sequences for an RNA polymerase. The genomic plasmid is transfected into cells with the helper plasmids that produce the proteins necessary for a functional ribonucleoprotein (RNP) complex. The RNA polymerase produces the viral RNA (vRNA) template that is subsequently encapsidated and then transcribed by the viral RNP complex, producing messenger RNA (mRNA) which is translated to produce the viral proteins. When viral transcription shifts to replication, full length anti-genome (cRNA) is produced, and is used as a template for new vRNA. This combines with the necessary proteins to form infectious virus.

polymerase provided by recombinant vaccinia virus. The first segmented negative-strand RNA viruses to be rescued were Bunyamwera virus in 1996 (15) and influenza A virus in 1999 (155). These systems were based on the T7 and Pol I polymerases, respectively. An improved rescue system for influenza virus, which used an ambisense coding strategy with both Pol I and Pol II promoters and decreased the number of required plasmids from 12 to 8 was described in 2000 (76). Since these early systems were described, a number of other full length infectious clone systems have been developed (41, 194, 215, 223). Although the number of available systems has increased substantially in recent years, a successful infectious clone system for a hantavirus has yet to be developed.

1.7 Rationale: Use of Recombinant VSV as a Vaccine Platform

VSV is a non-segmented, negative-sense single-stranded RNA virus belonging to the family *Rhabdoviridae*, genus *Vesiculovirus* (135). The use of this platform started with the development of the reverse genetics system in 1995 (111). The reverse genetic system has been shown to be very robust, with the ability to tolerate the addition of extra transcriptional units for the expression of foreign genes (67, 106, 195). The deletion of the VSV glycoprotein (G) from the recombinant genome (VSV Δ G) not only removes a key virulence determinant (140), but also allows for the insertion of a foreign, type I transmembrane glycoprotein that will be expressed on the surface of the rescued virions (182). Its use as a vaccine platform has been evaluated for a number of different viruses, including Lassa, Ebola, Marburg, West Nile, Influenza and Hepatitis B viruses with

great success (26, 51, 84, 87, 183, 199). VSV vaccines have been shown to strongly induce both cellular and humoral immunity in different animal models (87, 135). The efficacy of the VSV platform as a post-exposure treatment has been examined with VSV containing a filovirus glycoprotein in the NHP model with great success, depending on the time of administration (38, 58, 60). One of the main problems with the use of recombinant virus as a vaccine platform is that the target population may already contain antibodies against the virus vector. This is one of the main reasons that vaccines based on platforms such as human Ad5 and vaccinia virus have not been successful (188). Fortunately, the seroprevalence against VSV remains very low world-wide (135), with any neutralizing antibodies being directed against the VSV G. The removal and replacement of the VSV G from the virus backbone means that most individuals should not have a neutralizing response against the vector, and also suggests that the vector can be reused in the same population for protection against different diseases (182). Although non-replicating VSV pseudotyped with either HTNV, Seoul virus or ANDV glycoproteins have been described in the literature (114, 163, 179), a replication competent VSV expressing a hantavirus glycoprotein from its genome has never been attempted or tested as a potential vaccine candidate.

1.8 Hypothesis and Objectives

I have chosen ANDV as my model hantavirus, as it remains the only hantavirus with a lethal animal model in the Syrian hamster, allowing *in vivo* characterization of any results found *in vitro* (81). It also has a number of unique features, including its high

level of virulence and potential ability for human-to-human transmission (36, 141). Each year, it continues to be a large public health concern in areas of Argentina and Chile (142).

One of the major problems with the study of hantaviruses is the lack of a full-length reverse genetics system. The development of such a system would have many advantages. The development of chimeric hantaviruses containing sequences from non-pathogenic hantaviruses or a mixture of Old and New World hantavirus sequences might help understand the key mechanisms of viral pathogenesis. It might also allow an understanding of why ANDV, but not SNV or any other hantavirus, is so lethal in the Syrian hamster model (145, 216). Finally, a number of recent vaccine developments have been based on the manipulation of the virus genome to generate attenuated viruses that are no longer pathogenic (11, 12, 14, 68, 143). The development of a hantavirus vaccine using a reverse genetics system should be possible, and I hypothesize that the development of such a vaccine through the substitution of sequences from non-pathogenic hantaviruses with the ANDV genome would have the greatest potential for success.

Although a number of other different vaccine platforms have been tested as potential candidates against hantavirus infection, there remains no approved vaccine available for either Old or New World hantaviruses (138, 188). Both the N protein, as well as the G_N and G_C glycoproteins have been used as potential immunogens using recombinant virus and DNA platforms; however, the best protection appears to come from the expression of G_N and G_C together (79, 186). The exact immune mechanisms

required for protection remain unclear, and poorly characterized. The recombinant replication-competent VSV reverse genetic system has been used with great success as a vaccine candidate with a number of different viruses, and has a number of unique advantages when compared to other recombinant viral systems. I hypothesize that the expression of both ANDV glycoproteins by the recombinant VSV platform will be sufficient to protect hamsters from lethal disease. The requirements to test these hypotheses can be broken down into 7 main objectives.

1. Develop expression plasmid constructs for the ANDV proteins based on different promoter regions and characterize their expression *in vitro*.
2. Develop a minigenome expression plasmid based on different promoter regions and different reporter genes and successfully detect reporter signal *in vitro* using a series of optimization steps.
3. Develop a full length infectious clone system using the optimizations obtained in the development of the minigenome and successfully characterize and recover infectious virus *in vitro*.
4. Modify the pVSVXN2 Δ G expression plasmid to incorporate the ANDV GPC into the 4th transcriptional position of the virus genome, successfully recover infectious virus, and characterize *in vitro*.
5. Test the efficacy of protection of the vaccines from lethal disease *in vivo*.
6. Test the minimum requirements for the time between immunization and challenge, as well as post-exposure efficacy *in vivo*.

7. Characterize the immune response to determine the mechanism of protection at the different time points tested.

2.0 Materials and Methods

2.1 Cells and Viruses

HEK 293T (human embryonic kidney) cells were cultured in Dulbecco's Modified Eagle's Medium (DMEM, Sigma®) with 10% heat-inactivated fetal bovine serum (FBS, Wisent), 1% L-glutamine (L-glut, Gibco®) and 1% Penicillin/Streptomycin (P/S, Gibco®). Tissue culture dishes were coated with poly-D-lysine (1mg/ml, Sigma®) for at least 30 minutes (min) at 37°C to enhance attachment of cells. Dishes were subsequently washed with phosphate-buffered saline (PBS) prior to seeding of cells.

VeroE6 and COS-7 (both derived from African green monkey kidney) cells were cultured in DMEM supplemented with 10% FBS, 1% L-glut and 1% P/S.

All cells were incubated in 5% CO₂ and H₂O-saturated atmosphere conditions at 37°C in either 75 cm² (T75) or 150 cm² (T150) cell culture flasks. Cells were passaged by treatment with trypsin (0.25% Trypsin-EDTA (ethylenediamine tetraacetic acid), Gibco®) and diluted in culture medium every three to five days.

Escherichia coli (*E.coli*) Top 10 chemically competent cells (Invitrogen™) were made by growing 0.5ml of an overnight culture in 50ml (1:100 dilution) of Luria-Bertani (LB) broth at 37°C with shaking until the optical density (OD) at 660nm wavelength was within 0.5-0.8. Cells were incubated on ice for 20 min, pelleted by centrifugation at 2500 rpm at 4°C for 10 min and then re-suspended in 5 ml of TSS buffer (Appendix 1). Cells were then divided into 100µl aliquots and stored at -80°C.

ANDV, strain Chile 9717869 was kindly provided by Dr. C. Schmaljohn, U.S Army Medical Research Institute of Infectious Diseases (USAMRIID), Ft. Detrick, MD, USA. Virus stocks were prepared by infecting a 70% sub-confluent monolayer of VeroE6 cells in a T150 flask with a 1:100 dilution of previous ANDV stock in DMEM containing 2% FBS and 1% L-glut. After 10 days, supernatant from the flask was divided among three T150 flasks and the volume was topped up to 40ml. After another 10 days, the supernatants were collected and clarified by centrifugation at 500 x g for 10 min to remove any residual cell debris. Virus stocks were then divided into aliquots and kept at -80°C. ANDV titres of the stock were determined to be 2×10^5 focus-forming units (FFU)/ml in VeroE6 cells using a focus forming assay (Section 2.15.2). All infectious *in vitro* work with ANDV was performed in a biosafety level 3 (BSL-3) laboratory at the National Microbiology Laboratory (NML), Public Health Agency of Canada (PHAC) or the Integrated Research Facility (IRF) of the Rocky Mountain Laboratories (RML), Division of Intramural Research (DIR), National Institute of Allergy and Infectious Diseases (NIAID), National Institutes of Health (NIH).

2.2 Antibodies and Primers

See Appendix 2 for a list of primary and secondary antibodies used. Most antibodies used were obtained commercially.

See Appendix 3 for a list of primers used. Primers designed against ANDV were based on sequences from Genbank, Ascension Numbers: NC_003468.2 (L Segment), NC_003467.2 (M Segment) and NC_003466.1 (S Segment).

2.3 Molecular Biology Techniques

2.3.1 RNA Extractions

Viral RNA extractions of ANDV stocks were carried out to generate template for RT-PCR reactions (Section 2.3.3). Viral stocks, described in Section 2.1, were treated with TRIzol LS® (GibcoBRL). Briefly, the viral RNA was isolated from supernatants of infected cells in the following manner: 1) Addition and homogenization of infected supernatant with TRIzol LS®; 2) Phase separation of RNA, DNA and proteins with the addition of 350µl of chloroform to 1 ml of RNA/TRIzol homogenate. Centrifugation at 12000 rpm for 20 min allows clear development of the 3 phases. RNA is found in the aqueous phase, DNA is found in the interphase and the phenol phase, and protein is found in the phenol phase; 3) Collect the aqueous phase and precipitate the RNA through the addition of 500µl of isopropanol, and the addition of 1-2µl of glycogen to act as a carrier molecule to increase RNA precipitation from supernatants; 4) Pellet RNA by spinning at 12,000 rpm for 20 min, followed by RNA wash with 70% ethanol at 7,500 rpm for 5 minutes and 5) Redissolving the RNA in DNase/RNase free water after air-drying RNA pellet in a biosafety cabinet. Samples were aliquoted and stored at -80°C. All centrifugation steps were carried out at 4°C.

Viral and cellular RNA extractions from tissue samples were carried out to generate template for quantitative real-time RT-PCR (qRT-PCR) reactions (Section 2.3.5). Typically, a 100mg piece of lung, liver or spleen tissue was placed into individual tubes containing 1ml of RNAlater™ buffer (Qiagen) and stored overnight at 4°C, after which they were mechanically homogenized in 600µl of RLT lysis buffer

(Qiagen), clarified by low-speed centrifugation, and then diluted to 30mg equivalents with RLT buffer. For blood or cell culture supernatant, 140 μ l was mixed with 560 μ l lysis buffer AVL (Qiagen). Samples were extracted for RNA using the RNeasy® Mini kit (solid tissue) or QIAamp® Viral RNA Mini kit (blood) extraction kits (Qiagen). All RNA samples were quantified using Nanodrop™ 8000 spectrophotometer (Thermo Scientific), and diluted to 40ng/ μ l using DNase/RNase free water.

2.3.2 Polymerase Chain Reaction (PCR)

PCR was used to amplify or modify sections of genes from plasmid DNA. PCR reactions described in this manuscript were performed using one of two kits. Initially, the PfuTurbo® DNA polymerase kit (Stratagene) was used to construct the minigenome and expression plasmids (Sections 2.5 to 2.8). Subsequent PCR reactions were carried out using the iProof™ High Fidelity DNA polymerase kit (Bio-Rad). The PfuTurbo DNA polymerase was initially chosen as it was shown to have high PCR product yields and a high-fidelity with proofreading activity resulting in lower error rates. When the iProof™ High-Fidelity kit became available, it was shown to have an even greater fidelity and proofreading ability, the ability to produce longer, error-free fragments with a high yield, and a speed that reduced most reaction times by at least 75%. In general, a typical PfuTurbo™ 50 μ l PCR reaction consisted of 5 μ l of 10x PfuTurbo™ reaction buffer, 2.0 μ l of deoxynucleotide triphosphate (dNTP) solution (10mM each) (Invitrogen™), 3.0 μ l of 10 μ M forward primer, 3.0 μ l of 10 μ M reverse primer, 100ng of DNA plasmid, 1 μ l of PfuTurbo™ DNA polymerase and a volume of sterile water to

Materials and Methods

bring the final volume up to 50 μ l. A typical iProofTM 50 μ l PCR reaction consisted of 10 μ l of 5x iProofTM GC reaction buffer, 1 μ l of 10mM (each nucleotide) dNTP solution, 1 μ l of 10 μ M forward primer, 1 μ l of 10 μ M reverse primer, 1 μ l of 50mM MgCl₂, 1 μ l of 100% DMSO, 10ng of DNA plasmid, 0.5 μ l of iProofTM DNA polymerase and the remaining volume with sterile water. All reactions were set up on ice. All PCR reactions were carried out in a Biometra® thermocycler (Montreal Biotech Inc). See Appendix 3 for a list of primers used for PCR. General cycling conditions are outlined in Tables 1 and 2.

Table 1. General Cycling Conditions for PfuTurboTM Polymerase PCR

Cycle	Temperature	Length	# of Cycles
Initial Denaturation & Polymerase Activation	95°C	5 min	1x
Denaturation	95°C	30 sec	40x
Annealing	50-55°C	30 sec	
Extension	72°C	1 min/kb	
Final Elongation	72°C	7 min	1x
Final Cooling	4C	hold	1x

Table 2. General Cycling Conditions for iProofTM Polymerase PCR

Cycle	Temperature	Length	# of Cycles
Initial Denaturation & Polymerase Activation	98°C	30 sec	1x
Denaturation	98°C	10 sec	25x
Annealing	68-72°C	30 sec	
Extension	72°C	15 sec/kb	
Final Elongation	72°C	10 min	1x
Final Cooling	4C	hold	1x

2.3.3 Reverse Transcription-Polymerase Chain Reaction (RT-PCR)

RT-PCR was used to amplify viral genes from vRNA. RT-PCR reactions were done using one of two kits. The RobusT™ One-Step RT-PCR kit (Finnzymes) was used to generate the initial minigenome and expression plasmids (Sections 2.5 to 2.8). Subsequent reactions were carried out using a two-step RT-PCR procedure involving the Superscript® III reverse transcriptase (Invitrogen™) for reverse transcription, followed by the iProof™ High-Fidelity DNA polymerase kit described in Section 2.3.2 for the PCR step due to the high fidelity and reduced reactions times described in that section. A 50µl RobusT™ RT-PCR reaction was prepared as follows: 5µl of 10x reaction buffer, 1µl of 10mM (each nucleotide) dNTP solution, 1µl of 20µM forward primer, 1µl of 20µM reverse primer, 1.5µl of 50mM MgCl₂, 1µl of Avian Myeloblastosis Virus (AMV) reverse transcriptase, 2µl of DyNAzyme™ EXT DNA polymerase, a varying amount of RNA, and a volume of sterile water to bring the final volume up to 50µl. A 20µl Superscript® III RT reaction was prepared as follows: 1µl of 10µM forward primer, 1µl of 10µM reverse primer, 1µl of dNTP solution, 2µl of RNA and 8µl of sterile water. This mixture was incubated at 65°C for 5 min, followed by incubation on ice for 5 min. Subsequently, 4µl of 5x reaction buffer, 1µl of 0.1M dithiothreitol (DTT), 1µl of RNaseOUT™ recombinant ribonuclease inhibitor and 1µl Superscript III RT were added to a final volume of 20µl. This was incubated at 55°C for 60 min then the RT was inactivated at 70°C for 15 min. 1µl of RnaseH was added and incubated at 37°C for an additional 20 min. Finally, 2µl of RT reaction was added to the iProof™ PCR reaction described in Section 2.3.2. All reactions were set up on ice. All

Materials and Methods

RT-PCR reactions were carried out in a Biometra® thermocycler. See Appendix 3 for a list of primers which were used for RT-PCR. A general outline of cycling and incubation conditions is presented in Tables 3 and 4.

Table 3. General Cycling Conditions for RobusT™ RT-PCR

Cycle	Temperature	Length	# of Cycles
Reverse Transcription	60°C	60 min	1x
Initial Denaturation & Polymerase Activation	94°C	2 min	1x
Denaturation	94°C	30 sec	40x
Annealing	60°C	30 sec	
Extension	72°C	2 min/kb	
Final Elongation	72°C	15 min	1x
Final Cooling	4C	hold	1x

Table 4. General Incubation Conditions for Superscript® III RT-PCR

Components Added	Temperature	Length
10µM Forward Primer	65°C 4°C	5 min
10µM Reverse Primer		
RNA		5 min
dNTPs		
H ₂ O		
First-Strand Buffer	55°C	60 min
0.1M DTT	70°C	15 min
RNaseOUT		
Superscript III		
RNaseH	37°C	20 min

2.3.4 Amplicon Analysis

All PCR amplicons were verified for size and quality by separating a sample of the DNA on an agarose gel using gel electrophoresis and visualization by UV

illumination. A typical 50ml agarose gel was made with 400mg (0.8%) of agarose (Invitrogen™), 2µl of a 1% ethidium bromide solution (Fisher Scientific) used to stain DNA, and 50ml of 1x Tris acetate EDTA (TAE) buffer. 2µl of the reaction volume was mixed with the 6x Gel loading buffer (Appendix 1) and loaded into the gel. The 1 Kb Plus DNA molecular weight ladder (Invitrogen™) was also included with each run to verify the size of the amplicon (Appendix 4). Gels were placed in an electrophoresis tank containing the 1x TAE buffer at 100 volts (V) for approximately 45 minutes. DNA was visualized with a Hoefer™ MacroVue™ UV-25 transilluminator.

2.3.5 Quantitative Real-Time RT-PCR (qRT-PCR)

qRT-PCR was used to detect and quantify the amount of viral and cellular RNA present in tissue samples. RNA was extracted as described in Section 2.3.1. qRT-PCR primers and probes (Appendix 3) were designed using either Primer Express® Software v3.0 (Applied Biosystems) or directly designed and synthesized by TIB MOLBIOL based on sequence information of target transcripts. All experimental gene probes were labeled with 5' 6-Carboxyfluorescein (6-FAM) dye and quenched by BlackBerry Quencher (BBQ). All internal control gene probes were labeled with Yakima Yellow (YAK) and quenched by BBQ. qRT-PCR reactions were generated using one of two different kits. The QuantiTect® Probe RT-PCR kit was used for detection of ANDV RNA. The Rotor-Gene® Probe RT-PCR kit was used for detection of hamster cytokine mRNA transcripts. All experiments were carried out on the Rotor-Gene® 6000 thermocycler (Corbett Life Science). A general outline of cycling conditions is

Materials and Methods

presented in Tables 5 and 6. Data acquisition occurred at the end of each annealing/extension step in the green (510nm) and yellow (555nm) channels. Samples containing ANDV RNA were quantified against a standard curve of 10-fold serially diluted ANDV RNA extracted from ANDV stocks with a known titre. Hamster cytokine RNA samples were quantified using the $\Delta\Delta CT$ method (129, 226). Briefly, the cycle threshold (C_T) of each gene in a treated hamster was normalized to the C_T of internal reference gene RPL18 included in each reaction (ΔCT). This was then compared to the same normalized gene in an untreated control hamster ($\Delta\Delta CT$). The final value is expressed as fold change as calculated by $2^{-\Delta\Delta CT}$. A value above 1 fold indicates an increase relative to controls, whereas a value below 1 fold indicates a decrease.

Table 5. General Cycling Conditions for QuantiTect® qRT-PCR

Cycle	Temperature	Length	# of Cycles
Reverse Transcription	50°C	30 min	1x
Initial Denaturation & Polymerase Activation	95°C	15 min	1x
Denaturation	94°C	15 sec	40x
Annealing/Extension	60°C	1 min	

Table 6. General Cycling Conditions for Rotor-Gene® qRT-PCR

Cycle	Temperature	Length	# of Cycles
Reverse Transcription	50°C	10 min	1x
Initial Denaturation & Polymerase Activation	95°C	5 min	1x
Denaturation	95°C	5 sec	40x
Annealing/Extension	60°C	10 sec	

2.4 Molecular Cloning Techniques

Sequence specific primers (Appendix 3) were used to generate inserts by PCR or RT-PCR (Section 2.3). Amplicon size was verified by 0.8% agarose gel electrophoresis (Section 2.3.4). All amplicons were purified using a QIAquick® PCR purification kit (Qiagen), and eluted in 30µl of sterile water.

2.4.1 DNA Digestion

Amplified PCR or RT-PCR products were digested in parallel with the required sub-cloning or expression vector constructs and the necessary regular restriction enzymes (New England Biolabs, NEB) or FastDigest® restriction enzymes (Fermentas). A typical 30µl digestion was prepared: 3µl of restriction enzyme buffer, 2.0µg of vector DNA / 15µl PCR product DNA, 1-1.5µl of restriction enzyme 1 (typically 10-15 enzyme units), 1-1.5µl of restriction enzyme 2, 3µl of bovine serum albumin, and the remaining volume with sterile water to 30µl. Digestions were incubated at the required temperature (usually 37°C, except for BsmBI restriction enzyme incubated at 55°C) for 2–3 hrs for NEB enzymes or approximately 30 min to 1 hr at 37°C for FastDigest® enzymes. Restriction enzyme digests using enzymes with incompatible buffers or incubation temperatures were performed sequentially with the single enzymes and a purification step between each digest, or using the FastDigest® products, which use a single buffer and temperature for all enzymes. Digested PCR products and linearized DNA vectors were purified using the QIAquick® PCR purification kit. Digestions removing an insert

from a DNA vector for further cloning were separated on a 0.8% agarose gel and extracted using the QIAquick® gel extraction kit (Qiagen).

2.4.2 DNA Ligation

Following DNA digestion and purification of the vector and insert, 2µl from each was loaded onto a 0.8% agarose gel, separated by gel electrophoresis, and visualized by UV illumination to estimate the quality and quantity of digested DNA present. The insert and vector were ligated using T4 DNA ligase (5 units/µl, Invitrogen™). A typical 20µl DNA ligation reaction consisted of 2µl of 10x ligation buffer, 1-2µl of digested vector DNA, 5-15µl of digested insert DNA, 1.0µl of T4 DNA ligase and water to a final volume of 20µl. Ligation reactions were incubated at 14°C overnight.

2.4.3 DNA Plasmid Transformation

E.coli Top 10 chemically competent cells were transformed by first thawing cells on ice. Next, 5-10µl of the ligation reaction was added to 50µl of cells, followed by a 30 min incubation on ice. Cells were then heat shocked at 42°C for 45 sec and 200µl of SOC medium (Appendix 1) was added. Cells were then incubated at 37°C with horizontal shaking for 45 min. The bacterial culture was then plated on LB + Ampicillin (100 µg/ml) or LB + Kanamycin (35 µg/ml) plates, depending on the resistance marker used in the vector and incubated overnight at 37°C.

2.4.4 Screening and Verification of the Constructs by Restriction Digest

Selected bacterial colonies were cultured in 1.5ml of LB broth + appropriate antibiotic overnight at 37°C with shaking, as well as streaked onto a master plate that was also incubated at 37°C overnight. Plasmid DNA was subsequently extracted using the QIAprep® Spin Miniprep Kit (Qiagen) if DNA was to be sequenced, or by a “crude” miniprep method if screening colonies for positive clones, in order to lower overall cost. Briefly, the crude method used the same resuspension, lysis and neutralization buffer recipes (Appendix 1) contained in the Qiagen kit, but used the addition of 100% isopropanol to precipitate the plasmid DNA instead of the spin columns, followed by two washes with 70% ethanol. Extracted plasmid DNA was digested with specific restriction enzymes (NEB or Fermentas) in order to verify the presence of the correct insert. A typical 15µl digestion was prepared: 1.5µl of restriction enzyme buffer, 2µl plasmid DNA, 0.5µl of restriction enzyme 1, 0.5µl of restriction enzyme 2, 1.5µl of bovine serum albumin, and the remaining volume with sterile water to 15µl. Digestions were incubated at the required temperature for 1 hour. Positive colonies were then sequenced, using the dideoxy technique and ABI Prism® 3100 Genetic Analyzer (Applied Biosystems™), in order to ensure the presence and verify the correct sequence of the insert. Sequencing was carried out by an in-house DNA core facility.

2.5 Cloning Strategy – Creation of ANDV N Expression Constructs

In order to express recombinant ANDV N protein, the N amplicon was RT-PCR amplified (Section 2.3.3) from ANDV RNA derived from strain 9717869 (Section 2.1) and cloned (Section 2.4) directly into the pCAGGS mammalian expression vector using restriction enzyme sites EcoRI and XhoI. This is in contrast to the other constructs which were cloned initially into the pATXMCS3 or pATXMCS4 sub-cloning vectors (shown in Figure 8). A Kozak consensus sequence (CACC), which plays a major role in the initiation of the translation process, was placed immediately upstream of the ATG start site in each primer sequence, and an additional stop codon was added after the stop codon at the end of the ORF to ensure efficient termination of translation (Appendix 3). The N ORF was subsequently cloned into two other mammalian expression vectors; pTM1 (using the same EcoRI/XhoI restriction enzyme sites), and gWIZ (using SalI/NotI enzyme sites). These expression vectors are illustrated in Figure 9A. pCAGGS contains the CAG promoter, gWIZ contains the CMV promoter, and pTM1 contains the T7 promoter. These constructs were referred to as ANDV-N/pCAG, ANDV-N/gWIZ and ANDV-N/pTM1 respectively.

2.6 Cloning Strategy – Creation of ANDV Glycoprotein Expression Constructs

In order to express the recombinant ANDV glycoproteins, the ANDV GPC amplicon was generated by RT-PCR amplification (Section 2.3.3) from ANDV RNA derived from strain 9717869 (Section 2.1) and cloned (Section 2.4) into sub-cloning vector pATXMCS4 (Figure 8) using restriction enzyme sites KpnI and NheI. Similar to

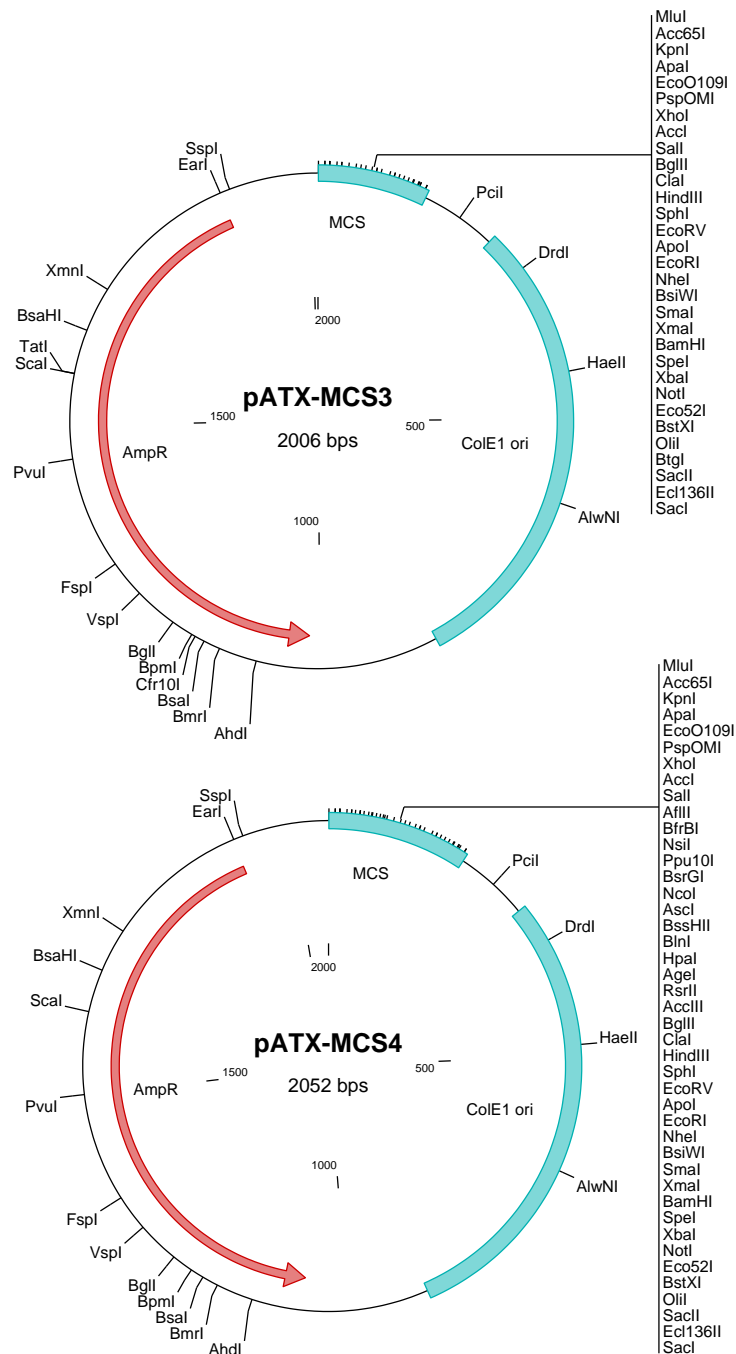


Figure 8. Sub-cloning Vectors. The pATXMCS3 and pATXMCS4 plasmids were used during the construction of all of the ANDV protein expression plasmids except N, as well as the construction of the different minigenome constructs. Both of these vectors contain an ampicillin resistance gene (AmpR) and an origin of replication (ColE1 ori), but no mammalian expression promoter. They both contain multiple cloning sites (MCS) with a large number of unique restriction enzyme sites.

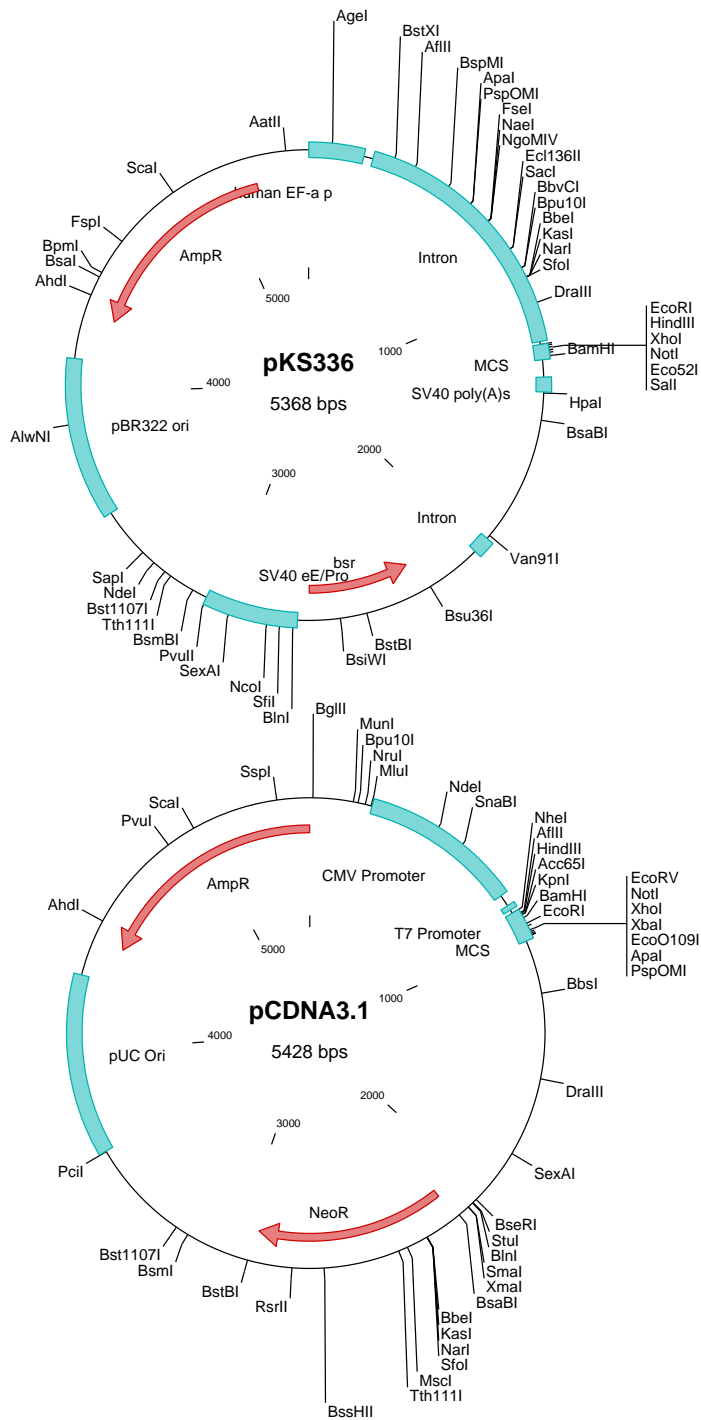
B

Figure 9. Expression Vectors. (A) The ANDV N construct was expressed from the pCAGGS, gWIZ and pTM1 expression vectors. The ANDV GPC, G_N and G_C constructs were expressed from pCAGGS. (B) The ANDV L constructs were expressed from the 3 constructs shown in A, as well as the 2 constructs shown in B.

the previous section, a Kozak consensus sequence (CACC) and additional stop codon were added to the cloning primers (Appendix 3). The resulting plasmid was referred to as ANDV-GPC/pATX4. The entire GPC ORF was subsequently excised from this vector by restriction enzyme digestion, and inserted into pCAGGS (Figure 9A) using the KpnI and NheI restriction enzyme sites. This construct was referred to as ANDV-GPC/pCAG.

Next, individual ANDV Gn and Gc expression plasmids were constructed by PCR (Section 2.3.2) amplification of regions of the ANDV-GPC/pCAG expression plasmid. Two stop codons were added to the downstream Gn primer, corresponding to position 1952 of the GPC ORF, to terminate expression immediately prior to the WASSA cleavage site. A start codon and Kozak sequence were added to the upstream Gc primer, corresponding to position 1902 of the GPC ORF, 50 nucleotides upstream of the cleavage site to allow correct processing of the N terminus of the Gc protein. Primers generated for creating the GPC ORF expression plasmid were used as the upstream Gn and downstream Gc primers (Appendix 3). The ANDV Gn and Gc amplicons were inserted into pCAGGS using the same restriction enzyme sites as full length GPC and were referred to as ANDV-Gn/pCAG and ANDV-Gc/pCAG.

2.7 Cloning Strategy – Creation of ANDV L Expression Constructs

In order to express the recombinant ANDV L protein, the L ORF was divided into 4 different segments based on the location of unique internal restriction digest sites to avoid the addition of any extraneous DNA sequence. Segment 1 used restriction

enzyme sites KpnI/SalI, segment 2 used NcoI/SphI, segment 3 used SphI/BsiWI and segment 4 used BsiWI/NotI. These amplicons were then generated by 4 separate RT-PCR reactions (Section 2.3.3) from ANDV RNA derived from strain 9717869 (Section 2.1) and cloned sequentially (Section 2.4) into sub-cloning vector pATXMCS3 (Figure 8). Similar to the previous section, a Kozak consensus sequence (CACC) and an additional stop codon were added to the cloning primers (Appendix 3). The construct was referred to as ANDV-L/pATX3. The fully assembled L ORF was then excised using restriction enzyme digest and cloned into mammalian expression vectors pCAGGS (using KpnI/NheI enzyme sites), pTM1 (using EcoRI/XhoI enzyme sites), and gWIZ (using SalI/NotI enzyme sites), as described in section 2.5. Two additional vectors were also used, including pKS336, containing a human elongation factor 1 α (HEF-1 α) promoter, and pCDNA3.1+, containing both CMV and T7 promoters (cloned into both using EcoRI/XhoI restriction enzyme sites). These expression vectors are illustrated in Figures 9A and 9B. These constructs were referred to as ANDV-L/pCAG, ANDV-L/gWIZ, ANDV-L/pTM1, ANDV-L/pKS336 and ANDV-L/pCDNA3.1 respectively.

The L protein does not have any commercially available antibodies available for detection of protein expression, so expression constructs containing a tag at either the N or C terminus of the L protein were created. Nucleotide sequences coding for the FLAG (amino acid sequence DYKDDDDK) or HA (amino acid sequence YPYDVPDYA) tags were added to the forward primer immediately downstream of the ATG start codon, or to the reverse primer immediately upstream of the stop codon. Primers from an internal

restriction site were used as the other forward/reverse primer (Appendix 3). This amplicon was then cloned into the ANDV-L/pATX3 vector after excision of the segment that it was replacing by restriction digestion. The HA and FLAG tagged L ORFs were subsequently cloned into the mammalian expression vectors as described above.

2.8 Cloning Strategy – Creation of Minigenome Constructs

In order to create the minigenome expression constructs, primers were designed to amplify the 3' (52 nucleotides) and 5' (203 nucleotides) non-coding regions (NCRs) of the ANDV M segment. Due to the relatively small size of these regions, internal primers were chosen in the coding region that generated amplicons of at least 1kb in length in order to facilitate the cloning process (Appendix 3) These amplicons were generated by RT-PCR (Section 2.3.3) from ANDV RNA derived from strain 9717869 (Section 2.1) and cloned (Section 2.4) into the sub-cloning vector pATXMCS3 (Figure 8). Next, primers were generated that removed the coding regions by PCR (Section 2.3.2), leaving the NCRs connected by a linker sequence containing 2 BbsI restriction enzyme recognition sites immediately downstream and upstream of the 3' and 5' sequences. The vector was re-ligated using an EcoRI restriction enzyme site located in the linker sequence. Three different reporter systems were chosen for the minigenome constructs; GFP, CAT and LUC. These genes were amplified by PCR from control mammalian expression plasmids and used to replace the linker sequence of the minigenome cassette using BbsI restriction enzyme digest of both the vector and the

amplicons. Minigenome cassettes containing the GFP, CAT and LUC genes were created and were referred to as ANDVM-GFP/pATX3, ANDVM-CAT/pATX3, and ANDVM-LUC/pATX3, respectively. Finally, primers were created to amplify the entire cassette by PCR and add BsmBI restriction enzyme sites to the 3' and 5' ends. These cassettes were cloned using the BsmBI restriction enzyme sites into the mammalian expression vectors under the control of the Pol I, Pol II or T7 promoters in the anti-sense (vRNA) orientation. The resulting plasmids were referred to as ANDVM-(Reporter Gene)/pRF240, ANDVM-(Reporter Gene)/pPol-II, and ANDVM-(Reporter Gene)/pT7. BsmBI and BbsI restriction enzymes were chosen for the cloning strategy because they are both type IIS restriction enzymes that cleave outside of their recognition site to one side. By choosing the appropriate primer sequences, it was possible to ligate the NCRs, reporter genes and mammalian expression vectors without the addition of extraneous DNA sequences, albeit with the destruction of the restriction enzyme site, preventing easy modification to the final constructs. Due to the addition of additional nucleotides to the transcripts produced from the Pol II and T7 polymerases, both the pT7 and pPol-II plasmids contain an HDV ribozyme sequence. The pPol-II plasmid also contains a hantavirus-specific hammerhead ribozyme sequence in order to ensure the appropriate vRNA ends. An outline of the entire cloning strategy is shown in Figures 10 and 11.

2.9 Cloning Strategy – Creation of Recombinant VSV Constructs

The recombinant VSV constructs were generated using vector pVSVXN2, kindly provided by Dr. J Rose, Yale University, New Haven, CT, USA. This plasmid

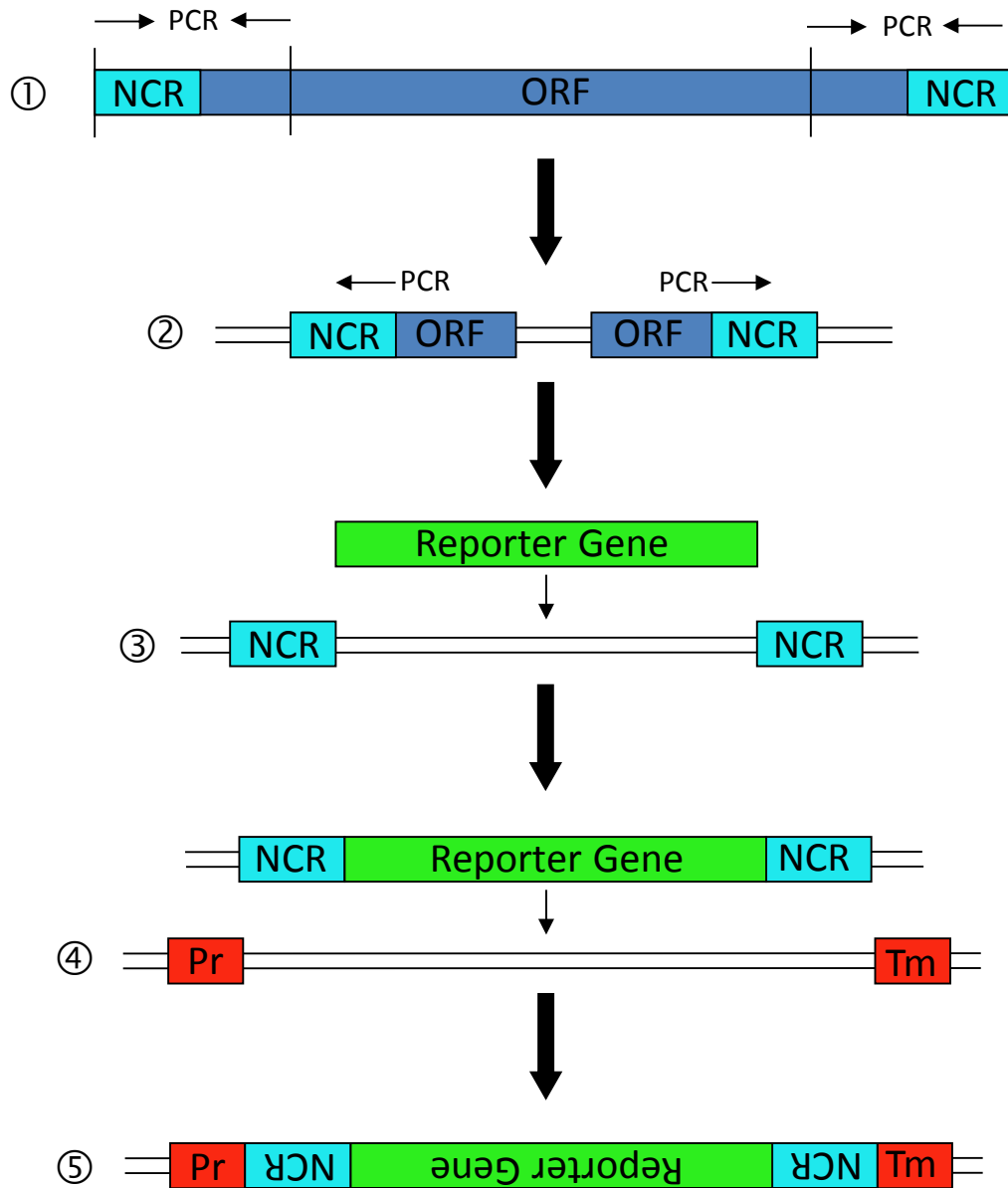


Figure 10. Cloning Strategy - Minigenome. (1) The ANDV non-coding regions (NCRs) were amplified by polymerase chain reaction (PCR) including portions of the open reading frame (ORF) due to short NCR length. Resulting amplicons were cloned into vector pATXMCS3. (2) Portions of the ORF were removed by PCR amplification around the vector which was subsequently re-ligated. (3) Reporter gene was cloned in between the NCRs using BbsI restriction enzyme digestion. (4) Minigenome cassette was cloned in the anti-genomic sense into vector containing RNA polymerase promoter (Pr) and termination (Tm) sites using BsmBI restriction enzyme digestion.

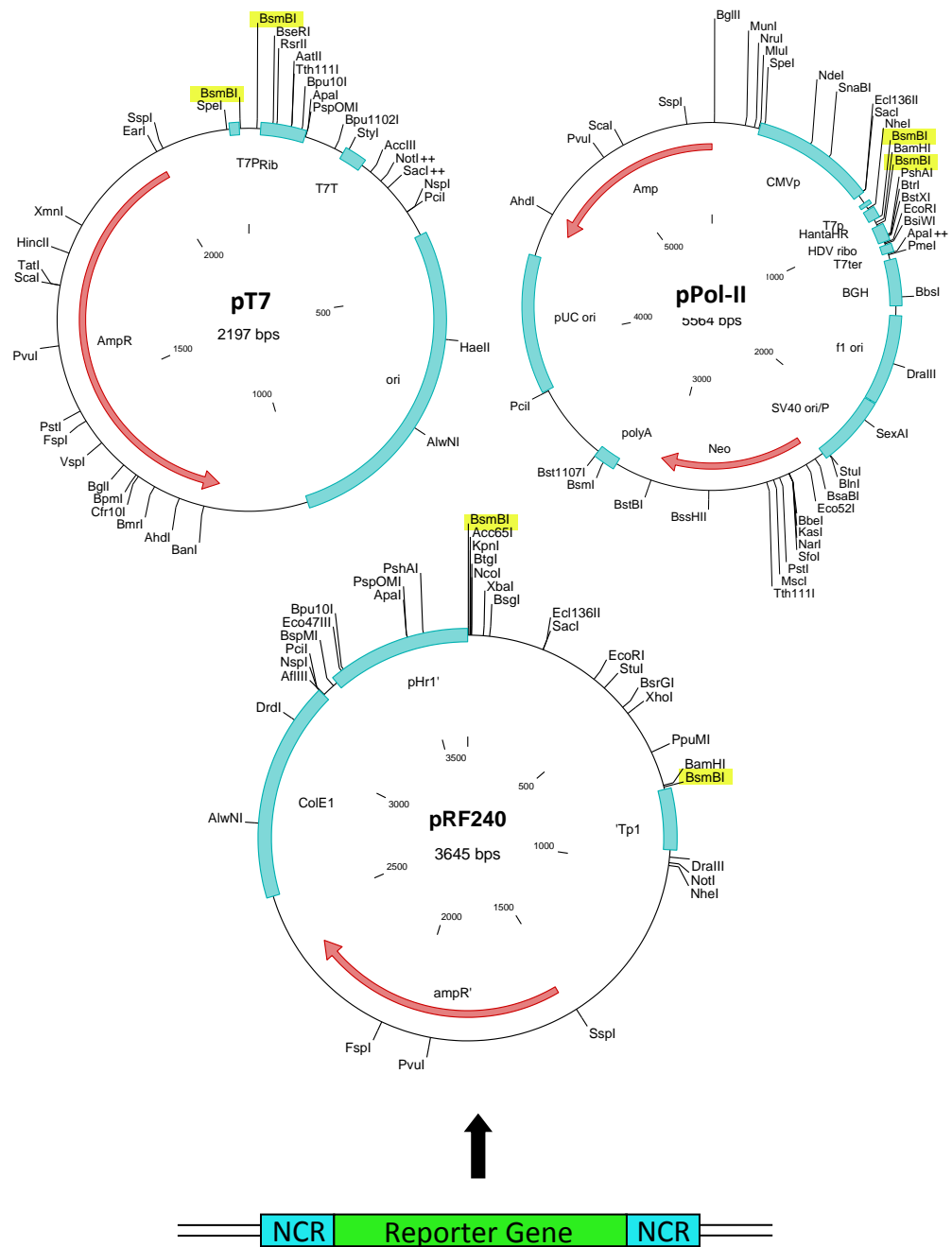


Figure 11. Cloning Strategy – Minigenome Insertion. The minigenome cassette containing the reporter gene flanked by the non-coding regions (NCRs) was cloned in the negative sense viral RNA (vRNA) orientation into 3 different plasmids containing different RNA polymerase promoter and termination sites using the BsmBI enzyme restriction sites, highlighted in yellow.

contains the positive-strand RNA complement of the VSV genome with an additional transcriptional site added (using the XhoI and NheI restriction enzyme sites) between the glycoprotein and polymerase genes as previously described (195). The plasmid contains the five VSV genes (nucleoprotein N, phosphoprotein P, matrix protein M, glycoprotein G and the polymerase L), in order flanked by the bacteriophage T7 promoter, the VSV leader, the hepatitis delta virus ribozyme, and the T7 terminator sequence. This vector was modified to delete the VSV G coding regions (pVSVXN2ΔG) and a second transcriptional site was added using the MluI and BlnI restriction enzyme sites. A number of different genes were amplified using PCR (Section 2.3.2) and cloned (Section 2.4) into the two sites contained within the vector. Due to the size of the vectors, all full-length plasmids were transformed and amplified in *E.coli* grown at room temperature over a few days to decrease the chance of mutations or removal of the vector. The ANDV GPC was cloned only using the MluI/BlnI site and was always cloned second in constructs containing two genes due to internal XhoI sites contained within the ANDV GPC ORF. Constructs were produced containing either the glycoprotein from *Zaire ebolavirus* strain Mayinga '76 (ZEBOV GP) as previously described (51, 87) or VSV G in the secondary position in addition to the ANDV GPC, because it was unknown if the VSVΔG/ANDVGPC virus would be successfully rescued with only the ANDV glycoproteins. The two different VSV vectors are illustrated in Figure 12. The genes that were cloned into the pVSVXN2ΔG vectors and the sites used are shown below in Table 7.

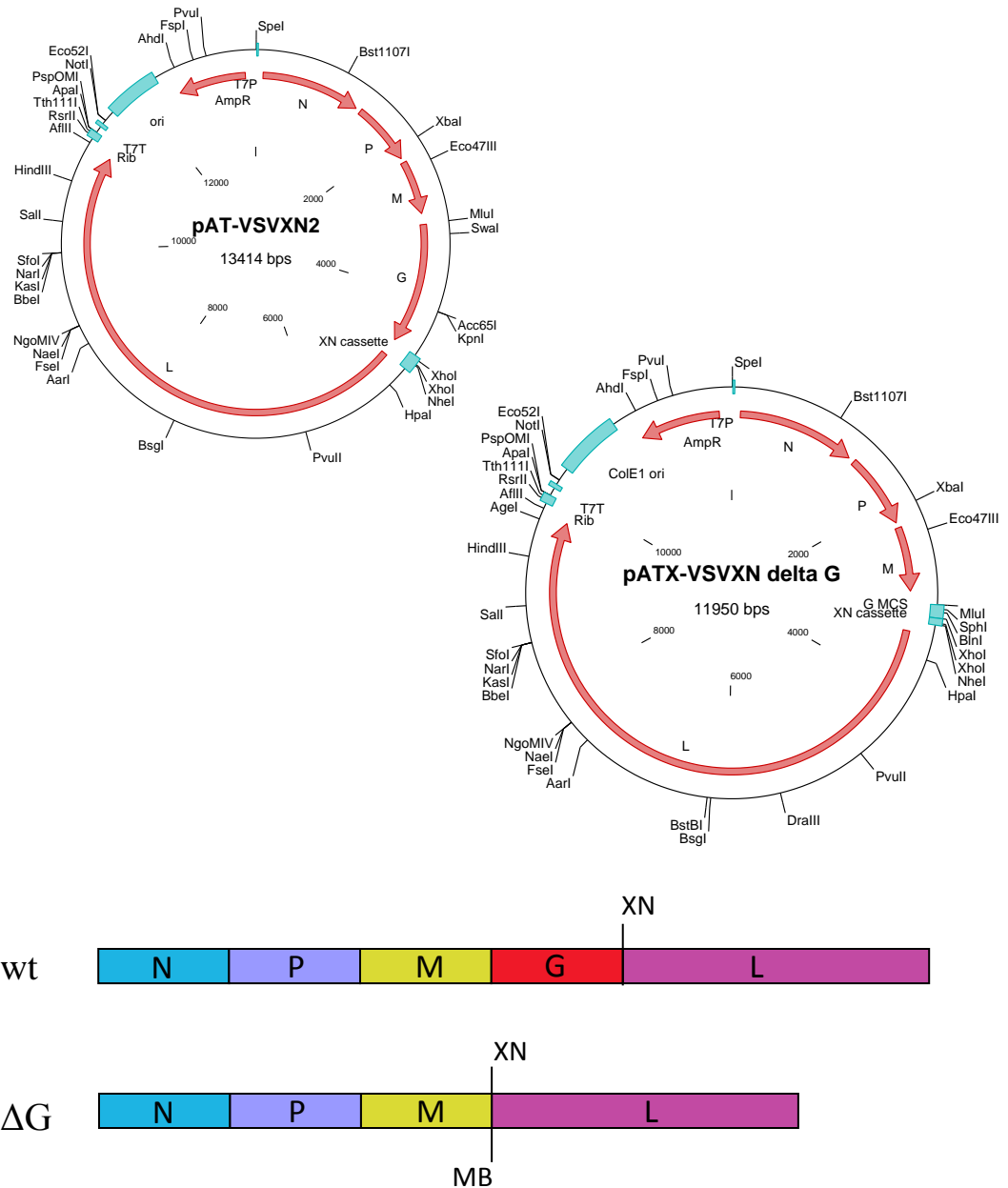


Figure 12. Cloning Strategy – Recombinant VSV. The VSVXN2ΔG plasmid deletes the VSV glycoprotein (G) gene from the wild-type (wt) plasmid and has two sites where additional transcriptional units may be inserted. The first uses the MluI and BlnI (MB) restriction enzyme sites, followed by the second, which uses the XhoI and NheI (XN) sites, highlighted in yellow on the vector map. N = Nucleoprotein, P = Phosphoprotein, M = Matrix protein, L = RNA dependent RNA polymerase

Table 7. Recombinant VSV Constructs

Virus Name	MluI/BlnI site	XhoI/NheI site
VSVΔG/ANDVGPC	ANDV GPC	---
VSVΔG/ZEBOVGP	ZEBOV GP	---
VSVΔG/ANDVGPC-ZEBOVGP	ANDV GPC	ZEBOV GP
VSVΔG/ANDVGPC-VSVG	ANDV GPC	VSV G

2.10 Transfection

Cells were transfected with plasmid DNA in order to express recombinant proteins. For protein expression assays, 293T or VeroE6 cells were typically used. Cells taken from a T75 stock flask were seeded into 6 well plates at a dilution necessary to obtain cells that were approximately 60% confluent the next day (for 293T cells) or in approximately 4 hours (for VeroE6 cells). FuGENE® 6 (FuGENE, Roche) or *TransIT*®-LT1 (LT1, Mirus®) were typically used as the lipid transfection reagents of choice. Briefly, 1-2µg of plasmid DNA was added to a tube containing 100µl of Opti-MEM®I Reduced Serum Media (Opti-MEM, Gibco®). In another tube, 3-12µl of transfection reagent was added to 100µl of Opti-MEM (1µg DNA: 3µl transfection reagent ratio for LT1, 1µg DNA: 6µl transfection reagent ratio for FuGENE). Reactions were incubated for approximately 5 min at room temperature, then mixed together and incubated for a further 15-30 min at room temperature. Finally, the volume in each tube was adjusted to 1ml with Opti-MEM. The media from the cells was removed and replaced by the transfection reaction. Cells were incubated for 24 hours at 37°C with 5% CO₂ and H₂O-saturated atmospheric conditions. The transfection reagent was then removed and fresh DMEM supplemented with 10% FBS, 1% L-glut and 1% P/S was added to the cells and allowed to incubate for an additional 24 hours.

2.11 Detection of Protein Expression by Immunostaining Techniques

2.11.1 Sodium Dodecyl Sulphate-Polyacrylamide Gel Electrophoresis (SDS-PAGE) Gels and Wet Transfer

Protein expression was typically assayed from either cell lysate (to examine cellular protein expression) or from cell culture media (to examine secreted proteins, or released virus particles). To collect cell lysate, transfected (Section 2.10) or infected cells from a 6 well plate were harvested by removing cell media, washing once with PBS to remove residual growth media, and then by adding a volume of PBS to each well and removing the cell monolayer with a cell scraper. The cell mixture was then lysed with an equal volume of 2X SDS Gel loading buffer (Appendix 1) and incubated at 95°C for 5 min. For secreted proteins or virus particles, cell culture media was directly mixed with an equal volume of 2X SDS gel loading buffer. Samples were run on SDS-PAGE gels to resolve proteins based on molecular weight. All gels included the See Blue Plus 2 (Invitrogen™) molecular weight marker, in order to estimate protein size (Appendix 4). Protein samples were separated by electrophoresis using the mini-Protean® III minigel system (Bio-Rad) at 120V for 1-1.5 hours. Proteins were resolved on 8-12% polyacrylamide SDS-PAGE gels (Appendix 1) and then transferred on a polyvinylidene fluoride (PVDF) membrane (Amersham Hybond™-P, GE Healthcare Life Sciences) using a mini Trans-Blot® wet transfer apparatus (Bio-Rad). Following electrophoresis, the gels, fibre pads and blotting paper were soaked in transfer buffer (Appendix 1) for 5 min and the PVDF membrane was activated by treatment in methanol for 5 min and then rinsed with transfer buffer. The apparatus was assembled in

the following manner: the cathode (black) side – fibre pad – blotting paper – polyacrylamide gel – PVDF membrane – blotting paper – fibre pad – anode (white) side. Air bubbles were removed by rolling a wet pipette across the surface of the polyacrylamide gel and PVDF membrane as they were added. The stacking gel of the SDS-PAGE gel was discarded prior to placement of the resolving gel. The apparatus was placed into the buffer tank with an ice pack and a magnetic stir bar. The tank was then filled with transfer buffer until the apparatus was entirely covered. Proteins were transferred at 100V for 1 hour, or at 30V overnight on top of a magnetic stir plate.

2.11.2 Western Blot

Following the transfer of proteins from the SDS-PAGE gel onto the PVDF membrane, the membrane was blocked with 5% skim milk powder in 0.1% Tween-20/PBS (PBST) overnight at 4°C to reduce non-specific binding of the antibodies. The blot was then incubated with primary antibody (diluted in blocking buffer) for 1 hour at room temperature, or overnight at 4°C with rocking (Appendix 2). Next, the blot was washed three times in PBST for 5 min each at room temperature and incubated with the secondary antibody (diluted in blocking buffer) for another 30 min to 1 hour at room temperature with rocking (Appendix 2). Following the incubation with the secondary antibody, the blot was again washed three times with PBST for 5 min each at room temperature. Proteins were visualized using the Amersham ECL PlusTM (GE Healthcare Life Sciences) Western Blotting Detection system. If necessary, blots were stripped of antibodies in order to be probed using another set of antibodies. In this case, blots were

incubated with stripping buffer (Appendix 1) for 30 min at 50°C. Blots were then thoroughly washed three times with PBST and assayed again as described above.

2.11.3 Immunofluorescent Assay (IFA)

IFA was typically carried out in VeroE6 cells, as the larger cytoplasm allowed easier visualization of the proteins of interest. In order to maintain cell structure, cells were fixed with either 3% PBS-buffered Formalin or 4% paraformaldehyde (PFA) for 10 min at room temperature, then permeabilized using 0.1% Triton®-X-100 (Fisher Scientific) for 15 min at room temperature. Many of the antibodies used (Appendix 2) were incompatible with this fixation method, so an alternative method of fixation, using an equal mixture of ice-cold acetone and methanol for 10 min at -20°C was more commonly used, albeit it with some loss of cell internal cell structure. This fixation method permeabilizes the cells, and therefore does not require an additional step for this process. After either fixation process, cells were blocked in 1% Bovine Serum Albumin (BSA)/PBS for 30 min at room temperature. Next, cells were washed three times with PBS. Cells were then typically incubated with primary antibody (Appendix 2) diluted in 1% BSA/PBS for 1 hour at room temperature or overnight at 4°C. Following incubation with the primary antibody, cells were washed three times with PBS. Next, cells were typically incubated with Alexa Fluor® 488 (green)-conjugated secondary antibodies (Invitrogen™, Appendix 2) diluted in 1% BSA/PBS for 1 hour at room temperature in the dark. Cells were washed a final three times with PBS and then visualized and imaged using a Zeiss Axiovert 200M fluorescent microscope. Controls to ensure that

cross-reactivity between antibodies or cells was not occurring were carried out for each experiment.

2.12 Minigenome Rescue

The plasmids required for rescue of the minigenome system were evaluated in a number of different mammalian cell lines. It was determined that optimal results occurred in COS-7 cells, an African Green Monkey kidney cell line. The COS-7 cells were transfected as described in Section 2.10. Briefly, plasmids expressing the ANDV L, GPC and N proteins and minigenome cassette (described in Sections 2.5-2.8, with different expression promoters) were transfected in varying concentrations relative to each other, as the optimal ratio of these plasmids has not been described in the literature. Negative controls usually consisted of the omission of either the L or minigenome cassette expression plasmids. Positive controls usually consisted of the reporter genes expressed from the CAG promoter in pCAGGS. Expression plasmids containing no insert were used to normalize the total amount of DNA transfected in each well.

2.13 Detection of Minigenome Reporter Signal

After transfection of cells with minigenome and helper constructs (Section 2.12), cells were allowed to incubate at 37°C for 48-72 hrs. Medium was then removed from each well, PBS was added and cell monolayers were detached using a cell scraper. Cells were pelleted by centrifugation at 3500 x g for 10 min to pellet cells, and then re-suspended in 100µl of Reporter Lysis Buffer (Promega). Cells were incubated at room

temperature for 15 min then pelleted by centrifugation at 3500 x g for 3 min to pellet cells. The supernatant was transferred to a clean tube and was assayed for either CAT or LUC activity immediately, or stored at -80°C for future analysis.

2.13.1 Chloramphenicol Acetyl Transferase (CAT) Assay and Thin-Layer Chromatography (TLC)

For the CAT assay, 55µl of supernatant was mixed with 15µl of *FAST CAT*® substrate reagent (Molecular Probes®, Invitrogen™). Next, 10µl of 9mM acetyl CoA (Sigma-Aldrich) was added to each tube. This mixture was incubated between 6 hrs and overnight. The reaction was stopped by the addition of 300µl of ethyl acetate (Fisher Scientific). Each sample was mixed by vortexing for 20 sec then placed in centrifuge at 12000 rpm for 3 min to separate the liquid phases. The top ~270µl of ethyl acetate was removed and transferred to a clean tube. This mixture was placed in a Savant DNA120 SpeedVac® (Thermo Scientific) at a low heat and allowed to completely dry (green solution turns to orange/yellow coloured precipitate). This precipitate was then re-suspended in a 20µl volume of ethyl acetate. This extract was either analyzed immediately by TLC or stored at -20°C for future analysis.

For TLC, 5µl of the *FAST CAT*® reference standard and 20µl of each ethyl acetate extract were spotted onto the bottom of a silica gel coated TLC plate (EM Science) and allowed to air dry. A glass chromatography chamber was then filled to a depth of approximately 0.5cm with chloroform:methanol (9:1 ratio v/v). The chamber was closed and allowed to equilibrate. Plates were then placed in the tank, allowing the

solvent to ascend. Once the solvent had reached a point close to the top of the plate, plates were removed and allowed to air dry. Spots were then visualized with a Hoefer™ MacroVue™ UV-25 transilluminator.

2.13.2 Luciferase (LUC) Assay

For LUC assay, 20µl of cell extract was placed in an opaque, flat-bottomed 96 well plate (Costar®) and assayed using the Dual-Luciferase® Reporter Assay (Promega). Both Luciferase Assay Reagent II (LAR II) and Stop & Glo® reagents were prepared as per manufacturer's instructions. Reagents were injected into plate sequentially and read by a Veritas™ 9100 luminometer (Turner Biosystems) with an acquisition time of 3 sec.

2.14 Rescue of Recombinant VSV

The transfection for the rescue of recombinant VSV was carried out in combination of both VeroE6 and 293T cells in order to maximize transfection efficiency (293T cells) and virus replication (VeroE6 cells). Briefly, a 1:6 dilution of ~90% confluent 293T cells and a 1:4 dilution of 100% confluent VeroE6 cells was taken from stock T75 flasks, combined in DMEM containing 3% FBS and 1% L-glut and then distributed into a 6 well plate. The next day, the expression plasmids necessary for virus rescue (VSV L/pBluescript (pBS), VSV N/pBS, VSV P/pBS, and full length VSV genome under the control of the T7 RNA promoter and T7 RNA polymerase expressed from the chicken β-actin promoter of pCAGGS (T7 poly/pCAG)) were combined using

Materials and Methods

the different ratios outlined in Table 8. These plasmids were added to a tube containing 100µl of Opti-MEM. Transfection reagent Lipofectamine™ 2000 (LP2000, Invitrogen™) was added to a second tube containing 100µl of Opti-MEM. These tubes were incubated at room temperature for 5 min, then combined and allowed to incubate for a further 15-30 min. After incubation, Opti-MEM was added to each tube to make a final volume of 1mL. The media from the cells was removed and replaced by the transfection reaction. Cells were incubated for 24 hours at 37°C with 5% CO₂ and H₂O-saturated atmospheric conditions. 1mL of fresh DMEM supplemented with 3% FBS, and 1% L-glut was added to the cells and allowed to incubate for up to an additional 7 days.

Table 8. DNA Transfection Amounts for VSV Rescue

Well	VSVXN2	T7 Polymerase	VSV N	VSV L	VSV P	LP2000
1	2.0µg	2.0µg	0.5µg	0.25µg	1.25µg	14µl
2	2.0µg	2.5µg	0.5µg	0.25µg	1.25µg	14µl
3	2.5µg	2.5µg	0.625µg	0.75µg	1.56µg	14µl
4	2.0µg	2.5µg	0.5µg	0.6µg	1.25µg	14µl
5	2.3µg	2.3µg	0.6µg	0.5µg	1.4µg	14µl
6	---	---	---	---	---	14µl

After incubation, a blind passage was carried out with 500µl of media from each well of the transfected plate being transferred to another 6 well plate containing fresh VeroE6 cells at 80% confluency. These new cells were monitored for cytopathic effect (CPE) compared to control wells to assess successful rescue of virus. Media and cells from any wells showing extensive CPE, with almost total destruction of the cell

Materials and Methods

monolayer (3+), were collected, and placed in centrifuge at 2500 rpm for 10 min to pellet the cells. Supernatant was transferred to a different tube, and the cell pellet was re-suspended using PBS. 140 μ l of either supernatant or cell lysate was added to 560 μ l of Buffer AVL (Qiagen) to extract RNA (Section 2.3.1) and to look for viral RNA by RT-PCR (Section 2.3.2) or 140 μ l of 2x SDS-PAGE buffer to look for expression of viral proteins by western blotting (Section 2.11.2). The remaining supernatant was divided into aliquots in 2ml cryovials and frozen at -80°C (p1 stock).

After confirmation of rescue by these methods, virus stocks were generated by splitting VeroE6 cells at 1:3 and seeding 3 T150 flasks to achieve 80-90% confluency by the next day. On infection day, p1 stocks were thawed and added to 30ml of DMEM without supplement at a 1:10,000 dilution (for VSV wt), a 1:1000 dilution (for VSV Δ G/ZEBOVGP) or a 1:200 dilution (for VSV Δ G/ANDVGPC). Media was removed from flasks and 10ml of infectious media was added to each flask. Flasks were incubated at 37°C for 1 hr, then 20ml of DMEM containing 3% FBS and 1% L-glut was added to each flask. Once the level of CPE reached 3+, cell monolayers were scraped, and supernatant/cell mixture was collected in 50ml conical tubes. Tubes were placed in centrifuge at 2500 rpm for 10 min to remove cell debris and then the supernatant was combined and transferred to new flask. FBS was added to a final concentration of 10%, then supernatant was aliquoted in 100 μ l, 500 μ l and 1ml aliquots and frozen at -80°C (p2 stock). Viral titres were determined by plaque assay (Section 2.15.1). A cartoon illustrating the entire rescue process is presented in Figure 13.

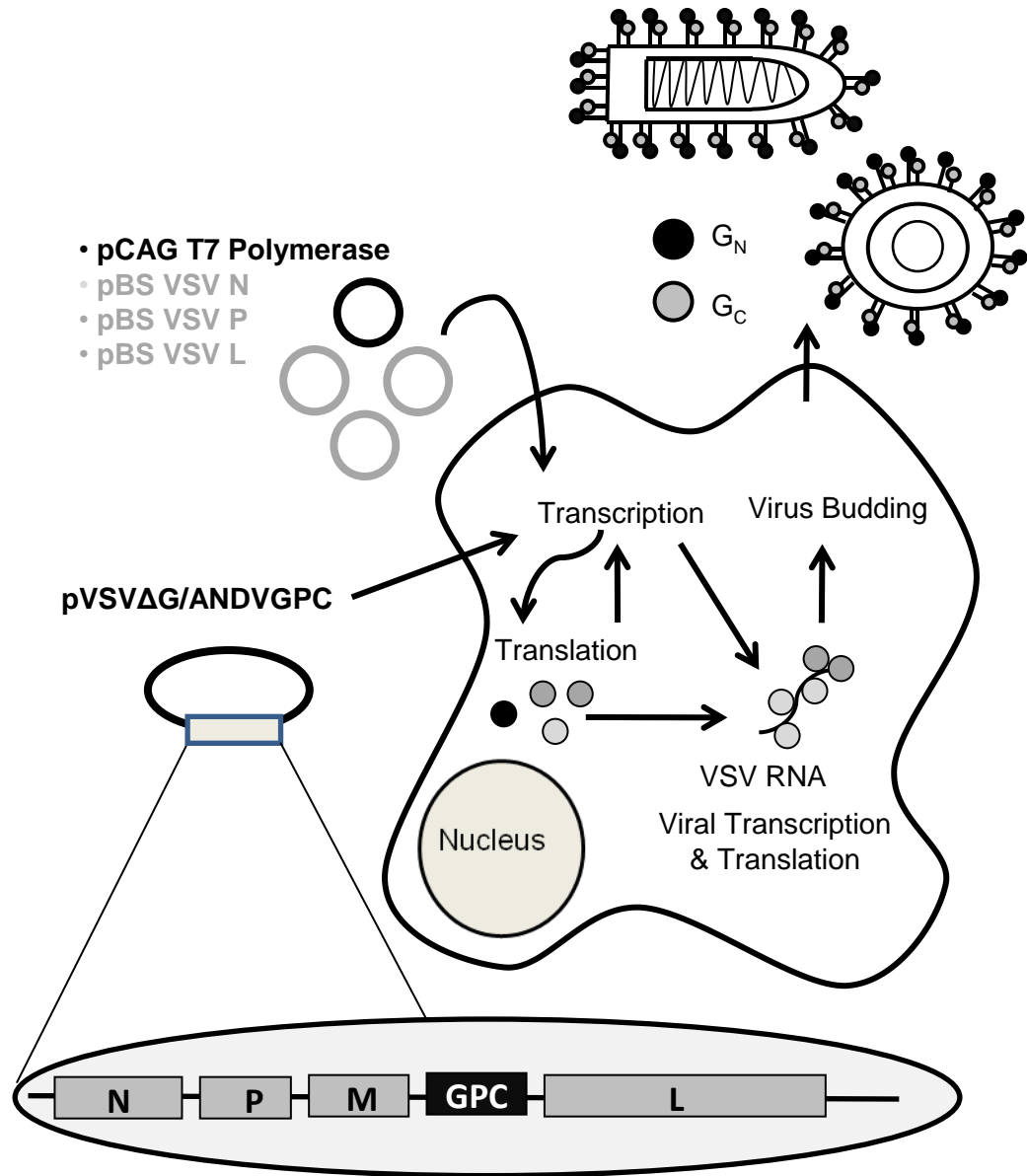


Figure 13. Rescue Strategy – Recombinant VSV. The pVSVΔG/ANDVGPC plasmid is transfected into 293T/VeroE6 cell mixture with necessary helper plasmids and T7 polymerase expression plasmid. The T7 polymerase protein transcribes the full length genomic plasmid and helper protein expression plasmids which then initiates viral transcription, translation and replication. Virus particle formation and budding occurs, and infectious virus is released from the cells, expressing the glycoprotein of interest on the envelope surface. N = Nucleoprotein, P = Phosphoprotein, M = Matrix protein, L = RNA dependent RNA polymerase, GPC = Glycoprotein precursor (cleaved to G_N and G_C glycoproteins), pBS = pBlueScript, pCAG = pCAGGS, T7 = T7 bacteriophage RNA polymerase.

2.15 Infectivity Assays

2.15.1 Plaque-Forming Assay

Plaque-forming assays were used to titre the recombinant VSVs, all of which cause CPE and plaque formation. These were carried out in enhanced BSL-2. To perform a plaque assay, VeroE6 were split 1:2 and seeded into 6 well plates to achieve a confluency of 100% by the following day. On infection day, 10-fold serial dilutions were carried out as follows: 30µl of p2 virus stock was added to 3ml of DMEM without supplement to achieve a 1:100 dilution (10^{-2}). Next, 300µl of the 1:100 dilution was added to 2.7ml of DMEM to achieve a 1:1000 dilution (10^{-3}). This continued up a dilution of 10^{-9} , using a fresh pipette tip between each dilution. Media was removed from each well of the plate and 500µl of each virus dilution was added per well. This was done in duplicate for each dilution, and a mock well was included that included DMEM containing no virus. Plates were incubated at 37°C for 1 hr, with rocking every 15 min to prevent the cell monolayer from drying out. Shortly before the end of the incubation, the cell overlay was prepared: 2% low-melting point agarose and 2x Minimum Essential Medium (Sigma®) containing 4% FBS were combined in equal amounts. Virus inoculum was removed from the cells and 2ml of overlay was added to each well, starting with the mock wells and then going from the lowest to highest amounts of virus. Agarose overlay was allowed to solidify at room temperature for 30 minutes, and then plates were placed upside down in 37°C incubator for 1-4 days. After incubation, 2ml of crystal violet (Appendix 1) was added to each well and allowed to sit

Materials and Methods

for 24 hrs. Cell overlays were then removed by using a pipette tip to cut around agarose, and cell monolayers were allowed to dry to allow clear visualization of the plaques. To calculate viral titre, the number of plaques were counted per well. Plaque numbers were used from dilutions that produced at least 20 plaques. The average number of plaques per well was then divided by the dilution factor and the initial volume of virus as shown below. Virus titres were expressed as plaque-forming units (PFU) per ml (PFU/ml).

Formula:
$$\frac{\text{Average Number of Plaques}}{(\text{Dilution Factor})(\text{Volume})} = \text{PFU/ml}$$

Example:
$$\frac{53 \text{ plaques}}{(10^{-6} \text{ dilution})(0.5\text{ml inoculum})} = 10.6 \times 10^7 \text{ PFU/ml}$$

2.15.2 Focus-Forming Assay

The focus-forming assay was used to titre ANDV, as hantaviruses do not cause CPE, and therefore do not cause plaque formation. All ANDV work was carried out in BSL-3 containment. For the focus-forming assay, VeroE6 were split 1:2 and seeded into 24 well plates to achieve a confluency of 100% by the following day. On infection day, 10-fold serial dilutions were carried out as described in the previous section for dilutions from 10^{-2} to 10^{-9} . Media was removed from each well of the plate and 100 μ l of each virus dilution was added per well. This was done in duplicate for each dilution, and a mock well was included that included DMEM containing no virus. Plates were incubated at 37°C for 1 hr, with rocking every 15 min to prevent the cell monolayer from drying out. A few minutes before the end of the incubation, the cell overlay was

Materials and Methods

prepared: sterile 3% carboxymethylcellulose (Sigma-Aldrich) and 2x Minimum Essential Medium containing 4% FBS were combined in equal amounts. Virus inoculum was removed from cells and 0.5ml of the overlay was added to each well, starting with mock wells and then going from lowest to highest amounts of virus. Plates were then incubated at 37°C for 7-10 days. After incubation, overlay was removed and cells were washed with PBS. Next, cells were fixed using a 1:1 mixture of acetone:methanol for 15 min at room temperature. Cells were then allowed to air dry in BSC, after which they could be removed from BSL-3 and brought to BSL-2 for staining. Cells were then covered with a 1:1000 dilution of hamster serum containing anti-ANDV N antibodies (Appendix 2) and incubated at room temperature for 1 hr. Cells were then washed twice with PBS, and then covered with a 1:500 dilution of HRP-conjugated goat anti-hamster IgG (Appendix 2) for another incubation for 1 hr. Cells were then washed 2 more times with PBS and covered with the NovaRED peroxidase substrate kit (Vector Laboratories) for 30 min. To calculate viral titre, the number of foci were counted per well. Dilutions were used that produced at least 20 foci. The average number of foci per well was then divided by the dilution factor and the initial volume of virus as shown in the previous section. Virus titres were expressed as focus-forming units (FFU) per ml (FFU/ml).

2.15.3 50% Tissue Culture Infectious Dose

The 50% tissue culture infectious dose (TCID₅₀) assay was used as an alternative method to titre the recombinant VSVs, all of which cause CPE and was carried out in

Materials and Methods

enhanced BSL-2. For the TCID₅₀ assay, VeroE6 were divided 1:3 and seeded into 96 well plates to achieve a confluency of 80-90% by the following day. On infection day, 10-fold serial dilutions were carried out as described in the previous sections for dilutions from 10⁻² to 10⁻⁹. Media was removed from each well of the plate and 100µl of each virus dilution was added per well. This was done in quadruplicate for each dilution, and a mock well was included that included DMEM containing no virus. Plates were incubated at 37°C for 1 hr, and then 100µl of DMEM containing 3% FBS and 1% L-glut was added to each well. Plates were then incubated at 37°C for 1-5 days. After incubation, wells that contained CPE were marked as positive. The TCID₅₀ was calculated using the Reed-Muench method (180) with the following equations, and viral titres were expressed as TCID₅₀/ml:

Formula: i. Proportionate Distance (PD) =

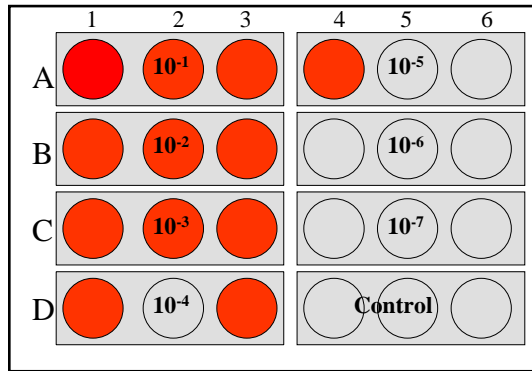
$$\frac{(\% \text{ CPE at dilution above } 50\%) - (50\%)}{(\% \text{ CPE at dilution above } 50\%) - (\% \text{ CPE at dilution below } 50\%)}$$

ii. -Log = dilution above 50% CPE ratio (i.e. 10⁻³ would be -3)

iii. ((PD) + (-log(dilution interval)))

iv. TCID₅₀ = 10^(ii + iii)

Example:



Dilution	Infected	% Infected
10-1	3/3	100
10-2	3/3	100
10-3	3/3	100
10-4	2/3	66
10-5	1/3	33
10-6	0/3	0
10-7	0/3	0

$$PD = \frac{(66 - 50)}{(66 - 33)} = 0.48$$

$$-\text{Log dilution above 50\%} = 4 \text{ (from } 10^{-4}\text{)}$$

$$4(-\text{Log}) + 0.48(PD) = 4.48$$

$$TCID_{50} = 10^{4.48} / 0.1\text{ml infection dose}$$

$$TCID_{50}/\text{ml} = 10^{5.48} \text{ or } 3.01 \times 10^5$$

2.16 Transmission Electron Microscopy (TEM) of VSV

For visualization of cell-associated VSV particles, VeroE6 cells grown on 13mm thermanox coverslips (Nunc) were infected with VSVΔG/ANDVGPC, VSVΔG/ZEBOVGP or VSV wt for 48 hours and subsequently fixed at 4°C with 2.5% glutaraldehyde in 0.1M sodium cacodylate buffer, pH 7.2 for 3 hours. Samples were

Materials and Methods

post-fixed 30 minutes with 0.5% osmium tetroxide/0.8% potassium ferricyanide in 0.1M sodium cacodylate, 1 hour with 1% tannic acid and overnight with 1% uranyl acetate at 4°C. Samples were dehydrated with a graded ethanol series, and embedded in Spurr's resin. Thin sections were cut with a Leica EM UC6 ultramicrotome (Leica), and stained with 1% uranyl acetate and Reynold's lead citrate prior to viewing at 120 kV on a Tecnai BT Spirit transmission electron microscope (FEI).

For visualization of purified VSV particles, T75 flasks containing VeroE6 cells with an 80-90% confluency were infected with either VSV Δ G/ANDVGPC, VSV Δ G/ZEBOVGP or VSV wt. The supernatant was collected and purified over a 20% sucrose cushion at 20,000 rpm for 2 hrs at 4°C, then subsequently re-suspended in PFA at 4°C. Fixed virus particles were then adsorbed to carbon and Formvar-coated grids and left overnight at 4°C. These grids were then transferred to 20 μ l droplets of blocking buffer containing 2% (m/v) globulin-free bovine serum albumin (BSA) in PBS, and irradiated at 150W in a Biowave model microwave processor (Ted Pella, Inc.) for a cycle of 1 min on, 1 min off, 1 min on. The grids were then washed once in blocking buffer, twice in PBS, twice in deionized water, and then negatively stained with 1% ammonium molybdate in water. The samples were examined at 80 kV in a model H7500 transmission electron microscope (Hitachi High Technology). Digital images were recorded for both methods using a model HR-100 CCD camera (Advanced Microscopy Techniques).

2.17 Growth Kinetic Analysis of VSV

VeroE6 cells were split at 1:3 and seeded in 12 well plates to achieve 80-90% confluency by the next day. Cells were then infected with VSV Δ G/ANDVGPC, VSV Δ G/ANDVGPC-ZEBOVGP, VSV Δ G/ZEBOVGP or VSV wt at an approximate multiplicity of infection (MOI) of 1 or 0.0001. Virus was allowed to adsorb to cells for 1 hr at 37°C, and then media was removed and cells were washed twice with DMEM to remove any residual virus. At pre-determined time points, cell monolayers and supernatant were collected from each virus in triplicate, and then centrifuged at 2500 rpm for 10 min to remove cellular debris, and stored at -80°C for analysis after all samples were collected. Virus titres at each time point were determined using TCID₅₀ assay (Section 2.14.3). The values from the 3 triplicate wells were averaged and the standard error was calculated.

2.18 Immunization and Challenge of Syrian Hamster Lethal Disease Model

All infectious *in vivo* work with ANDV was performed in BSL-4 at the IRF, RML, DIR, NIAID, NIH. All animal work was approved by the RML Institutional Animal Care and Use Committee (IACUC), and performed following the guidelines of the Association for Assessment and Accreditation of Laboratory Animal Care, International (AAALAC) by certified staff in an AAALAC approved facility.

5-6 week old female Syrian hamsters (*Mesocricetus auratus*) were group housed in microisolator units in BSL-4 for the entire length of the experiment. For immunization, hamsters were first anesthetized using inhalational isoflurane. Study

animals were then given 10^5 PFU of the VSV Δ G/ANDVGPC study virus diluted in 400 μ l of DMEM via intraperitoneal (i.p.) injection in two sites (200 μ l/site). Control animals received either 10^5 PFU of VSV Δ G/ZEBOVGP diluted in the same manner, or 400 μ l of DMEM containing no virus.

The LD₅₀ (dose leading to death in 50% of animals) of ANDV in this model was previously determined to be approximately 1.54 FFU (186). Hamsters were challenged with 100 x LD₅₀ (equal to 154 FFU) of ANDV given through i.p. route at 28, 14, 7 or 3 days after immunization, depending on the study. For testing the efficacy of the vaccine platform as a post-exposure treatment, hamsters were first challenged with 100 x LD₅₀ of ANDV, and then given VSV Δ G/ANDVGPC, VSV Δ G/ZEBOVGP or DMEM at 1, 3, or 5 days post-challenge.

2.19 Hamster Serological Assays

In order to detect and quantify the hamster immune responses, blood samples were collected both immediately before challenge by retro-orbital bleeding (28, 14, 7 or 3 days post-immunization) and 45 days after challenge from surviving animals by cardiac puncture and exsanguination (study end-point) into EDTA Microtainer® (BD) tubes. Whole blood was placed in centrifuge for 10 min and plasma was collected into individual 0.5ml cryovials. Samples were removed from BSL-4 and inactivated by gamma irradiation (2-5 Mrads).

2.19.1 Neutralization Assays

To determine if hamsters produced neutralizing antibodies against the ANDV glycoproteins, an 80% plaque reduction neutralization titre (PRNT₈₀) assay was performed using the VSVΔG/ANDVGPC virus as the neutralization target. Briefly, VeroE6 cells were split 1:2 and seeded into 24 well plates to reach a confluency of 100% by the following day. Next, hamster serum was mixed with DMEM without supplement using 2-fold serial dilutions starting at an initial screening dilution of 1:40 and then further diluted until an end-point was reached. VSVΔG/ANDVGPC was mixed with a volume of DMEM to obtain a final titre of 1×10^3 . 150μl each of virus and diluted hamster serum were combined and incubated at 37°C for 1 hr. Media was then removed from plates and 130μl of virus/serum mixture was added to each well in duplicate. This mixture was allowed to adsorb to cells at 37°C for 1 hr, and then the mixture was removed and a 0.5ml overlay of equal amounts of 3% carboxymethylcellulose and 2x Minimum Essential Medium containing 4% FBS was added. Plates were incubated at 37°C for 3 days, and then crystal violet (Appendix 1) was added to each well, and allowed to sit for 24 hours. Semi-solid overlay and crystal violet were then removed with a serological pipette, and cell monolayers were allowed to dry. Plaques were counted and the PRNT₈₀ value was determined to be the last dilution at which there was at least an 80% reduction in the number of plaques compared to control wells containing no serum.

To ensure that the target of the neutralization was the ANDV glycoproteins, and not another component of the VSV backbone, we validated our assay by doing an 80%

focus reduction neutralization titre (FRNT₈₀) assay using native ANDV as the neutralization target with a subset of our total number of samples. The assay was carried out in a manner identical to the PRNT₈₀ assay described above, except that the ANDV was diluted to a titre of approximately 2.5×10^4 and plates were incubated for between 7 and 10 days. Plates were fixed and foci were stained as described in Section 2.15.2. Foci were counted and the FRNT₈₀ value was determined to be the last dilution at which there was at least an 80% reduction in the number of foci compared to control wells containing no serum.

2.19.2 N-Specific Indirect Enzyme-Linked Immunosorbent Assay (ELISA)

Seroconversion against the N protein was determined using an N-specific indirect ELISA with *E. coli* recombinantly expressed and purified SNV N as the antigen, due to the cross-reactivity of the hantavirus N proteins. Round-bottom 96 well flexible microtiter plates (VWR) were coated with 100µl of SNV N protein re-suspended in PBS. Plates were placed in a sealed container at 4°C overnight. The next day, plates were washed three times with PBST using a mechanical plate washer. Excess fluid was removed from wells by tapping plate on a paper towel. Hamster serum samples were diluted to 1:40 using PBST as a screening dilution and then diluted using 2-fold serial dilutions until an endpoint was reached. 100µl of each dilution was added to each well, and incubated at 37°C for 1 hr in a sealed plastic container humidified using a moist paper towel. Serum samples were removed, and each well was washed 3 times using PBST. Next, HRP-conjugated goat anti-hamster IgG (Appendix 2) was

diluted to 1:1000 using PBST and 100µl was added to each well. Plates were incubated at 37°C for 1 hr in the sealed humidified container. Antibody solution was removed, and each well was again washed 3 times using PBST. Finally, ABTS peroxidase substrate kit (KPL) was prepared according to included instructions, and 100µl was added to each well. Colour was allowed to develop for 30 min in the dark, and then measured using an ELISA plate reader at OD₄₀₅. Net OD was calculated by subtracting the OD value of the control wells containing no serum from each study sample. Samples were considered positive if they were greater than the cut-off point, determined to be the OD value of the negative control serum plus 3 standard deviations.

2.20 qRT-PCR Hamster Cytokine Assay

At 28, 14, 7, 3 or 1 day after immunization with VSVΔG/ANDVGPC or VSVΔG/ZEBOVGP, 6 hamsters per group were anesthetized, exsanguinated via cardiac puncture, and necropsied. 6 hamsters received an injection of DMEM to establish baseline cytokine mRNA levels and were euthanized at 3 or 1 day after injection. RNA was extracted from an approximately 100mg piece of lung and spleen tissue as previously described in Section 2.3.1. qRT-PCR (Section 2.3.5) was conducted on RNA extracts using a Rotor-Gene RG-3000 instrument (Corbett Life Science). All RNA samples were normalized to 200ng of RNA per reaction. TaqMan primer/probe sets for myxovirus resistance protein-2 (Mx-2), signal transducer and activator of transcription-1 (STAT-1), interferon regulatory factor-1 (IRF-1) or interferon γ (INF- γ) were chosen as representative components of the innate immune response (Appendix 3).

3.0 Results

3.1 Cloning and Expression of ANDV Proteins in Mammalian Expression Constructs

As the first step in the development of the reverse genetic systems based vaccines, it was necessary to create plasmid-based expression constructs that would express the different ANDV proteins *in vitro*. To increase our chances of successful expression of each protein, a number of different expression constructs under the control of different mammalian promoters were created for the N and L proteins. For the ANDV glycoproteins, only the pCAGGS vector was used, as another member of the lab was able to successfully clone hantavirus glycoproteins using this vector. The successful cloning of the different amplicons into sub-cloning vectors and expression constructs was confirmed by nucleotide sequence analysis in both directions for each cloning step.

3.1.1 ANDV N Constructs

The ANDV N construct was successfully amplified by RT-PCR from ANDV RNA derived from the Chilean isolate 9717869 and cloned directly into the mammalian expression vector pCAGGS using the EcoRI and XhoI sites. The construct was referred to as ANDV-N/pCAG. Constructs ANDV-N/pTM1 and ANDV-N/gWIZ were successfully generated by either directly cloning (pTM1) using the same EcoRI and XhoI sites, or by PCR amplification using primers containing SalI and NotI restriction

enzyme sites (gWIZ). Confirmation of all inserts by restriction enzyme digest at expected size of 1.3 kb is shown in Figure 14.

3.1.2 ANDV Glycoprotein Constructs

The ANDV GPC construct was successfully amplified by RT-PCR from ANDV RNA derived from the Chilean isolate and cloned into the sub-cloning vector pATXMCS4 using sites KpnI and NheI. The construct was then cloned into the mammalian expression vector pCAGGS using the same digest sites. This construct was referred to as ANDV-GPC/pCAG. Next, individual ANDV G_N and G_C expression plasmids were successfully constructed by PCR amplification of ANDV-GPC/pCAG, using internal primers with the WASSA cleavage site as the separation point. Amplicons were inserted into the pCAGGS vector using the same KpnI and NheI sites. Confirmation of all inserts by restriction enzyme digest at expected sizes of 3.5 (GPC), 2.0 (G_N) and 1.5 kb (G_C) are shown in Figure 15.

3.1.3 ANDV L Constructs

The ANDV L constructs were successfully amplified by RT-PCR from ANDV RNA derived from the Chilean isolate and cloned into the sub-cloning vector pATXMCS3. A cloning strategy was used that broke the L ORF into 4 separate segments, which were amplified independently, inserted into the sub-cloning vector, and ligated together using unique restriction sites found within the ORF sequence. This

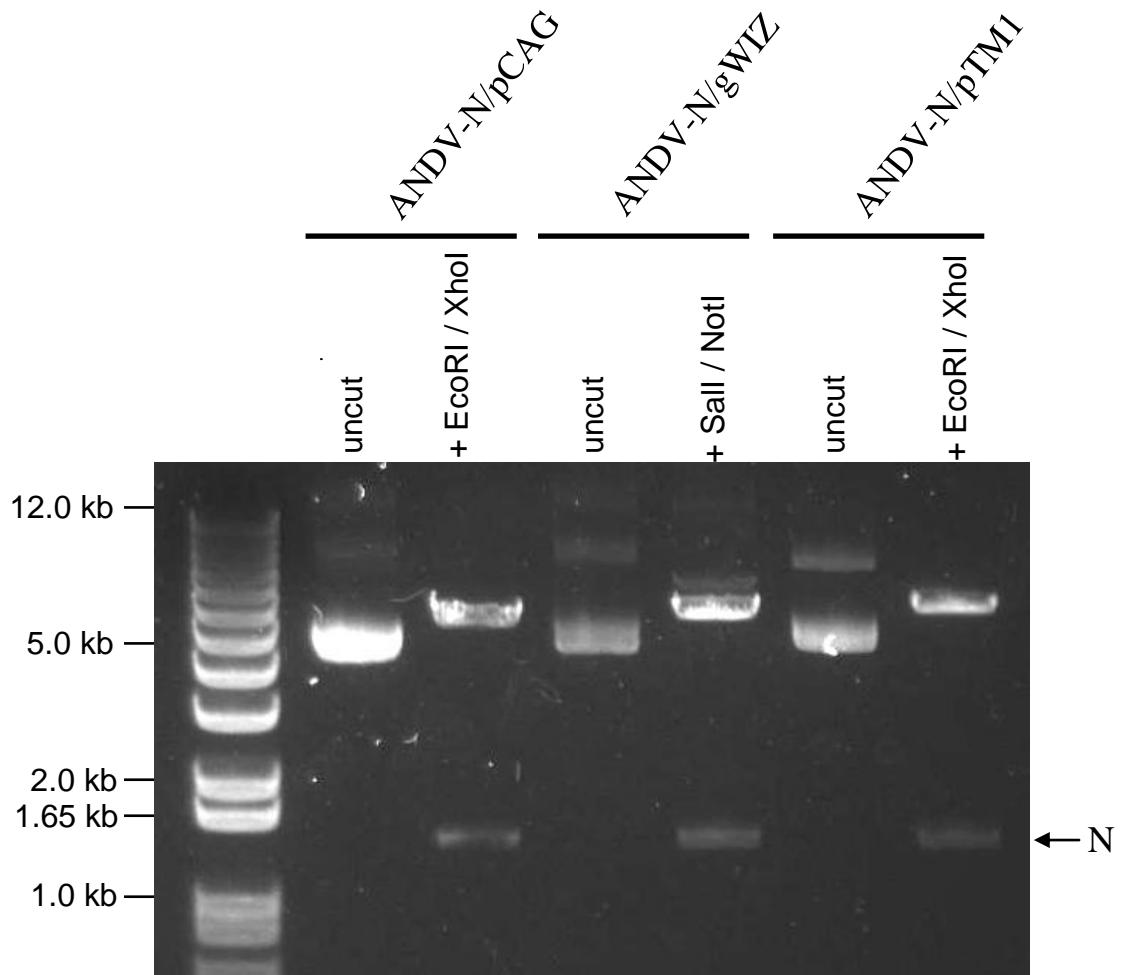


Figure 14. Restriction Enzyme Digest Confirmation – N Constructs.

Digestion of ANDV nucleocapsid protein (N) open reading frame (ORF) in pCAGGS, gWIZ and pTM1 expression plasmids with the restriction enzymes used for cloning and digestion indicated above. Top bands represent the expression plasmids and the bottom band represents the N ORF. 1 Kb Plus DNA ladder is used on left hand side and values are expressed in kilobases (kb).

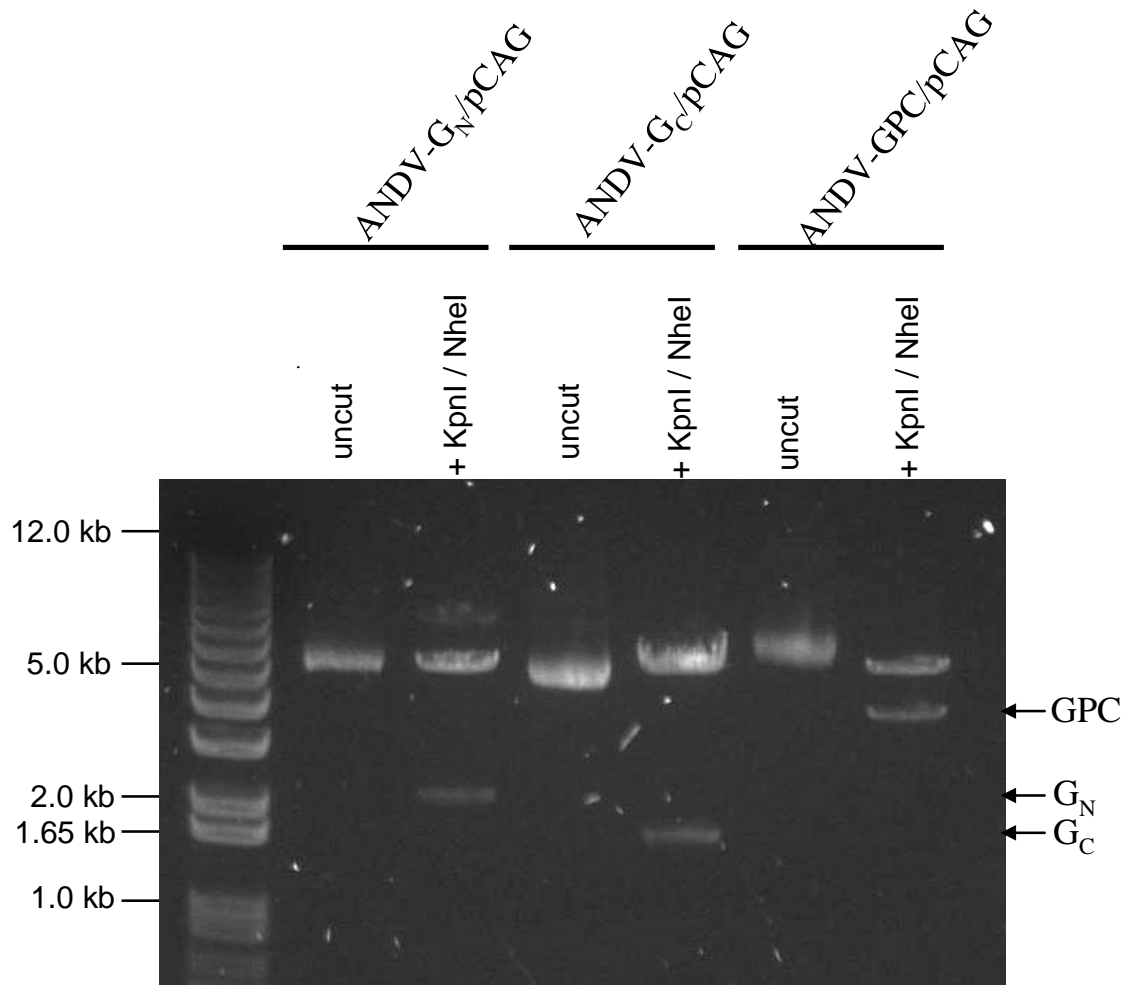


Figure 15. Restriction Enzyme Digest Confirmation – Glycoprotein Constructs. Digestion of pCAGGS expression plasmids containing the glycoprotein precursor (GPC), or the individual G_N or G_C glycoprotein open reading frames (ORF) with the restriction enzymes used for cloning and digestion indicated at the top. Top bands represent the expression plasmid and bottom band represents G_N, G_C or full length GPC ORFs. 1 Kb Plus DNA ladder is used on left hand side and values are expressed in kilobases (kb).

Results

strategy was successful, with a minor modification. During the initial cloning steps, it was quickly realized that the combination of the Kozak sequence with the ATG start site generated an additional NcoI site that was intended to be used to insert the second segment. To overcome this, segment 1 was inserted and then removed by NcoI digestion (leaving segment 1 with an NcoI site at each end). Segment 2 was then cloned in, and segment 1 was then re-inserted to successfully achieve a construct containing both pieces, without affecting the sequence in any way. Proper orientation of the sequence was checked by restriction enzyme digest. Subsequently, segment 3 and 4 were inserted. The full-length L ORF was then PCR amplified and cloned into pCAGGS using KpnI and NheI sites, gWIZ using SallI and NotI sites, or pTM1, pKS336 and pCDNA3.1 using EcoRI and XhoI sites. These constructs were referred to as ANDV-L/pCAG, ANDV-L/gWIZ, ANDV-L/pTM1, ANDV-L/pKS336 or ANDV-L/pCDNA3.1, respectively. Confirmation of all inserts by restriction enzyme digest at expected size of 6.5 kb is shown in Figure 16.

There are no commercially available antibodies to detect L protein expression, so modifications were made to the constructs to include either the HA or FLAG tag on either the N or C terminus of the protein. This was done by PCR amplification including the HA or FLAG tag sequence as part of the forward or reverse primer, and an internal restriction site in the other. Constructs were successfully completed that included one of these two tags at either of the ends of the protein.

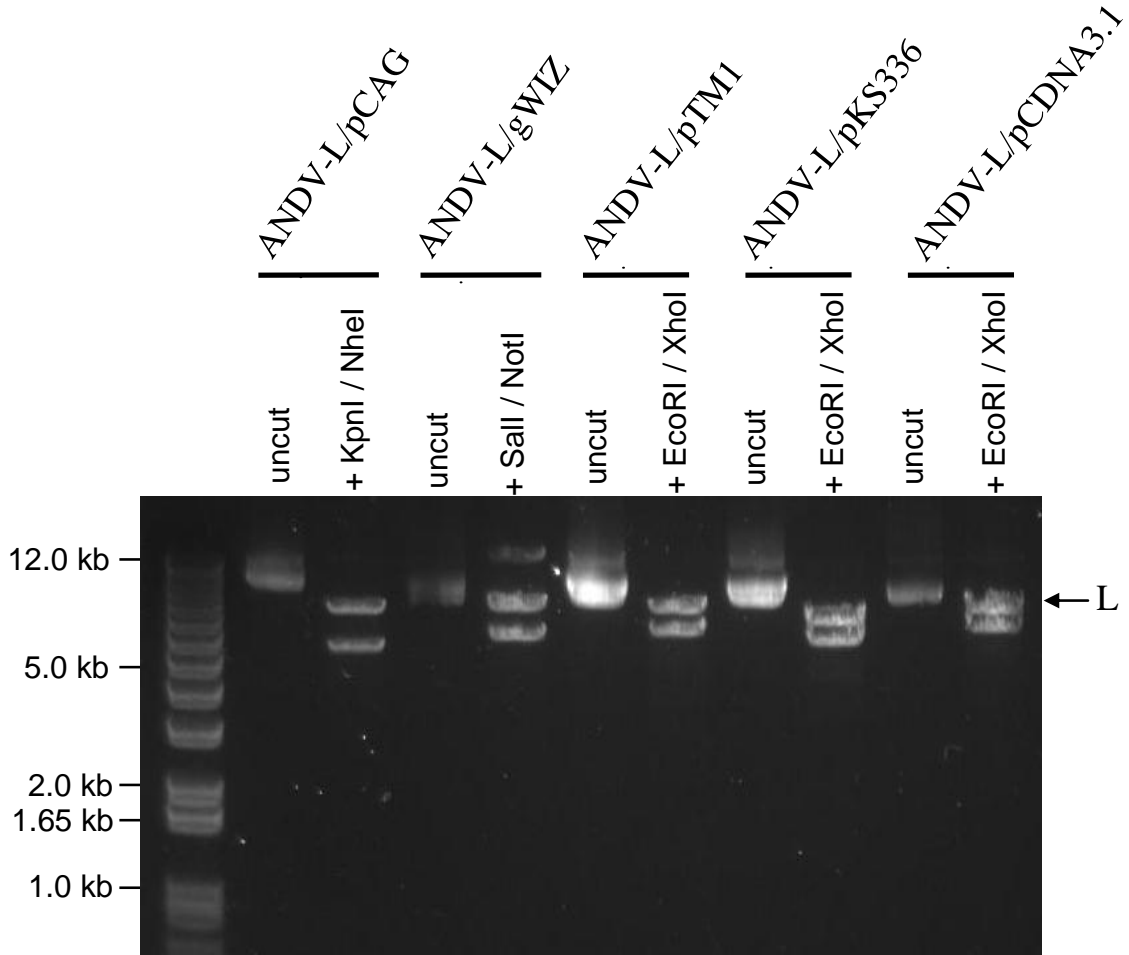


Figure 16. Restriction Enzyme Digest Confirmation – L Constructs. Digestion of polymerase protein (L) open reading frame (ORF) in pCAGGS, gWIZ, pTM1, pKS336 and pCDNA3.1 expression plasmids with the enzymes used for cloning and digestion indicated at top. Top bands represent the L ORF and bottom band represents expression plasmids. 1 Kb Plus DNA ladder is used on left hand side and values are expressed in kilobases (kb).

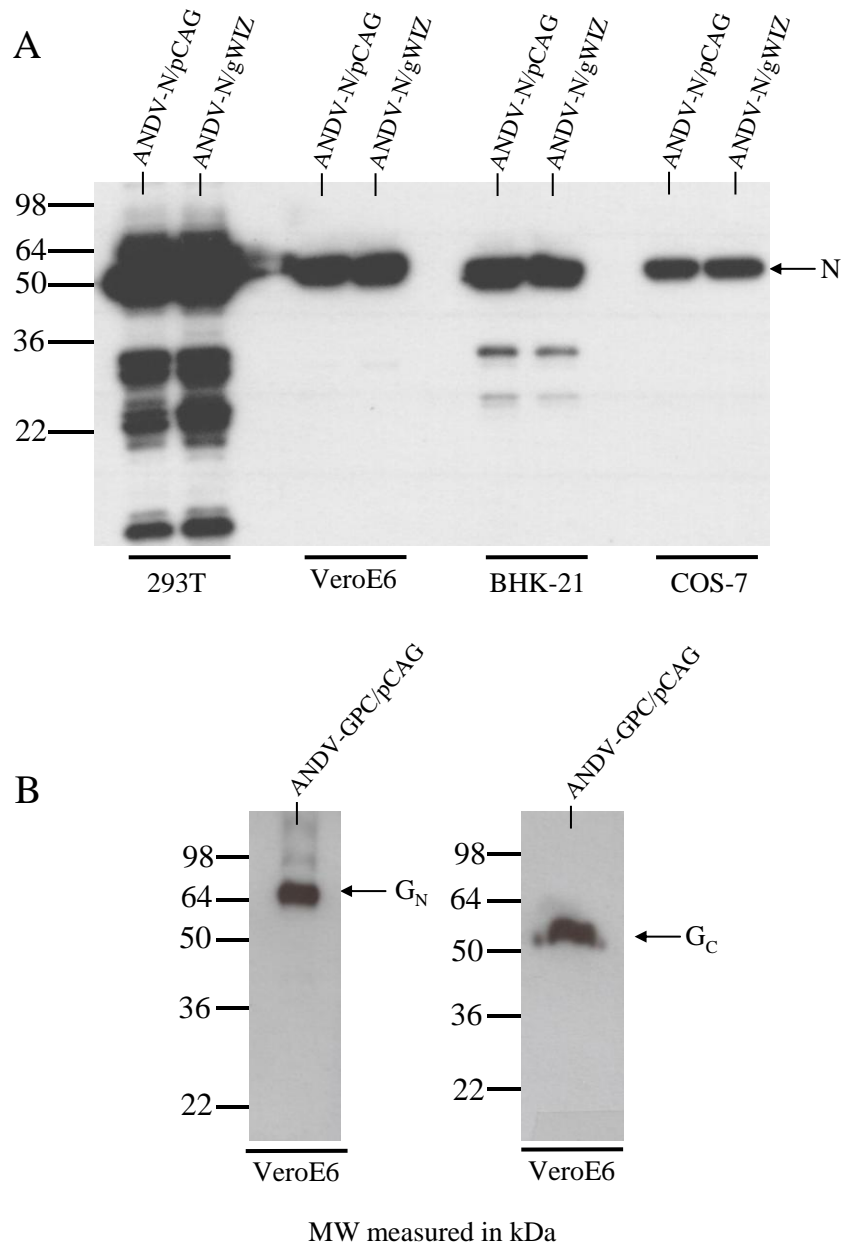


Figure 19. Western Blot – N and GPC Expression Constructs. Confirmation of expression of different ANDV protein expression plasmids using anti-N, G_N or G_C - specific monoclonal antibodies. (A) Comparison of nucleocapsid protein (N) construct expression in human embryonic kidney (293T), African green monkey kidney (VeroE6 and COS-7) or baby hamster kidney (BHK-21) cell lines. (B) Detection of G_N and G_C expression from ANDV glycoprotein precursor (GPC) expression construct in VeroE6 cells. Apparent molecular weight (MW) is indicated on the left hand side of each blot and is expressed in kiloDaltons (kDa).

3.1.4 Confirmation of Protein Expression

To confirm protein expression from the constructs, different cell lines were transfected with each of the constructs using a lipid-based transfection reagent (Appendix 5). Expression was first confirmed by western blot, as shown in Figure 17. There was little difference between the ANDV-N/pCAG and ANDV-N/gWIZ construct expression levels, with the amount of expression determined more by the cell type used. Both proteins were highly over-expressed in 293T cells, with expression levels in VeroE6, COS-7 and BHK-21 cells being lower, but very similar to each other. The ANDV-N/pTM1 construct typically expressed at a slightly lower level (data not shown), most likely due to the need to include the T7 polymerase expression plasmid in the transfection mixture, and the requirement for the presence of both plasmids in the same cell to achieve successful expression.

The expression of both G_N and G_C glycoproteins was successfully achieved from the ANDV-GPC/pCAG construct, and were detected independently using glycoprotein-specific monoclonal antibodies. As should be expected, no full-length GPC protein was detected due to co-translational cleavage into G_N and G_C .

To detect expression of the L protein, the different tagged constructs were used in order to be able to use either anti-HA or anti-FLAG antibodies. However, expression of the L protein from any of the constructs was not detected. Further analysis using non-immune protein staining methods including silver staining and Coomassie blue staining were also unsuccessful in detecting L protein expression.

After confirmation of expression of N protein and glycoproteins by western blot, expression was also examined by IFA, shown in Figure 18. It was determined that the commercial antibodies used worked much better using a methanol:acetone fixation process compared to the use of formalin or PFA. N, G_N and G_C were successfully expressed from the ANDV-N or ANDV-GPC constructs. The G_N antibody did not work very well for this particular assay, with lower levels of labelling that made imaging difficult.

Expression of the tagged L proteins was unsuccessful for almost every expression construct tested. The only L construct that was successfully expressed was with a FLAG tag attached to the N terminus expressed from the pKS336 expression vector. However, it is unknown if full-length L is being detected, or just a portion of the L protein containing the FLAG tag in frame, although the FLAG tag was not detected at a lower molecular weight by western blot. In addition, overall expression levels were extremely low, even in 293T cells.

Overall, the ANDV N, G_N and G_C proteins seemed to be both easily and successfully expressed from all expression constructs in all cell lines tested. Unfortunately, expression of the L protein was not detected in most attempts, and if it was, it was only at very low amounts. This may help explain why the expression of so few hantavirus polymerase proteins have been described in the literature (42, 109).

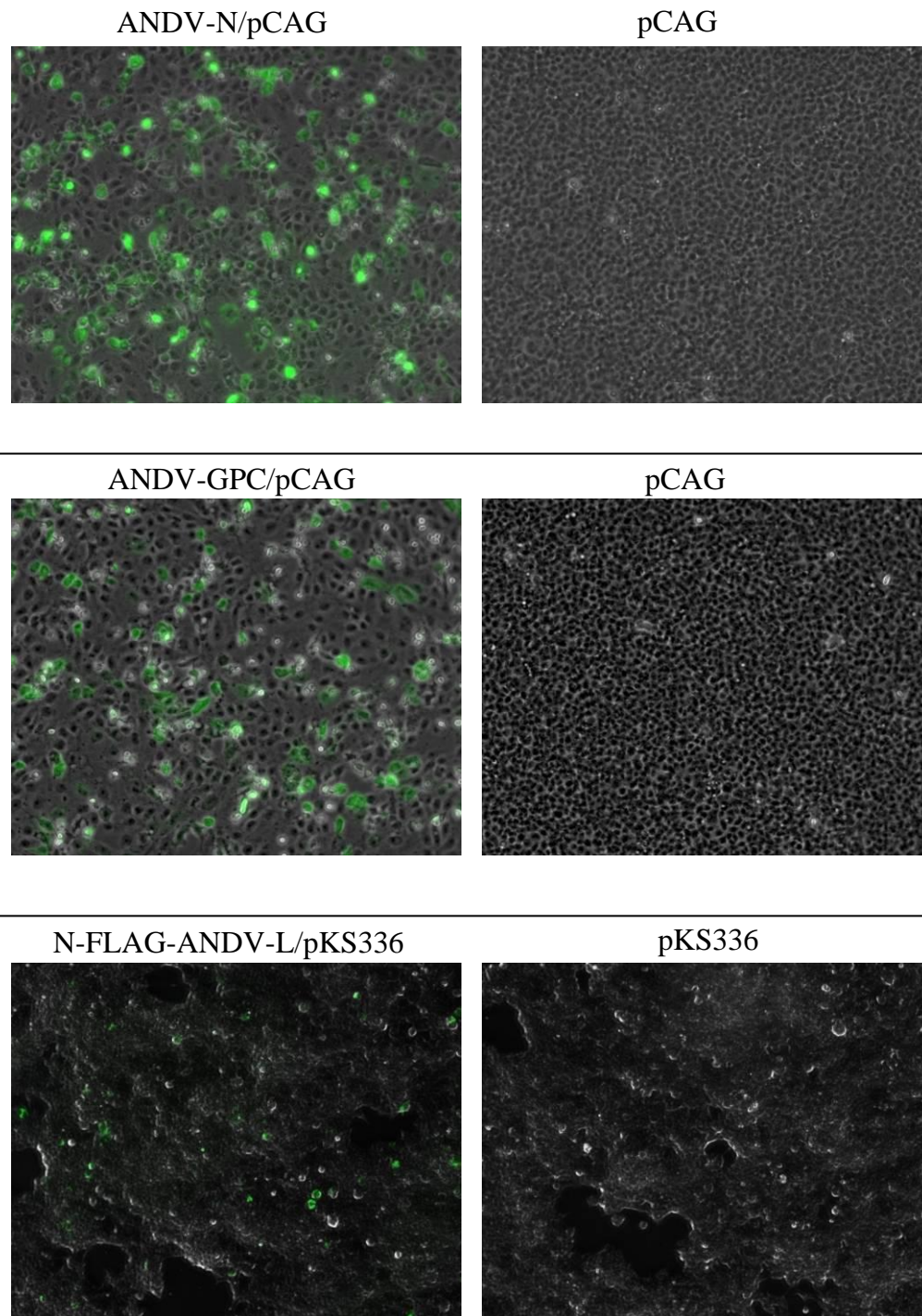


Figure 18. IFA – N, GPC and L Expression Constructs. Confirmation of expression of different ANDV protein expression plasmids using anti-N, G_C or FLAG-specific monoclonal antibodies and anti-mouse Alexa Fluor 488 secondary antibody. VeroE6 cells were used for N and GPC, and 293T cells were used for N-terminal FLAG-tagged L protein. Negative controls were transfected with empty vector. Expression from other N and glycoprotein constructs was equivalent and are not shown. FLAG-tagged L was only detected when expressed from the pKS336 mammalian expression plasmid. pCAG = pCAGGS.

3.2 Cloning and Rescue of Minigenome Constructs

As the first step towards the production of a reverse genetic system, a series of minigenome expression plasmids were created in order to determine if reporter gene expression could be rescued after the addition of the RNP constituents *in vitro*. Previous reports with other *Bunyaviridae* members had suggested that the M segment may have the strongest promoter compared with the other segments (45); therefore, the M segment NCRs were used as the basis for the minigenomes. The NCRs were amplified by RT-PCR from ANDV RNA derived from the Chilean isolate 9717869 and inserted in pATXMCS3. The CAT, LUC or GFP reporter genes were then inserted between the NCRs and cloned into expression vectors containing the T7, Pol I or Pol II RNA polymerase promoters in the anti-sense orientation. All steps of the cloning process were done using type IIS restriction enzymes (BsmBI, BbsI) that cut outside of their recognition site in order to avoid the addition of extraneous sequence into the different expression cassettes.

Based on the previous experiments looking at expression of N protein in different cell lines (Figure 17), COS-7 cells were used for most minigenome rescue attempts, as the expression levels appeared much more controlled in this cell line. However, many different cell lines were also evaluated during the optimization process. For the rescue experiments, one of the minigenome expression vectors was transfected into COS-7 cells with both an N and L expression construct and a T7 polymerase expression construct if necessary. Total amounts of DNA transfected were normalized using empty vector, with negative controls omitting one of the necessary helper proteins.

Results

Positive controls consisted of the reporter gene being expressed from the pCAGGS expression vector. 48-72 hrs post-transfection, cells were either visualized by fluorescence microscopy (GFP), or the cell lysates were collected and analyzed for CAT or LUC expression using the appropriate substrates. To optimize the process, a number of different variables were tested, such as: the ratio of helper and minigenome plasmids, the use of the different expression constructs containing different mammalian or RNA polymerase promoters, the types and concentrations of transfection reagents, as well as the use of different cells lines (Appendix 5). Unfortunately, minigenomes containing the GFP or LUC reporter genes were not successfully rescued. Minigenomes containing the CAT reporter gene were rescued, and are shown in Figure 19. Despite numerous optimization attempts using different experimental conditions, it was incredibly difficult to obtain the same results across multiple identical experiments. This data showed that rescue of the minigenome was possible, but that reproducibility was an issue preventing the further use of the system to address experimental questions. The cause of this problem was most likely insufficient expression of functional L protein. To address this problem, attempts were made to rescue the minigenome reporter using a helper ANDV infection of the transfected cells as a means of providing functional L protein. Unfortunately, ANDV grows very poorly and slowly in cell culture, and the appropriate conditions for both sufficient virus growth and plasmid-based protein expression were difficult to obtain. Also, the use of ANDV required BSL-3 containment, meaning that the GFP reporter gene was the only minigenome construct that could be evaluated due to the

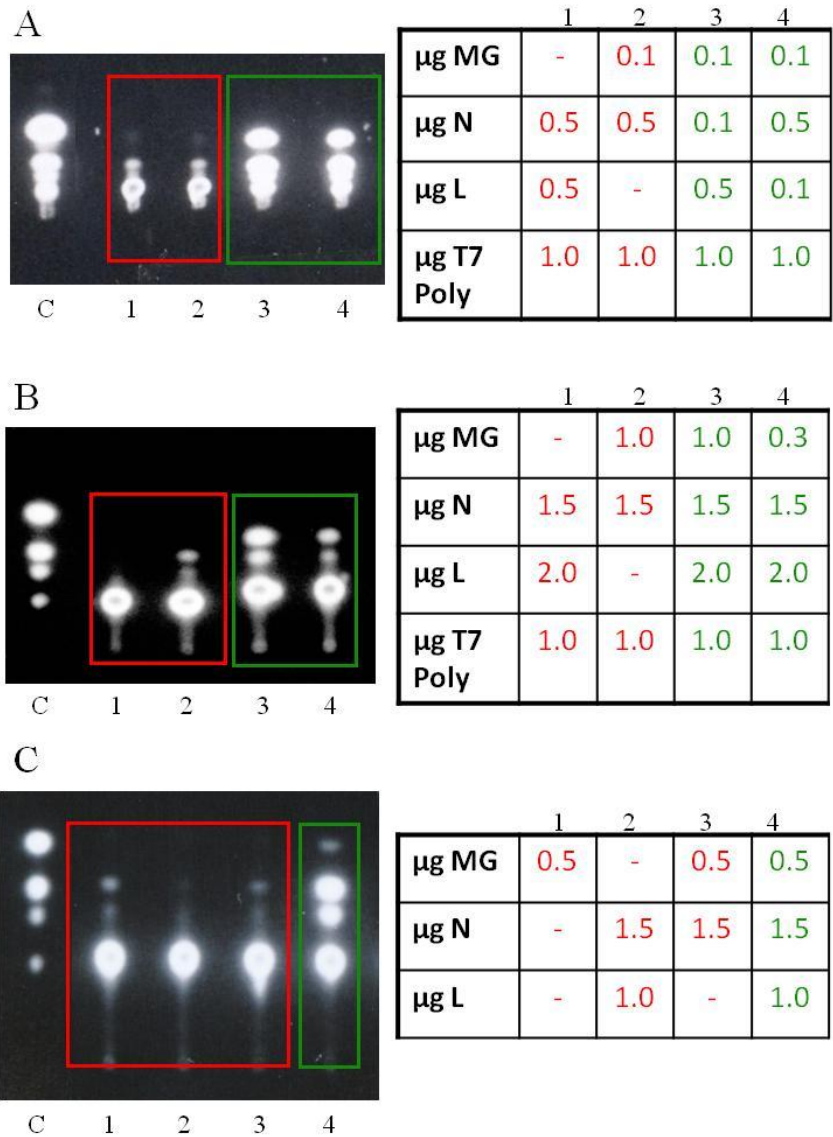


Figure 19. Rescue of CAT Minigenomes. Functional chloramphenicol acetyl transferase (CAT) enzyme acetylates the chloramphenicol substrate using acetyl-CoA. Different acetylation products were separated by thin-layer chromatography (TLC) and visualized using UV light. Red boxes outline negative controls (omitting a plasmid) and green boxes outline positive samples. The first lane in each picture represents the positive control (CAT/pCAGGS, C). (A) Rescue using T7 RNA promoter based minigenome and helper plasmids. (B) Rescue using T7 RNA promoter based minigenome and CMV promoter based helper plasmids. (C) Rescue using Pol I RNA promoter and CMV promoter based helper plasmids. Values in boxes represent amount of plasmid used, expressed in μg . MG = Minigenome, N = Nucleocapsid protein, L = RNA dependent RNA polymerase.

inactivation requirements of taking the cell lysate out of containment, and the lack of required equipment inside.

After many attempts of rescuing the minigenome constructs, it was realized that the system would not be reliable enough to warrant further development of the full-length reverse genetics system. The reproducibility issues suggest that there are some unknown factors about obtaining high levels of expression of functional hantavirus L protein, and seems to be a significant issue with the further development of these systems. Therefore, further vaccine development focused primarily on the recombinant VSV platform.

3.3 Cloning and Rescue of Recombinant VSV

Although non-replication competent recombinant VSV particles pseudotyped with hantavirus glycoproteins provided *in trans* had previously been produced (163, 179), no replication-competent vectors expressing the hantavirus or any other bunyavirus glycoproteins from the viral genome had ever been successfully rescued. The VSV and hantavirus life-cycles follow different pathways, with VSV assembly and budding occurring from the plasma membrane, in contrast to hantaviruses using the Golgi membranes. It was unknown how attenuated the viruses might be, and whether successful rescue of these viruses would even be possible; therefore constructs were made that contained either the ZEBOV or VSV glycoproteins in addition to the ANDV GPC to avoid issues with particle maturation and budding.

Results

To generate the different VSV Δ G constructs, the ZEBOV GP and VSV G ORFs were first PCR amplified and inserted into the XhoI and NheI sites of pVSVXN2 Δ G. Once these constructs were confirmed by nucleotide sequencing, the ANDV GPC ORF was inserted into the constructs containing ZEBOV GP, VSV G or no additional glycoprotein, using the MluI and BlnI sites. The resulting plasmids were referred to as pVSV Δ G/ANDVGPC, pVSV Δ G/ANDVGPC-ZEBOVGP and pVSV Δ G/ANDVGPC-VSVG. Confirmation of all constructs by restriction enzyme digestion is shown in Figure 20.

Constructs were then transfected into a combination of VeroE6 and 293T cells with different amounts of DNA for each expression plasmid, based on amounts that had been previously established by others for successful VSV rescue. The VSV Δ G/ZEBOVGP and VSV wt viruses were successfully rescued by other members of the laboratory group using these methods, and were used as control viruses for all further experiments. The supernatant from transfected cells (p0 plates) was transferred onto fresh VeroE6 cells 3 days post-transfection (p1 plates). Approximately 1 to 2 days after blind passage, the plates infected with supernatants derived from transfections with dual glycoprotein VSV vectors (VSV Δ G/ANDVGPC-ZEBOVGP and VSV Δ G/ANDVGPC-VSVG) showed extensive signs of CPE, signalling successful rescue of these viruses. Both the ZEBOV GP and VSV G are cytotoxic, and the viruses containing these glycoproteins show CPE that was identical to the CPE seen with rescues from single glycoprotein VSV vectors (VSV Δ G/ZEBOVGP and VSV wt).

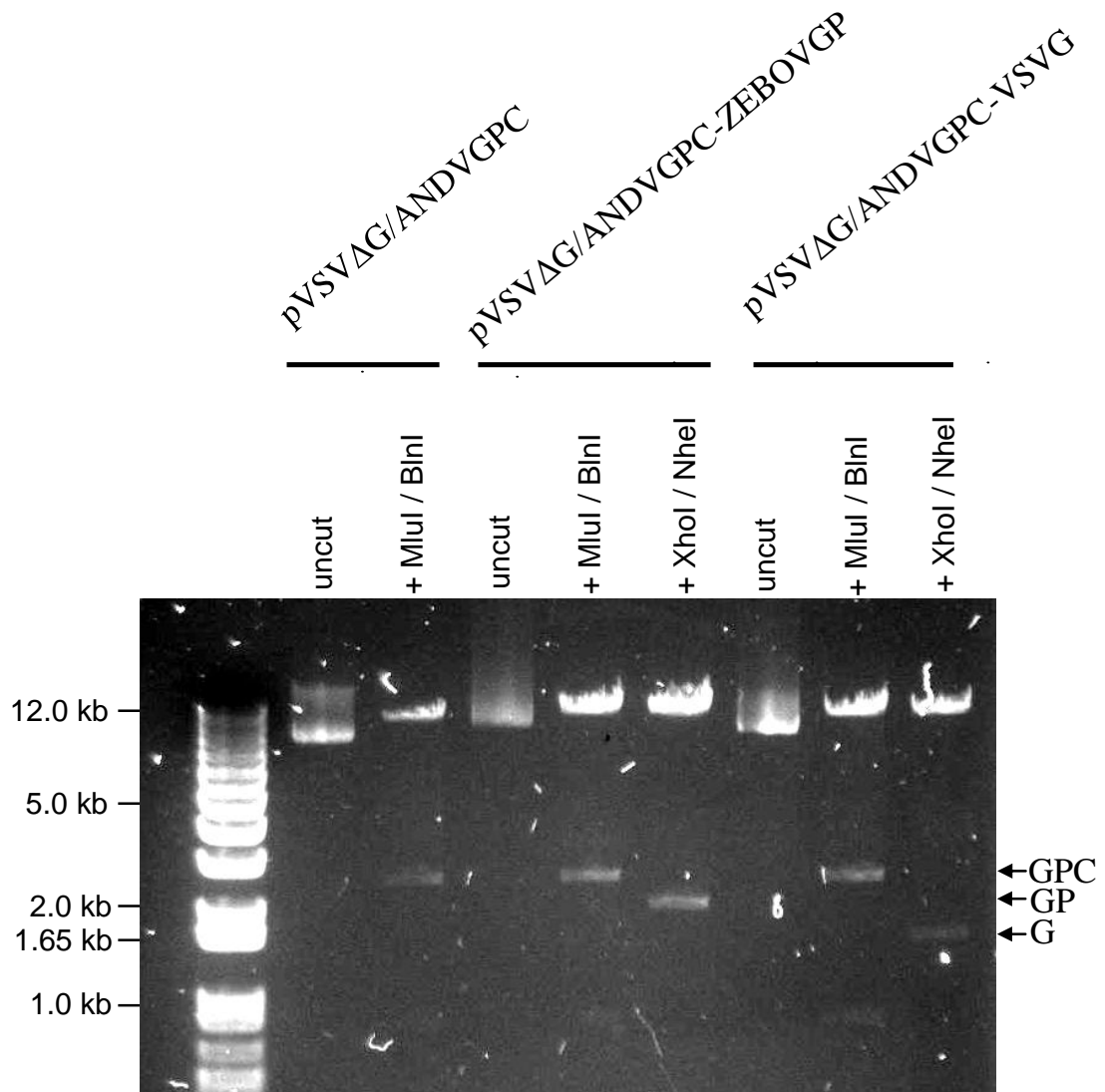


Figure 20. Restriction Enzyme Digest Confirmation – VSV Full Length Constructs. Digestion of the pVSVΔG/ANDVGPC, pVSVΔG/ANDVGPC-ZEBOVGP and pVSVΔG/ANDVGPC-VSVG full length VSV expression plasmids opening reading frames (ORFs) for the Andes virus glycoprotein precursor (ANDV GPC), Zaire ebolavirus glycoproteins (ZEBOV GP) or vesicular stomatitis virus glycoprotein (VSV G) with restriction enzymes used for cloning and digestion indicated at top. Top bands represent the full length plasmid and bottom bands represent the glycoprotein ORFs. 1 Kb Plus DNA ladder is used on left hand side and values are expressed in kilobases (kb).

Results

Initial attempts at rescuing VSVΔG/ANDVGPC were unsuccessful, and no CPE was seen in either the p0 or p1 plates. Based on information that successful rescue of VSVΔG containing the Lassa virus glycoproteins took a much longer incubation time of 1-2 weeks instead of 3 days (personal communication, Heinz Feldmann), the p0 plates containing VSVΔG/ANDVGPC were allowed to incubate for a longer period of time, with supernatant being transferred at 5, 7, 10 and 14 days. Rescue of VSVΔG/ANDVGPC was successful in all plates that were incubated for a minimum of 7 days before supernatant transfer, and CPE was seen in the p1 plates within 2-4 days. Unlike ZEBOV GP and VSV G, the ANDV glycoproteins are not inherently cytotoxic and therefore CPE takes longer to develop. This may be caused by another cytotoxic VSV protein, such as the M protein (103), or because of differences in replication between the viruses. Confirmation of successful rescue was done by western blot and RT-PCR of clarified supernatants, as shown in Figures 21 and 22. Titres of viral stocks were obtained by plaque assay, and are shown below in Table 9. Titres obtained for VSVΔG/ANDVGPC were typically lower compared to the other viruses and the inclusion of the ANDV GPC with either the ZEBOV GP or VSV G glycoproteins typically resulted in a lower titre when compared to the individual viruses without it.

Table 9. VSV titres

Virus Name	Glycoprotein 1	Glycoprotein 2	Titre (PFU/ml)
VSVΔG/ANDVGPC	ANDV GPC	---	2.2×10^6
VSVΔG/ANDVGPC-ZEBOVGP	ANDV GPC	ZEBOV GP	7.2×10^6
VSVΔG/ANDVGPC-VSVG	ANDV GPC	VSV G	5.4×10^7
VSVΔG/ZEBOVGP	ZEBOV GP	---	5×10^7
VSV wt	VSV G	---	3×10^8

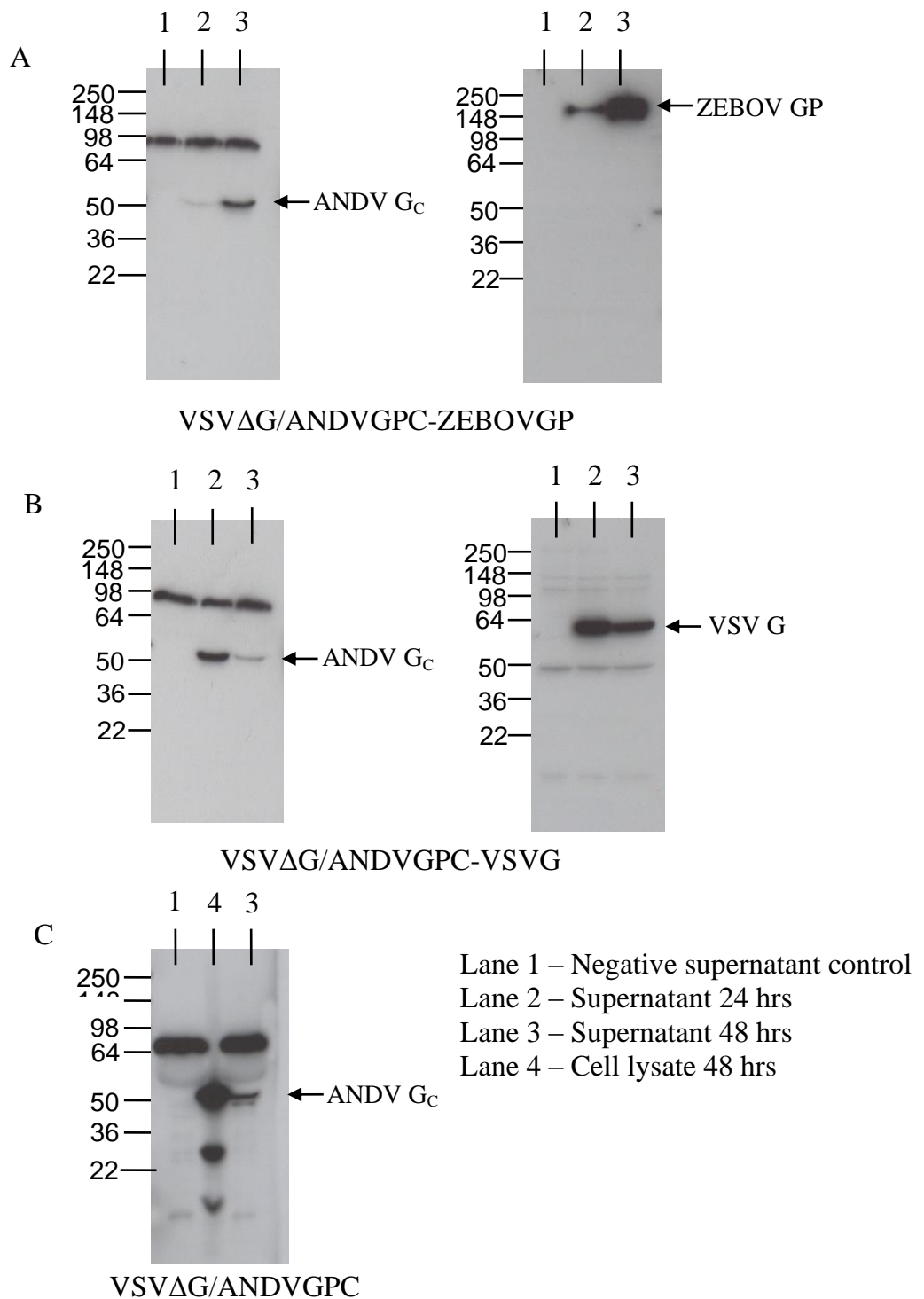
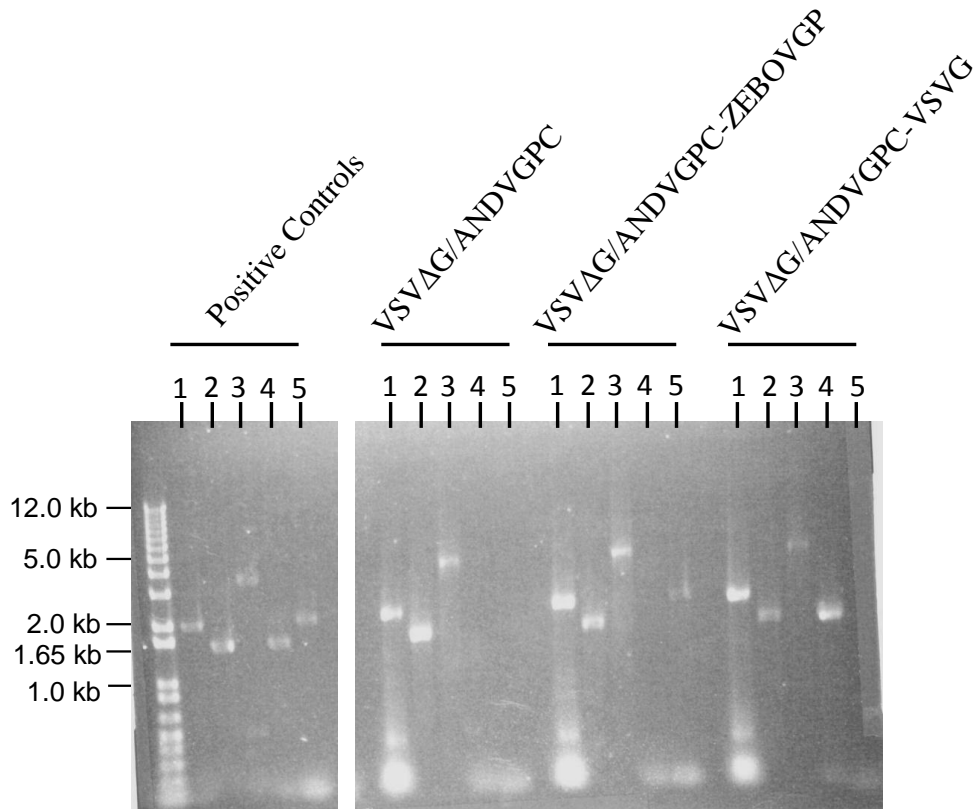


Figure 21. Western Blot – Rescue of Recombinant VSV. Confirmation of rescue of VSV containing the Andes virus glycoproteins (VSVΔG/ANDVGPC) alone, or in conjunction with Zaire ebolavirus glycoproteins (VSVΔG/ANDVGPC-ZEBOVGP) or VSV wild-type glycoprotein (VSVΔG/ANDVGPC-VSVG). Molecular weight (MW) is indicated on the left hand side of each blot and is expressed in kiloDaltons.



Primers used:

1. ANDV G_N
2. ANDV G_C
3. ANDV GPC
4. VSV G
5. ZEBOV GP

Figure 22. RT-PCR – Rescue of Recombinant VSV. Confirmation of the rescue of different recombinant VSVs by extracting viral RNA from clarified supernatant and using RT-PCR with Andes virus glycoprotein precursor (GPC), individual ANDV G_N & G_C glycoproteins, vesicular stomatitis glycoprotein (VSV G) or Zaire ebolavirus glycoprotein (ZEBOV GP) specific forward and reverse primers as shown in the legend. Positive controls consist of the PCR of DNA vectors containing the different genes using the same forward and reverse primers.

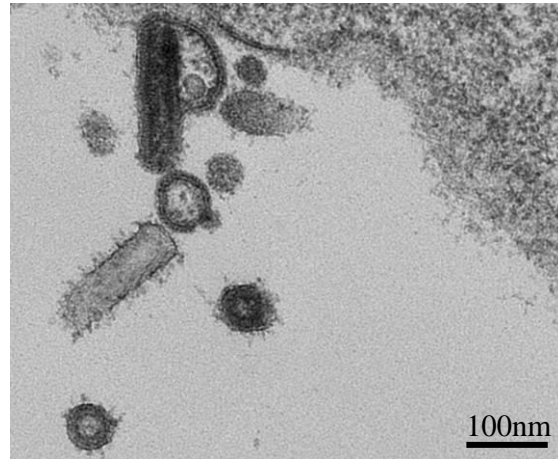
3.4 *In Vitro* Characterization of Recombinant VSV Vaccine

After successful rescue of the VSV Δ G/ANDVGPC virus, it was decided that this virus would be the ANDV vaccine of choice, as it contains only the ANDV glycoproteins. Both the VSV wt and VSV Δ G/ZEBOVGP viruses were used as controls throughout the various experiments, and the inclusion of either the VSV or ZEBOV glycoproteins in the vaccine construct would have made interpretation of the results difficult. In order to carry out any protection studies with the vaccine, it was first necessary to characterize the VSV Δ G/ANDVGPC *in vitro*.

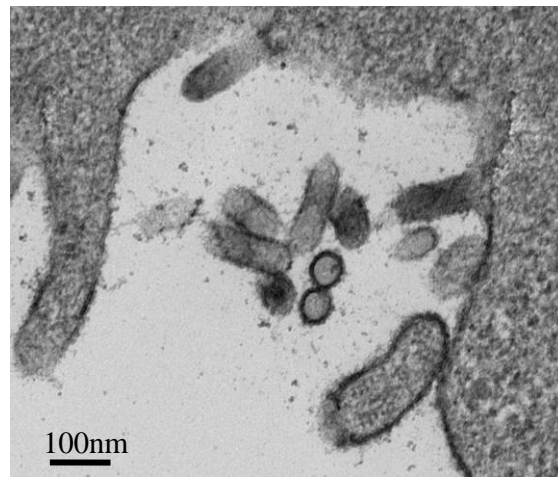
3.4.1 TEM Imaging of VSV

To verify that the rescued viruses had the typical bullet-shaped VSV particle morphology, VeroE6 cells grown on thermanox coverslips or in T75 flasks were infected with VSV Δ G/ANDVGPC, VSV Δ G/ZEBOVGP or VSV wt. Cells grown on coverslips were used to visualize intracellular virus particles and virus being released from the plasma membrane, as shown in Figure 23. Supernatants from T75 flasks were first purified on a 20% sucrose cushion to remove any cellular debris and then used to visualize released virus particles, as shown in Figure 24. Purified virus particles were also confirmed with western blot using glycoprotein-specific monoclonal antibodies to ensure that there was no-cross contamination between the different viruses, as shown in Figure 25. All images showed virus particles with a bullet-shaped morphology and a glycoprotein fringe around the exterior of the particle, suggesting little difference between VSV Δ G/ANDVGPC, VSV Δ G/ZEBOVGP and wild-type virus. A number of

VSV Δ G/ANDVGPC



VSV wt



VSV Δ G/ZEBOVGP

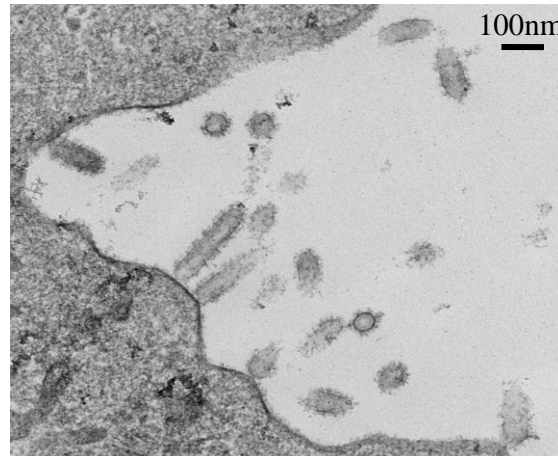
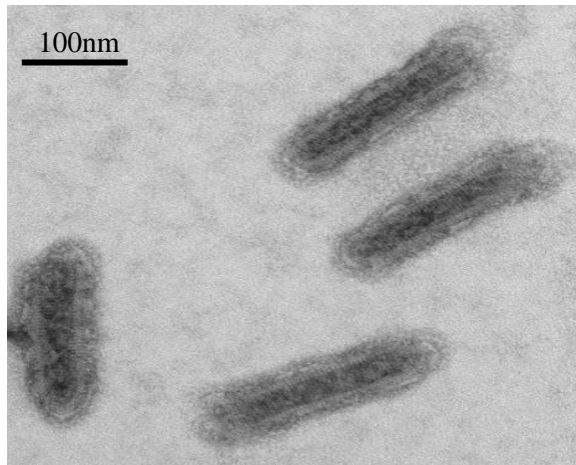
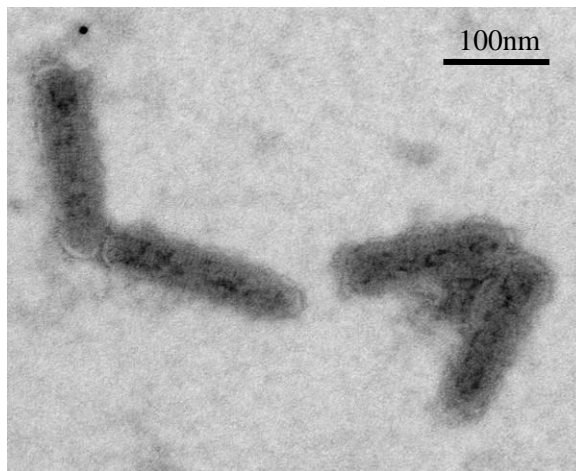


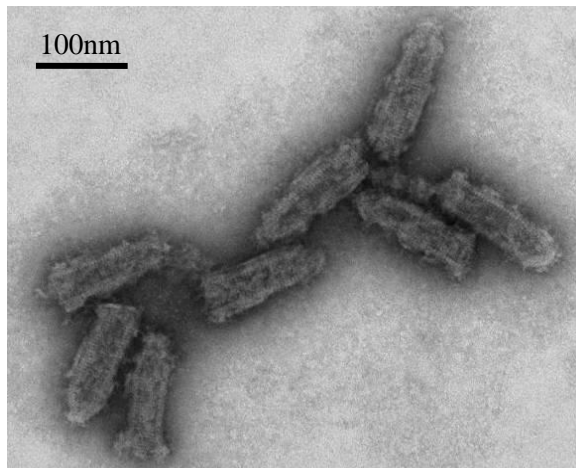
Figure 23. TEM – Recombinant VSV Infected Cell Monolayer. VeroE6 cells plated on Thermanox coverslips were infected with VSV expressing the ANDV glycoproteins (VSV Δ G/ANDVGPC), the Zaire ebolavirus glycoproteins (VSV Δ G/ZEBOVGP), or VSV wild-type (wt) fixed and visualized by transmission electron microscopy (TEM). Bullet-shaped particles were visualized budding from the cell plasma membrane. The scale is indicated in a corner of each panel with bar representing 100 nanometres (nm).



VSVΔG/ANDVGPC



VSV wt



VSVΔG/ZEBOVGP

Figure 24. TEM – Purified Recombinant VSV. 20% sucrose cushion purified VSV expressing the ANDV glycoproteins (VSVΔG/ANDVGPC), the Zaire ebolavirus glycoproteins (VSVΔG/ZEBOVGP), or VSV wild-type (wt) were fixed and visualized with transmission electron microscopy (TEM). Bullet-shaped particles can be visualized with glycoprotein fringe surrounding each particle. The scale is indicated in the corner with the bar representing 100 nanometres (nm).

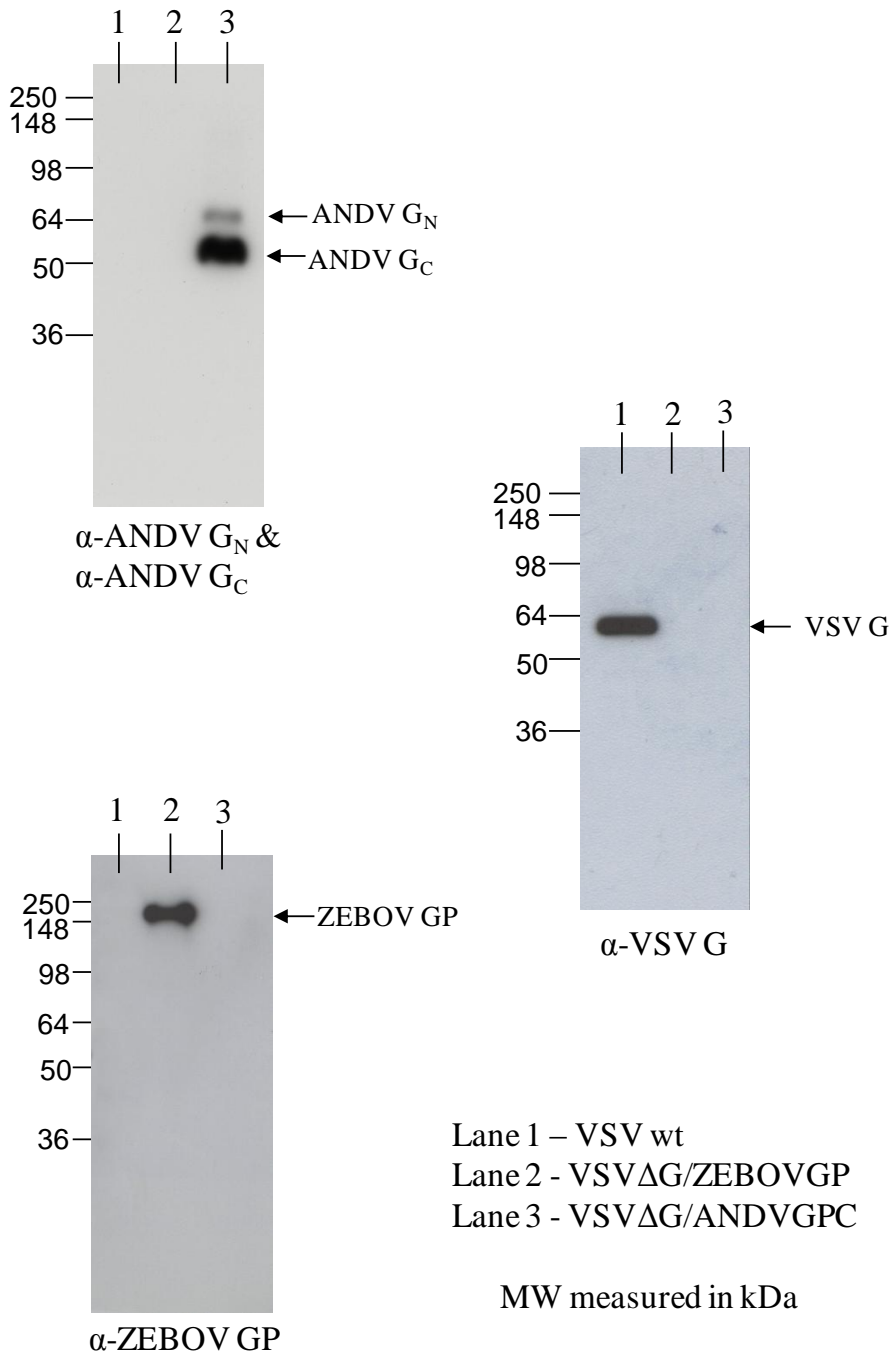


Figure 25. Western Blot – Purified Recombinant VSV. Western blot analysis of 20% sucrose purified virus particles using VSV expressing the ANDV glycoproteins (VSVΔG/ANDVGPC) the Zaire ebolavirus glycoproteins (VSVΔG/ZEBOVGP) or wild-type VSV glycoprotein (G) using glycoprotein-specific monoclonal antibodies. Molecular weight (MW) is indicated on the left hand side of each blot and is expressed in kiloDaltons (kDa).

different attempts were made to use immuno-EM to label the ANDV glycoproteins with gold-labelled antibodies in order to visualize the ANDV glycoproteins and compare glycoprotein incorporation to the other viruses, but all attempts were unsuccessful. A number of different fixation methods were attempted, including various amounts of glutaraldehyde, PFA: alone and in conjunction with inactivation by gamma-irradiation. It appears that these fixation methods are incompatible with our commercial antibodies, and no other vendor supplies antibodies against the ANDV glycoproteins. Additional attempts using hamster serum containing anti-ANDV glycoprotein antibodies were also unsuccessful, partially due to the extraneous material in the serum and the lack of commercially available anti-hamster gold-labelled secondary antibodies.

3.4.2 Growth Kinetic Analysis of VSV

To get an idea of how quickly the different recombinant VSVs replicate in comparison to one another, the growth kinetics of the different viruses were compared over a 48 hr (high MOI) or 96 hr (low MOI) period, with samples being collected at different time points. Virus titres were calculated by using the TCID₅₀ assay and expressed as TCID₅₀/ml. 4 different viruses were compared; VSV wt, VSVΔG/ANDVGPC, VSVΔG/ANDVGPC-ZEBOVGP and VSVΔG/ZEBOVGP. At a “high” MOI of approximately 1, all viruses grew at a similar level, with very little discernable difference between viruses, except for VSV wt, as shown in Figure 26A. Therefore, the experiment was repeated at a “low” MOI of approximately 10⁻⁴, as shown in Figure 26B. At a low MOI, the VSV wt titre began to rise between 3 and 6 hrs and

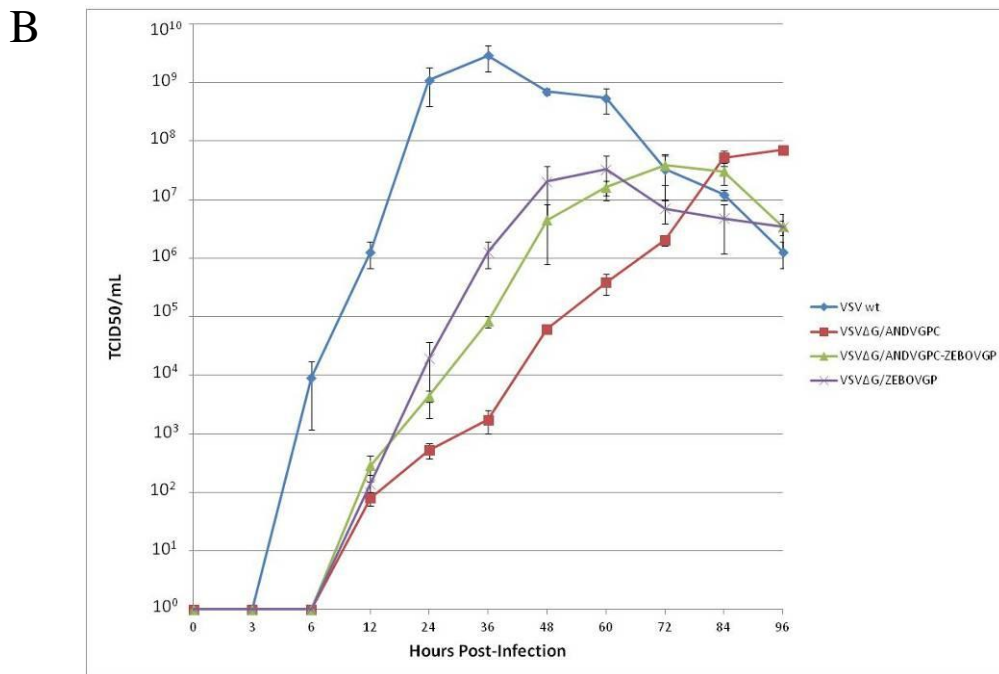
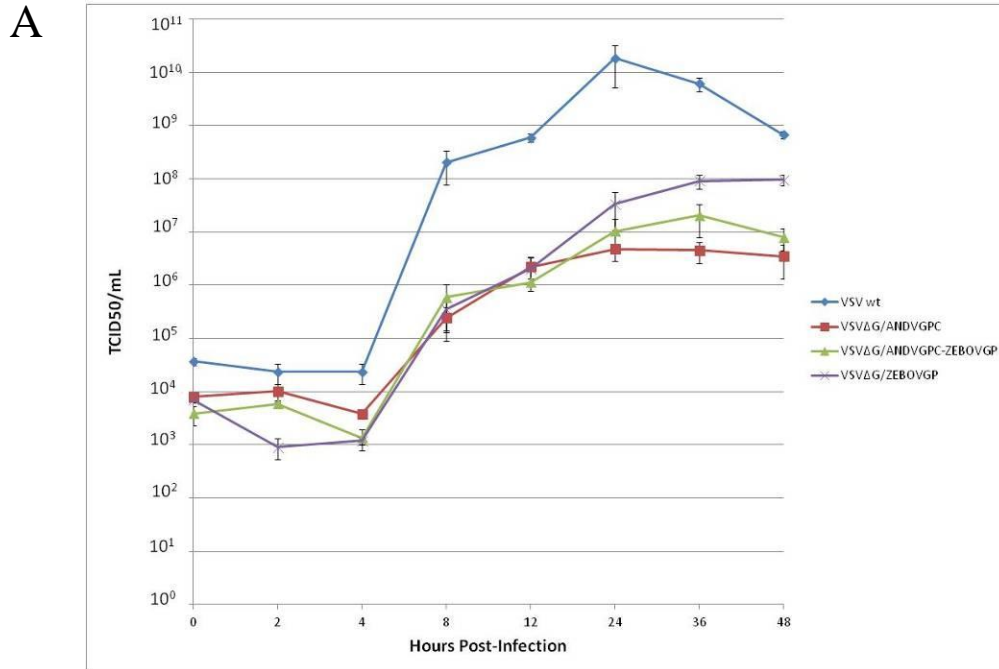


Figure 26. Recombinant VSV Growth Kinetic Study. (A) Growth kinetic comparison of VSV wild-type (wt), or VSV containing the ANDV glycoproteins (VSVΔG/ANDVGPC), the Zaire ebolavirus glycoproteins (VSVΔG/ZEBOVGP) or both (VSVΔG/ANDVGPC-ZEBOVGP) at a high multiplicity of infection (MOI) of 1. (B) The same comparison of viruses at a low MOI of 10^{-4} . Each time point was collected in triplicate, and 50% tissue culture infectious dose (TCID₅₀) analysis was carried out in quadruplicate. Error bars represent the standard error of the mean.

reached a maximal peak of around 3×10^9 by 36 hrs. In comparison, the other viruses began to rise between 6 and 12 hrs and reached a maximal peak of between 10^7 and 10^8 for VSV Δ G/ZEBOVGP at 60 hrs, VSV Δ G/ANDVGPC at 96 hours and the VSV Δ G/ANDVGPC-ZEBOVGP virus at 72 hrs post-infection. Although all three viruses appear to be greatly attenuated compared to VSV wt, it is unclear if this reflects a reduction in viral entry, replication or budding. The maximum titre for each virus corresponds to the maximum amount of CPE and destruction of the cell monolayer. Reductions in titres following this point are most likely due to a lack of viable cells to continue to maintain production of infectious virus and the degradation of infectious virus particles contained in the supernatant.

3.5 *In Vivo* Protection Studies

3.5.1 Vaccine Efficacy Against Lethal ANDV Challenge

Once the viruses were characterized *in vitro*, the VSV Δ G/ANDVGPC virus was tested for its efficacy as an ANDV vaccine in the lethal Syrian hamster model. For the *in vivo* work, DMEM and/or VSV Δ G/ZEBOVGP were used as negative controls. In contrast to the recombinant VSV vaccine vectors (VSV Δ G/ANDVGPC and VSV Δ G/ZEBOVGP), which are attenuated and cause no detectable signs of illness in the hamsters, VSV wt has been demonstrated to be highly lethal in Syrian hamsters at even low doses, and therefore could not be used as a negative control (49, 50).

For the initial protection study, two groups of hamsters were immunized with 10^5 PFU of either VSV Δ G/ANDVGPC (n=18, study virus) or VSV Δ G/ZEBOVGP

Results

(n=15, control virus) using the i.p route at two different injection sites. 28 days after immunization, both groups of hamsters were challenged with a lethal dose of 100 x LD₅₀ (approximately 154 FFU) via the i.p route using two different injection sites, as described previously (186). Although ANDV has been shown to be lethal through a variety of different injection routes (79), the i.p route was chosen. Serum samples were collected from each animal by retro-orbital bleeding immediately before challenge to measure the immune responses. 3 hamsters from each group were euthanized at 5 and 8 days post-challenge (6 animals per group total) to measure the level of ANDV replication, leaving 12 and 9 hamsters in the VSVΔG/ANDVGPC and control groups to monitor survival. All hamsters immunized with VSVΔG/ANDVGPC showed no signs of disease and survived the challenge, as shown in Figure 27. All control hamsters died between days 8 and 11, showing signs of disease, such as respiratory problems, beginning with rapid, shallow breathing that quickly advanced to severe dyspnea, a rapid decrease in activity levels and grooming after the onset of symptoms and the presence of blood around the nostrils and mouth in some animals. All surviving hamsters were monitored for 45 days after challenge for any delayed signs of illness. Hamsters were then euthanized using exsanguination via cardiac puncture, with serum samples collected to measure immune responses.

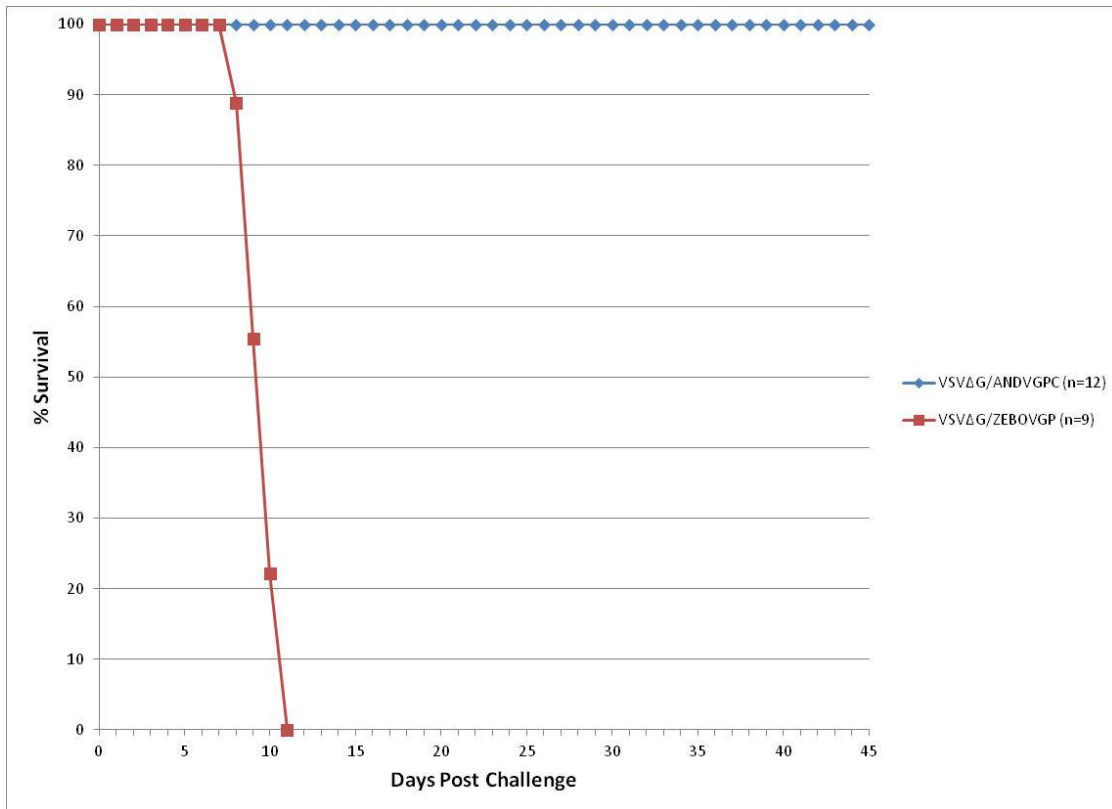


Figure 27. Vaccine Protection Study. 18 hamsters were immunized with 10^5 plaque forming units (PFU) of VSV containing the ANDV glycoproteins (VSVΔG/ANDVGPC, study vaccine), and 15 hamsters were immunized with the Zaire ebolavirus glycoproteins (VSVΔG/ZEBOVGP, control), both through the intraperitoneal (i.p) route. 6 animals from each group were euthanized for tissue collection at days 5 and 8, leaving 12 and 9 animals in each group, respectively. 28 days after immunization, all hamsters were challenged with 100 times the 50% lethal dose ($100 \times LD_{50}$) of ANDV i.p. and monitored for survival. Controls died between days 8 and 11.

3.5.2 Detection and Quantification of ANDV Replication

3.5.2.1 ANDV RNA

To measure the amount of ANDV replicating in infected hamsters, lungs, liver and blood were collected from the hamsters euthanized at 5 and 8 days after challenge. RNA was extracted from these different tissues and used in qRT-PCR using ANDV S-segment specific probe/primers to detect and quantify ANDV RNA. All animals immunized with VSV Δ G/ANDVGPC showed no detectable ANDV RNA in any of the tissues tested at either 5 or 8 days post-challenge, shown in Figure 28. In contrast, the control immunized animals showed the presence of ANDV RNA in all samples tested, with an increase of approximately 0.5 to 1 log base between 5 and 8 days. The amount of ANDV RNA was quantified using a standard curve created from 10-fold serial dilutions of ANDV with a known infectious titre. Although the amount of ANDV RNA may not directly correlate with the infectious titres due to the presence of defective viral particles, it was sufficient for a relative comparison between the samples.

3.5.2.2 N Protein-Specific Seroconversion

As an indirect measure of ANDV replication by looking at the immune response against the virus, serum samples were collected from all hamsters both immediately pre-challenge, as well as 45 days post-challenge from all survivors. An ELISA using bacterially expressed, recombinant SNV N was used to detect and quantify the presence of ANDV N-specific IgG antibodies. Antibodies against the N protein of most Old and New World hantaviruses are cross-reactive, and therefore the production of a specific

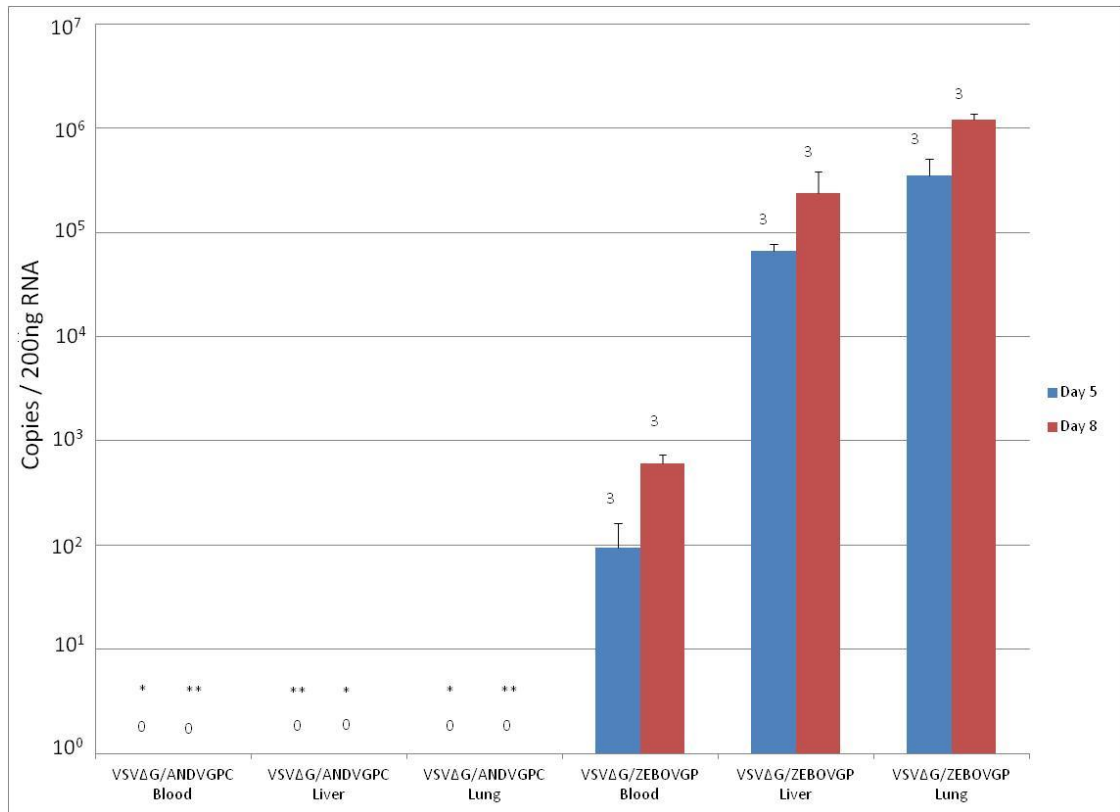


Figure 28. Detection of ANDV RNA. At 5 and 8 days post-challenge, 3 animals from each group were euthanized and 3 tissues from each animal (blood, liver and lung) were analyzed by quantitative real-time RT-PCR (qRT-PCR) using ANDV S segment-specific primer/probe for the presence of ANDV RNA. Tissue samples were normalized to 200ng of RNA per reaction. The data represents the average of a triplicate analysis of tissues from 3 animals per group. Numbers above bars represent number of hamsters positive for ANDV RNA in each group (n=3). Error bars represent 2 times the standard error of the mean (* = $p < 0.05$, ** = $p < 0.001$, Student's t-test).

recombinant ANDV N protein was unnecessary. The results from the ELISA are shown in Figure 29. All samples were screened at a dilution of 1:40, and positive samples were diluted out using 2-fold serial dilutions until the endpoint was reached. As expected, the serum samples collected pre-challenge in both groups were uniformly negative due to no previous exposure to ANDV. No serum samples were collected from the control groups post-challenge as there were no hamsters that survived challenge. Serum samples collected post-challenge from the VSV Δ G/ANDVGPC immunized group showed either no (n=9) or low (n=3) levels of ANDV N seroconversion. ELISA testing of human diagnostic samples typically set a cut-off of 1:100 as a positive sample, and all 3 samples remain below this level, questioning the significance of those results. Overall, the data from this experiment combined with the data from the previous section suggests a mostly sterile immunity, with little or no ANDV replicating in hamsters that had previously been immunized with the VSV Δ G/ANDVGPC vaccine.

3.5.3 Measurement of Immune Response

3.5.3.1 Humoral Response - Neutralizing Antibodies

Previous studies with DNA-based vaccines have shown that a neutralizing antibody response against the ANDV glycoproteins can be an important mechanism for protection (79). In order to detect and quantify the presence of ANDV neutralizing antibodies, a PRNT₈₀ assay was done using the recombinant VSV Δ G/ANDVGPC virus as the virus to be neutralized. The results of the PRNT₈₀ are shown in Figure 30. Pre-challenge serum samples collected from the control group showed no detectable ANDV

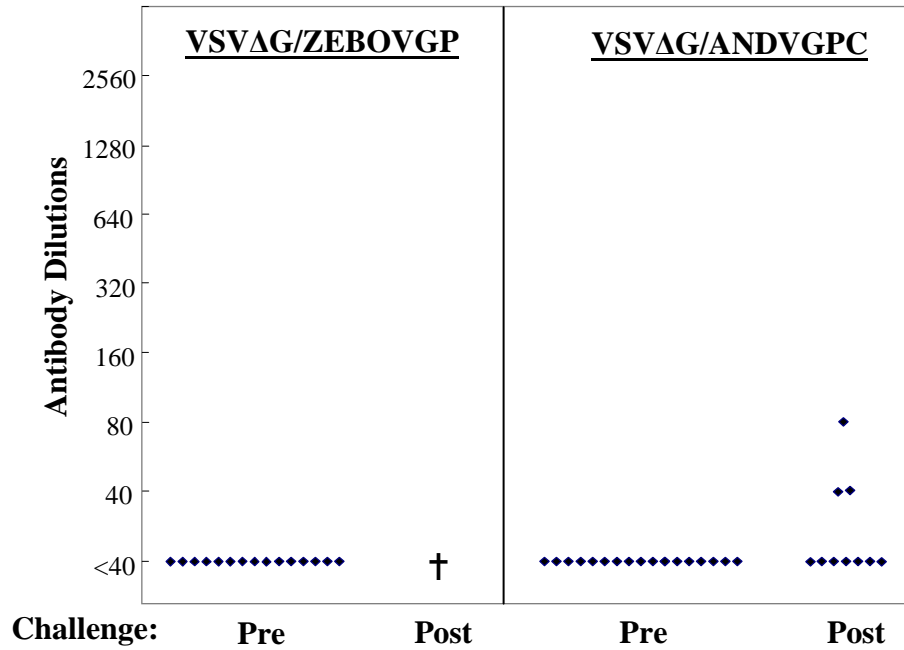


Figure 29. N Protein-Specific Seroconversion. Serum samples were collected from hamsters from both study (VSVΔG/ANDVGPC) and control (VSVΔG/ZEBOVGP) groups immediately before challenge (28 days post-immunization, Pre) and 45 days post-challenge from all surviving animals (Post). All samples were screened at a dilution of 1:40 using N-specific ELISA and were considered negative if there was no reaction. Positive samples were diluted out until an endpoint was reached. Recombinant N was used as the ELISA antigen. Each dot represents an individual animal. † indicates no surviving animals in group.

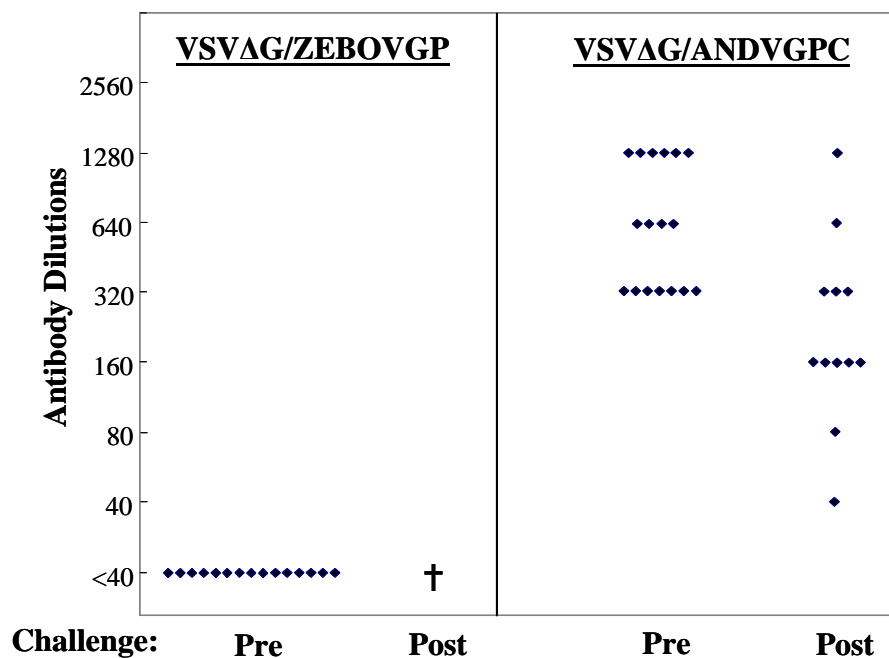


Figure 30. ANDV Glycoprotein Neutralizing Antibodies. Serum samples were collected from hamsters from both study (VSVΔG/ANDVGPC) and control (VSVΔG/ZEBOVGP) groups immediately before challenge (28 days post-immunization, Pre) and 45 days post-challenge from all surviving animals (Post). All samples were screened at a dilution of 1:40 using 80% plaque reduction neutralization (PRNT₈₀) and were considered negative if there was less than 80% neutralization. Positive samples were diluted out until an endpoint was reached. Recombinant VSVΔGANDVGPC was used as the antigen. Each dot represents an individual animal. † indicates no surviving animals in group.

neutralizing antibodies, as expected. Post-challenge serum samples were not collected from the control group, as there were no hamsters that survived challenge. Pre-challenge serum samples collected from the VSVΔG/ANDVGPC immunized group showed high levels of neutralizing antibodies, with titres between 320 and 1280. The titres showed a slight decrease when measured in the post-challenge samples. Although these results are in agreement with those seen in the DNA-based studies, they are in contrast to the Ad5-based vaccine study, where little or no neutralizing antibodies were detected (79, 186). Overall, neutralizing antibodies appear to be an important mechanism of protection for the VSVΔG/ANDVGPC vaccine platform.

3.5.3.2 Validation of Assay

The PRNT₈₀ assay done with VSVΔG/ANDVGPC was chosen over the neutralization of native ANDV for a number of reasons. First, ANDV does not plaque, and therefore requires a much more time-consuming FRNT₈₀ assay that requires staining of the infected cells with an ANDV N antibody, followed by a peroxidase-labelled secondary antibody with the appropriate substrate. ANDV also grows very slowly in cell culture, and the assay requires 8-10 days of incubation time. VSVΔG/ANDVGPC will plaque, and therefore only needs to be stained with crystal violet in order to visualize the plaques, which requires an incubation time of only 2-3 days before analysis. Finally, all work with ANDV is required to be completed in BSL-3, whereas VSVΔG/ANDVGPC can be worked with in an enhanced BSL-2. Unfortunately, because the VSVΔG/ANDVGPC was used for the initial immunization, there was a chance that

Results

neutralizing antibodies may be directed towards another part of the VSV vector. Therefore, we validated our choice of the PRNT₈₀ assay by completing the FRNT₈₀ with a subset of our samples, shown below in Table 10. The neutralization titres obtained with the serum samples against ANDV were all either identical or within +/- 1 dilution factors compared to the titres obtained with the same samples against VSVΔG/ANDVGPC, which could be accounted for by simple experimental variation. In addition, the serum samples from VSVΔG/ANDVGPC immunized hamsters did not neutralize VSVΔG/ZEBOVGP or VSV wt, whereas the serum samples from the VSVΔG/ZEBOVGP immunized control did neutralize VSVΔG/ZEBOVGP. Finally, serum containing antibodies directed against ANDV (taken from initial LD₅₀ experiments) was able to successfully neutralize VSVΔG/ANDVGPC at a titre of 160, but had no effect on either VSVΔG/ZEBOVGP or VSV wt. All of the data taken together show that the neutralization response is glycoprotein-specific, and that VSVΔG/ANDVGPC is a valid substitute for ANDV in our assays.

Table 10. Comparison of VSVΔG/ANDVGPC and ANDV Neutralization Titres

Serum Sample	VSVΔG/ANDVGPC PRNT ₈₀	ANDV FRNT ₈₀
1	320	320
2	640	320
3	320	320
4	80	160
5	40	80
6	1280	640
7	160	160
8	160	80
9	160	160
10	160	320
11	320	320
12	160	160

3.6 Time to Protection and Post-Exposure Vaccine Efficacy

After demonstrating that the VSV Δ G/ANDVGPC fully protected hamsters from lethal ANDV challenge when administered 28 days before challenge, the next step was to identify the efficacy of the vaccine when given at time points closer to challenge, or when given post-exposure.

3.6.1 Time to Protection Survival Study

For the time to protection study, groups of hamsters were immunized with VSV Δ G/ANDVGPC (n=10 per time point, study virus), VSV Δ G/ZEBOVGP (n=6 per time point, control virus) or DMEM (n=3 per time point, control) at 14, 7 and 3 days prior to lethal ANDV challenge. Blood samples were collected by retro-orbital bleeding immediately prior to challenge, or 45 days post-challenge by cardiac puncture from all surviving hamsters to monitor the immune responses. As shown in Figure 31, all hamsters immunized with VSV Δ G/ANDVGPC survived challenge when immunized at 14, 7 or 3 days before challenge, with no signs of disease. All hamsters receiving DMEM control showed signs of disease, and died between days 9 and 10 for all time points tested. All hamsters receiving the VSV Δ G/ZEBOVGP control vaccine 14 days before challenge died between days 8 and 12. Interestingly, 3/6 hamsters receiving the vaccine 7 days before challenge and 5/6 hamsters receiving it at 3 days before challenge survived lethal challenge, with only some animals showing signs of disease. All hamsters were monitored for 45 days after challenge for delayed signs of disease. This result was unexpected, and suggests that the VSV Δ G/ZEBOVGP vaccine induces a

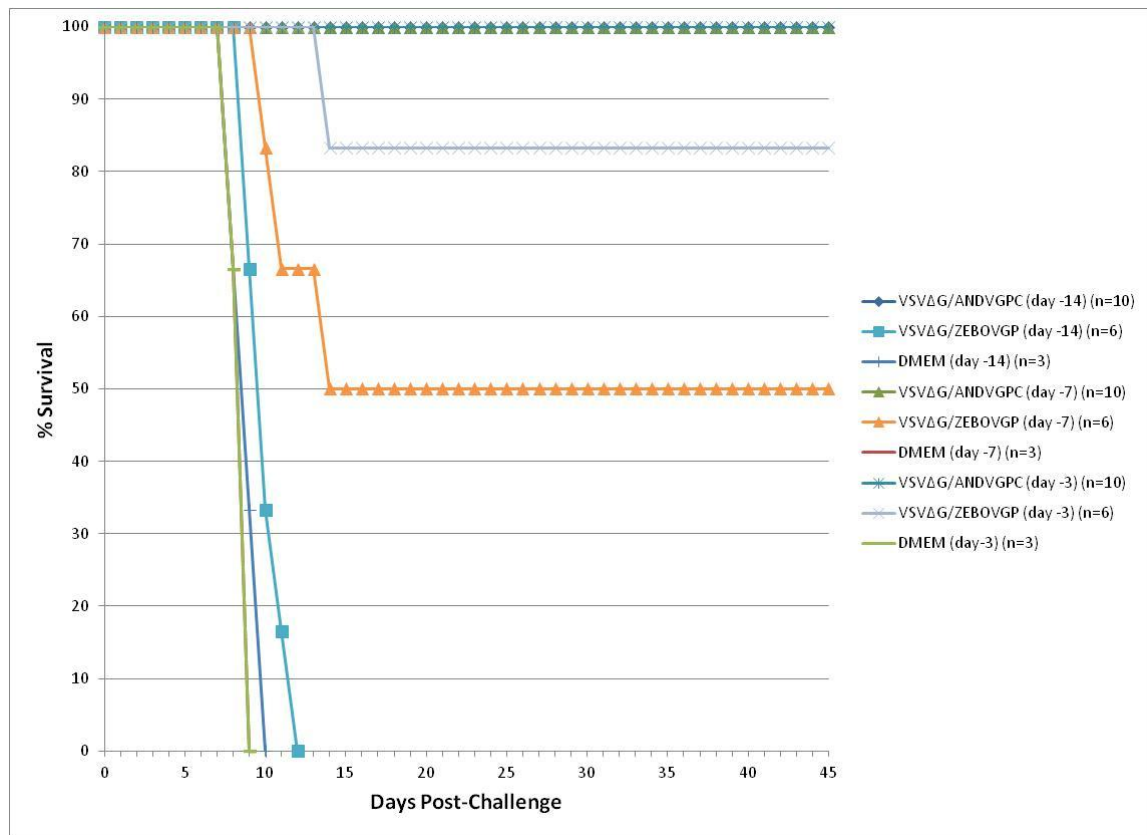


Figure 31. Time to Protection Study. Hamsters were immunized with 10^5 plaque forming units (PFU) of VSV containing the ANDV glycoproteins (VSVΔG/ANDVGPC, study virus), the Zaire ebolavirus glycoproteins (VSVΔG/ZEBOVGP, control) or Dulbecco's Modified Eagle's Medium (DMEM, control) through the intraperitoneal (i.p) route. All hamsters were challenged with 100 times the 50% lethal dose ($100 \times LD_{50}$) of ANDV i.p. 14, 7 or 3 days post-immunization and monitored for survival. Controls died between days 8 and 12.

fairly strong immunogen-independent effect against heterologous ANDV challenge if given shortly before challenge, most likely indicating strong innate immune responses.

3.6.2 Post-Exposure Survival Study

For the post-exposure study, hamsters were put in the same 3 groups described in the previous section. All groups were challenged with ANDV at day 0 then given either the study or control VSV vaccine or DMEM at 1, 3 or 5 days post-challenge. As shown in Figure 32, hamsters receiving the VSV Δ G/ANDVGPC vaccine showed a 90% rate of survival when injected at 1 day post-challenge, but no protection when given at 3 days post-challenge. In contrast, 100% of hamsters receiving the VSV Δ G/ZEBOVGP vaccine at 1 day post-challenge survived lethal ANDV challenge, with 4/6 surviving when injected 3 days post-challenge. All hamsters receiving either the VSV Δ G/ANDVGPC or VSV Δ G/ZEBOVGP vaccines at 5 days post-challenge did not survive. Any hamsters receiving the DMEM control did not survive lethal challenge at any of the time points tested, with animals dying between days 8 and 10. All hamsters were monitored for 45 days post-challenged for delayed signs of disease. This result was also unexpected, but taken with the time to protection data, confirms that VSV Δ G/ZEBOVGP is capable of protecting against lethal ANDV challenge using a non-specific immune stimulation, most likely through the strong induction of innate immune responses.

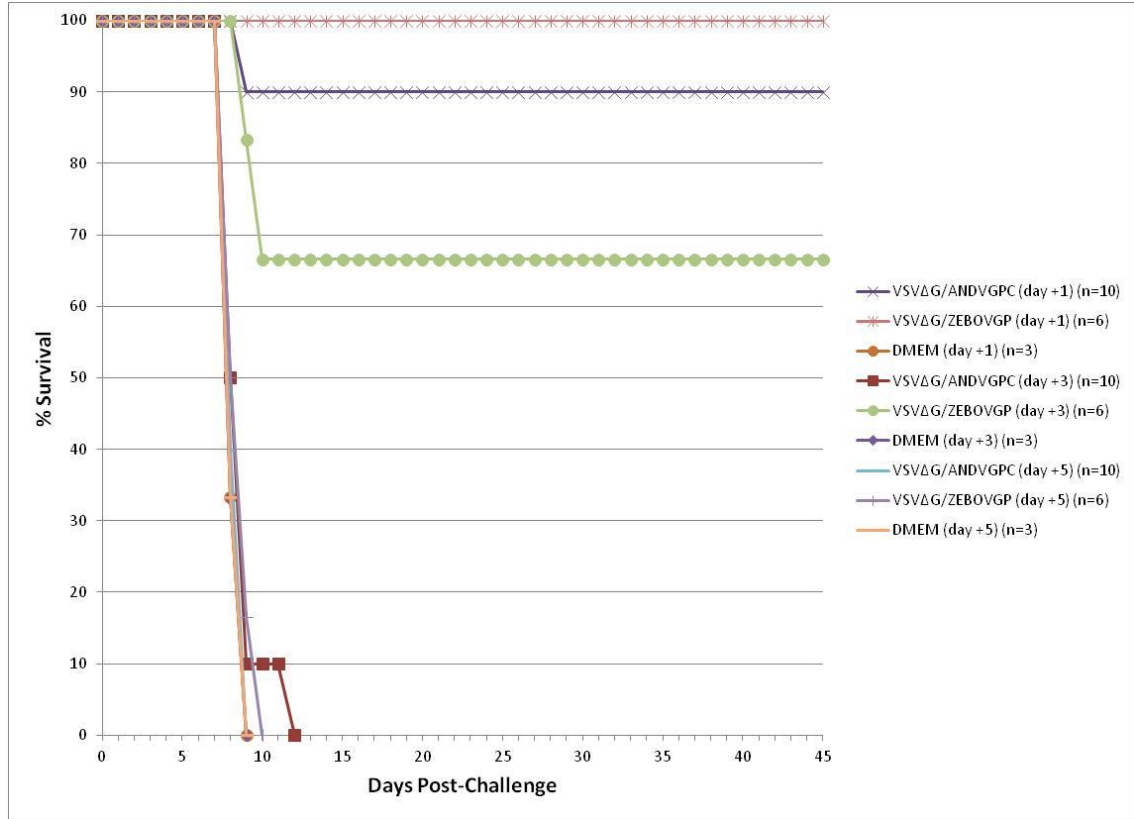


Figure 32. Post-Exposure Study. Hamsters were challenged with 100 times the 50% lethal dose ($100 \times LD_{50}$) of ANDV intraperitoneally (i.p), and then given 10^5 plaque forming units (PFU) of VSV containing the ANDV glycoproteins (VSVΔG/ANDVGPC, study virus), the Zaire ebolavirus glycoproteins (VSVΔG/ZEBOVGP, control) or Dulbecco's Modified Eagle's Medium (DMEM, control) also through the i.p route at 1, 3 or 5 days post-challenge and monitored for survival. Controls died between days 8 and 12.

3.6.3 Time to Protection – Measurement of Immune Response

3.6.3.1 Time to Protection – ANDV Replication

Unlike the previous study, tissue samples were not collected to detect the presence of ANDV RNA. Rather, the N-specific ELISA was used to measure the amount of seroconversion against the N protein as an indirect measure of ANDV replication. Serum samples collected 45 days post-challenge from surviving animals were tested for anti-N antibodies, and the results are illustrated in Figure 33. The results from the initial protection study (Section 3.5), with animals immunized at 28 days prior to challenge are included for comparison. Hamsters immunized with VSV Δ G/ANDVGPC 28, 7 or 3 days prior to challenge showed little or no detectable seroconversion. In contrast, hamsters immunized at 14 days prior to challenge showed very high levels of seroconversion. This data suggests that ANDV is able to replicate to higher amounts in the hamsters immunized at this time point, causing a production of antibodies against the N protein present in the challenge virus; however, all animals are still able to clear the infection and do not display any signs of illness. Serum samples from animals surviving post-exposure treatment were also tested, and showed incredibly high levels of seroconversion in all animals (titres of >20480), as would be expected from the challenge occurring prior to the treatment (data not shown).

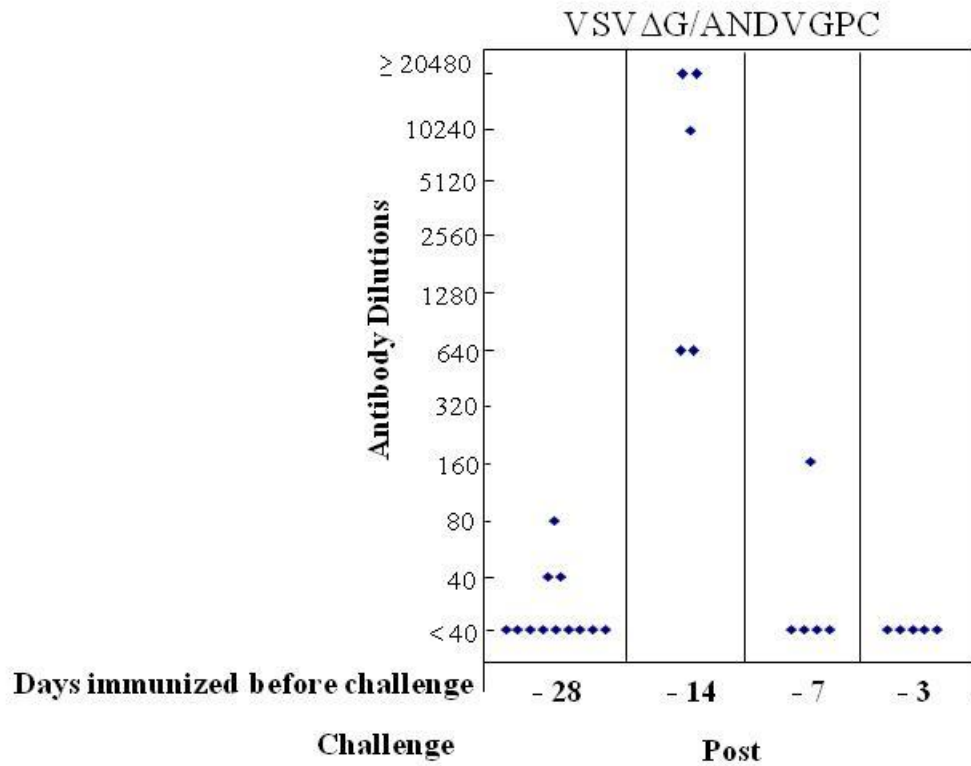


Figure 33. Time to Protection N Protein-Specific Seroconversion. Serum samples were collected from hamsters 45 days post-challenge (Post) from all surviving animals. All samples were screened at a dilution of 1:40 using N-specific ELISA and were considered negative if there was no reaction. Positive samples were diluted out until an endpoint was reached. Recombinant N was used as the ELISA antigen. Each dot represents an individual animal.

3.6.3.2 Time to Protection – ANDV Glycoprotein Neutralizing Antibodies

Serum samples collected from the VSV Δ G/ANDVGPC immunized hamsters immediately before challenge and 45 days post-challenge were tested for the presence of neutralizing antibodies against the ANDV glycoproteins using the PRNT₈₀ assay. As shown in Figure 34, hamsters start to develop low to moderate levels of neutralizing antibodies at 14 days post-immunization, with moderate to high levels by 28 days. No neutralizing antibodies are detectable at either 7 or 3 days post-immunization. At 45 days post-challenge, all hamsters show similar levels of neutralizing antibodies, however, the day 28 samples appear to be slightly lower, and the day 14 samples appear to be slightly higher. These results support the idea that protection in the 28 and 14 day hamsters must be based on an adaptive response, compared to a non-specific innate response in the 7 and 3 day animals due to the lack of any detectable neutralizing antibodies prior to challenge. Serum samples collected from control animals immunized with VSV Δ G/ZEBOVGP or DMEM were also tested for neutralizing antibodies against the ANDV glycoproteins, and the results were uniformly negative (data not shown).

3.6.3.3 Time to Protection – Stimulation of Innate Immune System

After demonstrating that hamsters receiving the VSV Δ G/ZEBOVGP control vaccine exhibited some survival when immunized 7 or 3 days prior to challenge, it was necessary to determine if innate responses were the primary determinant of protection in these cases. Unfortunately, there are only very few commercially available reagents to test this, and those designed for other rodent species exhibit little or no cross-reactivity.

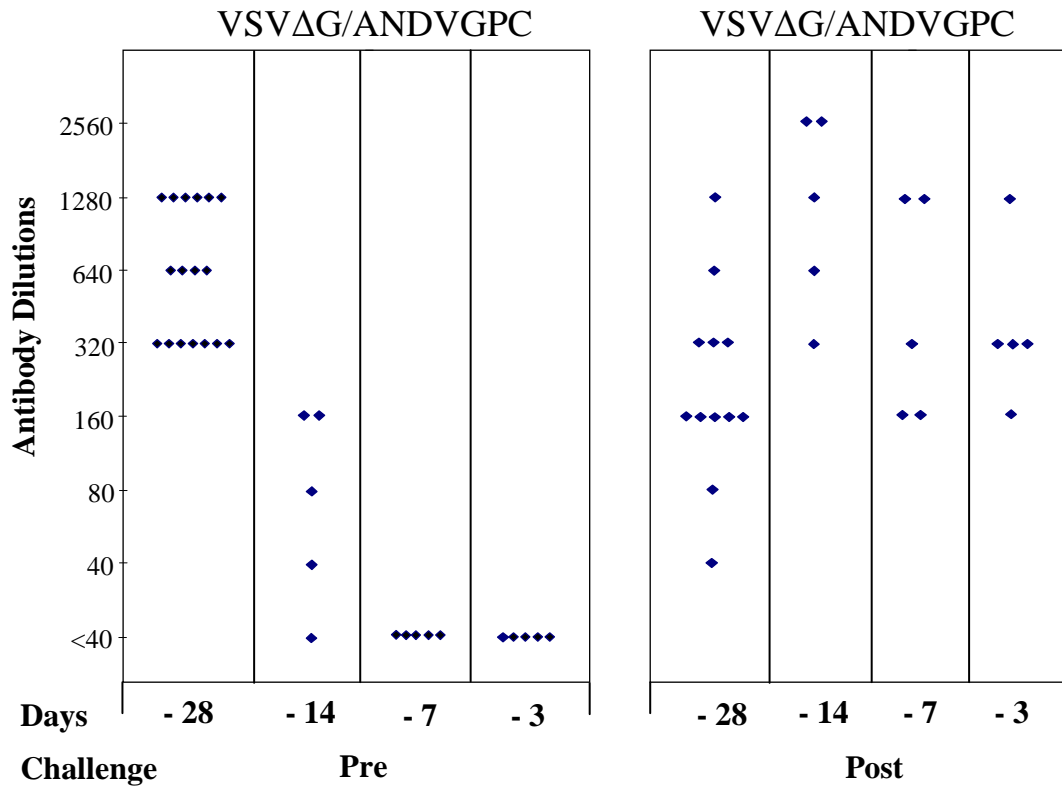
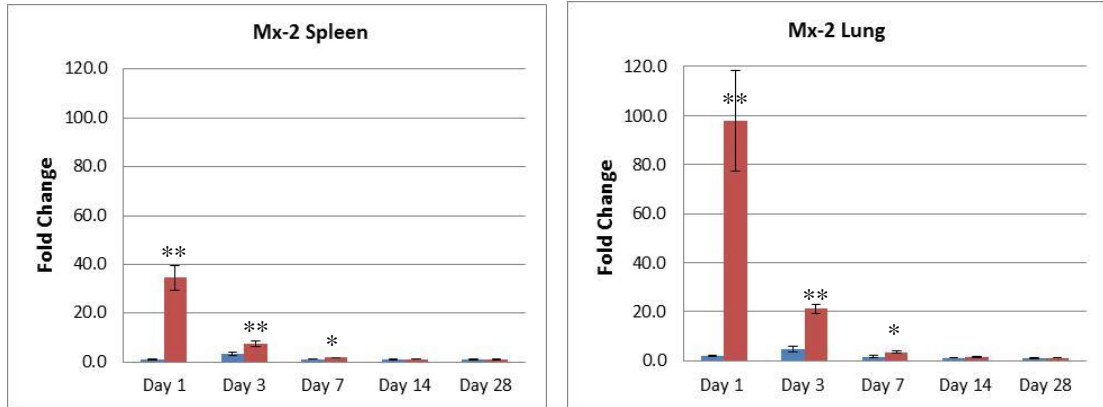


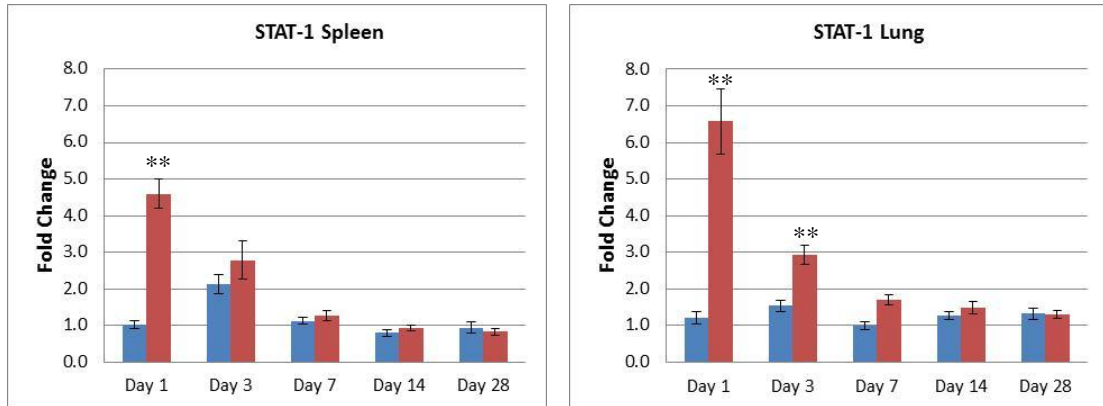
Figure 34. Time to Protection ANDV Glycoprotein Neutralizing Antibodies. Serum samples were collected from hamsters immunized with VSV expressing the ANDV glycoproteins (VSVΔG/ANDVGPC) immediately before challenge (Pre) and 45 days post-challenge from all surviving animals (Post). All samples were screened at a dilution of 1:40 using 80% plaque reduction neutralization (PRNT₈₀) and were considered negative if there was less than 80% neutralization. Positive samples were diluted out until endpoint was reached. Recombinant VSVΔG/ANDVGPC was used as antigen. Each dot represents an individual animal.

Therefore, there are currently no available methods to detect and quantify the expression of hamster cytokines and chemokines. Fortunately, a recently published manuscript by another member of the lab established a qRT-PCR assay to monitor hamster cytokine expression at the mRNA transcript levels (226). We chose 4 distinct genes that represented different components of the innate immune response; Mx-2, STAT-1, IRF-1 and IFN- γ , and determined their transcript levels in spleen and lung tissue compared to DMEM-immunized control hamsters. The results are shown in Figure 35. For all genes tested, the VSV Δ G/ZEBOVGP immunized hamsters exhibited much higher levels of cytokine transcripts in both tissues tested, with the maximum peak being seen at 1 day post-immunization, as opposed to 3 or 7 days when compared to VSV Δ G/ANDVGPC. Levels typically returned close to normal by 7-14 days post-immunization, although IFN- γ levels remained elevated in the spleen for the entire period for the VSV Δ G/ZEBOVGP immunized hamsters. This data shows that the VSV Δ G/ZEBOVGP vaccine seems to stimulate the innate immune system more quickly and more robustly when compared to the VSV Δ G/ANDVGPC vaccine, which may help to explain the observed protection.

A



B

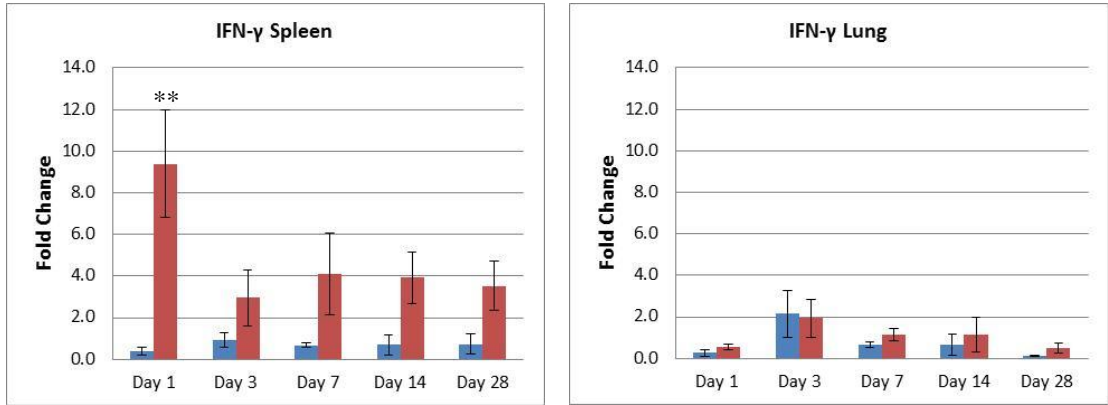


VSVΔG/ANDVGPC

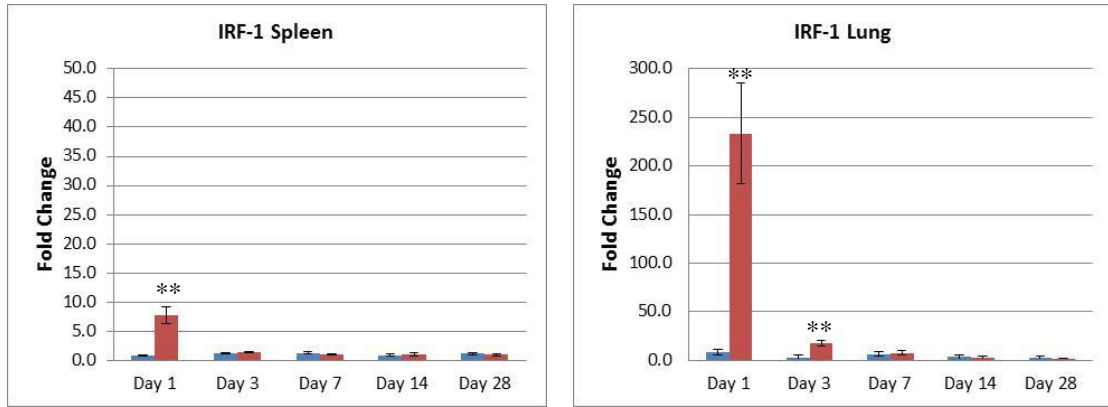


VSVΔG/ZEBOVGP

C



D



■ VSVΔG/ANDVGP ■ VSVΔG/ZEBOVGP

Figure 35. Hamster Real-Time Cytokine Assay. Hamsters were immunized with either VSVΔG/ANDVGP or VSVΔG/ZEBOVGP (n=6 per group/time point) and euthanized at 1, 3, 7, 14 or 28 days post-immunization. Specific primers/probes were used for (A) Myxovirus resistance protein-2 (Mx-2), (B) Signal transducer and activator of transcription-1 (STAT-1), (C) Interferon gamma (IFN-γ), or (D) Interferon regulatory factor-1 (IRF-1). Samples were normalized to an internal reference gene (RPL18) and expressed as fold change compared to DMEM control hamsters using the $\Delta\Delta CT$ method. Error bars represent the standard error of the mean. **/* indicate significant difference between viruses. (**= $p < 0.001$, * = $p < 0.05$, Student's t-test)

4.0 Discussion

Although the incidence of HPS cases in North and South America remains low in comparison to HFRS cases in Europe and Asia, the significantly higher case fatality rate and the lack of any approved, licensed, vaccines or any effective treatments for the disease suggest an urgent need for the development of such measures (138, 188). This study focused on the development of a vaccine that would be effective in the protection of the Syrian hamster from lethal ANDV infection. The results illustrate the successful production of an ANDV minigenome system, but also show the problems that exist with the development of an ANDV infectious clone system and its use for vaccine development. The results also show the successful use of the replication competent recombinant VSV Δ G/ANDVGPC as a vaccine and post-exposure treatment against ANDV infection and some insights into the mechanisms behind this protection.

4.1 Cloning and Expression of ANDV Proteins *In Vitro*

All molecular cloning steps were successful, with the production of a number of different constructs containing the ANDV protein ORFs. Expression of the ANDV N protein, as well as the G_N and G_C proteins from the GPC ORF was shown by western blot or IFA from a variety of different constructs and in a variety of different cell lines. These 3 proteins are the primary antigens of choice for vaccine development, and a recent review of several studies suggests that these proteins appear to be easy to express from a variety of different expression platforms (138). The vectors used for this study have relatively strong mammalian expression promoters, and this resulted in the strong

Discussion

expression of the proteins in cell culture. The biggest difference in protein expression levels was seen in 293T cells compared to the other cell lines tested, and may be due to a few reasons. First, these cells are known to be very easily transfected through a variety of different transfection methods, including lipid-based transfection reagents and calcium phosphate methods. Second, the inclusion of the SV40 large T-antigen in this cell line allows for the episomal replication of transfected plasmids that contain an SV40 origin of replication (65, 71). This allows further amplification of the plasmids, typically leading to a higher level of protein expression over a greater length of time. The high levels of protein expression, however, may also lead to proteasomal degradation of the proteins, leading to the smaller molecular weight bands that appear whenever the cell lysate was used for western blot. Although VeroE6 and COS-7 cells are less easily transfected than 293T cells, through a variety of optimizations including plating and transfecting the cells a few hours apart, a much higher level of protein expression was achieved. Although COS-7 cells also contain the large T-antigen, expression levels were not nearly as high as 293T cells (64). VeroE6 cells also survive much longer when they reach confluency, with larger cytoplasm volumes that make visualization of the proteins easier using IFA. Fortunately, a number of commercial ANDV antibodies became available shortly after the start of the experiment, with the exception of any antibodies that recognized the L protein (Appendix 2). These antibodies worked exceptionally well in western blot, but had a number of limitations when used in IFA. This suggests that the antibodies must recognize epitopes within the primary amino acid sequence, or epitopes that are hidden when in the native protein conformation. Therefore, the use of

fixatives such as formalin or PFA that preserve internal cell structural integrity was incompatible with detection by these antibodies, and therefore prevented studies designed to look at cellular trafficking of the ANDV proteins and possible regions of co-localization using these antibodies.

The L protein proved to be a much greater challenge to express and detect. Only a few publications have described the successful expression of a hantavirus L protein. The detection of the protein has been described through functional minigenome assays, the detection of an L-GFP fusion protein by fluorescent microscopy, and by antibodies produced from an L peptide (42, 109, 225). In order to detect the expression of the ANDV L protein, fusion constructs were created with the commonly used HA and FLAG tags, which were added to either the N or C terminus of the L protein. Even with the inclusion of the tags, detection of the protein by western blot was unsuccessful with all of the expression constructs tested. In addition, non-immune specific detection methods that non-specifically label all proteins in a mixture such as silver staining and Coomassie blue staining did not detect a protein in the expected 250 kDa range (109). Detection of the protein was finally successful with the FLAG tag at the N terminus of the L protein in the pKS336 expression vector, although it is unusual that detection only occurred with this vector and tag combination. Unfortunately, because the tag is located at the N terminus of the protein, it is unknown if full-length L is being detected, or if it is only a small protein portion containing the tag in the same frame. There are a few possible explanations for the inability to detect the full-length L protein. First, there may be an issue on the RNA level, where the transcripts may be spliced or modified,

preventing their translation and expression. Second, the full length protein may be produced, but may be targeted for cleavage or proteasomal degradation almost immediately after its production, due to its size or possible toxicity. To address the RNA question, an *in vitro* RNA transcription kit was used to produce the L mRNA transcripts, which were subsequently transfected into cell culture. This was also unsuccessful in producing detectable L protein. To address these issues with the expression of the L protein, perhaps future work can focus on the use of northern blotting or mass spectrometry to see if the problem exists at the RNA or protein level.

4.2 Cloning and Rescue of Minigenome Constructs

Minigenome cassettes containing the M-segment NCRs and the CAT, LUC or GFP reporter genes were successfully inserted into the T7, Pol I and Pol II RNA promoter expression plasmids in the vRNA orientation. These minigenome cassettes were inserted in the vRNA orientation because they can be directly transcribed by the viral RNP complex to produce the reporter gene signal, whereas those in the cRNA orientation must first undergo a round of replication to produce the vRNA transcripts. Previously described minigenomes for Ebola and Marburg viruses used the vRNA orientation, and showed a higher reporter signal compared to constructs in the cRNA orientation (66, 153). All members of *Bunyaviridae* contain the 3 genomic segments S, M and L, presumably with differences in relative promoter strength between them. Reports with the Uukuniemi virus minigenome suggested that the NCRs of the M segment contained the strongest promoter, and was therefore the basis of the

minigenome constructs in this study (45). One of the key aspects of successful minigenome rescue is to determine the appropriate biological conditions necessary for viral transcription and replication, by varying the ratio between the plasmids that express proteins forming the RNP complex and vRNA transcripts (15, 28). A variety of different ratios of the N, L and minigenome plasmids were tried, using all of the different expression constructs described in this study in a variety of different cell lines. Unfortunately, detection of minigenome expression containing the LUC or GFP reporter genes was unsuccessful. Expression of the CAT enzyme expressed from the minigenome containing the CAT reporter gene was successfully detected, suggesting that some functional L protein was being produced.

Unfortunately, despite numerous optimizations the system continued to have issues with reproducibility. It is unclear why this was the case, although unreliable expression of the L protein is probably a major factor, as demonstrated by the difficulty in its detection. Another explanation is the possible presence of a cryptic promoter in the NCRs, which has been described for other bunyaviruses and can cause an imbalance in the signal to noise ratio (42, 45). Finally, most of the other bunyaviruses contain non-structural proteins such as NSs that can influence minigenome replication (193). Although NSs proteins have only been described for TULV and PUUV (90), potential NSs sequences exist in many of the hantavirus genomes in an alternative reading frame, including ANDV (205). Unfortunately, the role of these putative proteins on minigenome replication varies considerably depending on the genus; some display an inhibitory effect (10, 218), while others display an enhancement (83) or no effect at all

(45). An N expression construct with the removal of the potential NSs ORF from the ANDV N expression plasmid by elimination of an internal ATG start site and the creation of an internal stop site without any effect on the N protein sequence was created, but unfortunately displayed no detectable effect on the success of minigenome rescue.

Although manuscripts have been published describing a minigenome system for the Old World hantavirus HTNV (42, 225), this study represents the first New World hantavirus reverse genetics system to be described. Despite these advances, a successful full-length infectious clone system has still not been established for any member of the *hantavirus* genus, and was not attempted with the ANDV constructs due to the reliability issues, which also prevented the development of a vaccine candidate through these means. Future work needs to be continued with hantavirus reverse genetics, as the field is currently being held back by the lack of this much-needed tool.

4.3 Cloning and Rescue of Recombinant VSV Constructs

The different VSV constructs containing the ANDV GPC based on the previously described pVSVXN2ΔG vector (51, 196) were successfully rescued with only a minimal amount of optimization required. The VSV vector expressing the ANDV GPC is unique in that it represents the first glycoprotein from a member of the *Bunyaviridae* family to be expressed in a replication-competent recombinant VSV backbone, although replication-incompetent VSV have previously been pseudotyped with either Old World (HTNV and Seoul virus) (114, 163) or New World (ANDV)

(179, 186) hantavirus glycoproteins by other groups. The different bunyaviruses are generally believed to mature and bud through the Golgi membranes, where glycoprotein incorporation would occur, although alternative pathways have been suggested (193). This is in contrast to many other virus families that replicate in the cytoplasm, where maturation of the virus particles and glycoprotein incorporation usually occurs at the plasma membrane, as it does for VSV (135). This served as the main rationale behind creating the VSV constructs that expressed either the ZEBOV or VSV glycoproteins in addition to the ANDV GPC; essentially, the hope that the ANDV glycoproteins would be successfully expressed intracellularly, even if there was no or only low incorporation of the proteins into the rescued virus particles. The fact that recombinant VSV containing the ANDV glycoproteins was able to be rescued independently of another glycoprotein seems to indicate that a certain portion of these proteins are transported to the plasma membrane, as has been suggested for both Old World (HTNV and Seoul virus), as well as New World (Black Creek Canal virus) hantaviruses (163, 178), perhaps directly through an interaction with the VSV matrix protein or indirectly due to the increased expression of the protein from the VSV system. However, this process appears to be less optimal, as demonstrated by a number of different factors. First, rescue of the virus took over twice as long (minimum of 7 days) compared with the other constructs (3 days). Second, the VSV Δ G/ANDVGPC virus had slower growth kinetics, and virus titres were generally slightly lower than was achieved for other viruses. Both of these factors suggest an overall greater attenuation of this vector, although the specific details of this attenuation are unknown.

In vitro characterization of the growth kinetics of all VSVs showed attenuation compared to VSV wt; these viruses take longer to reach their peak titres, which remain lower than what is seen in wild-type. It is unclear if this attenuation of the viruses reflects a decreased efficiency in viral entry, replication or budding, but is most likely beneficial for their use as a vaccine platform, due to a decrease in potential side-effects from high levels of virus replication. Western blots of cell lysates showed protein being expressed at high levels within the cells, and samples of purified virus particles suggested incorporation of the foreign glycoproteins into the virus particles as described previously for other glycoproteins using the recombinant VSV system (51, 195). This would seem to suggest that the virus should be able to strongly stimulate both cellular and humoral adaptive host immune responses. Visualization of the virus particles by TEM showed the bullet-shaped particles characteristic of the *Rhabdoviridae* family. There does not appear to be much difference in the virus morphology across the different recombinant VSVs looked at, with no significant differences in particle size. Unfortunately, numerous attempts to use immuno-EM to label the virus particles were unsuccessful. Possible explanations are that the commercial antibodies do not appear to be compatible with the different fixation methods used or do not bind efficiently to the glycoprotein epitopes in their natural conformation. This would be in concurrence with the results that the antibodies work well in western blot with denatured proteins, but not with IFA or co-localization studies where protein structural integrity is desired. Therefore, confirmation of the incorporation of the ANDV glycoproteins was done through indirect means, including the presence of the ANDV glycoproteins and the

absence of others as detected by western blot in purified virus particle samples, and the neutralization of the VSV Δ G/ANDVGPC virus using serum containing anti-ANDV antibodies using a PRNT₈₀ assay.

4.4 *In Vivo* Protection Studies

4.4.1 Efficacy of VSV Δ G/ANDVGPC as a Vaccine Platform

Many other vaccine platforms have been previously evaluated for their success as a hantavirus vaccine, including inactivated virus, recombinant protein subunits, recombinant viral vectors and DNA vaccines, each with varying degrees of success (138, 188). The biggest obstacle in the development of these vaccines has been the lack of a lethal animal model, meaning that vaccine efficacy was measured by the ability of the vaccine to prevent virus replication in an animal that shows no signs of illness from infection. The characterization of the Syrian Golden hamster as a lethal model for ANDV infection in 2001 has finally allowed the evaluation of different ANDV vaccines using the model, as well as some insights into the mechanisms behind successful protection (81).

The recombinant VSV platform was chosen as a potential ANDV vaccine because it has been shown to stimulate both a strong cellular and humoral adaptive immune response in different animal models (87, 135). VSV does not appear to cause any serious disease in humans, and seroprevalence in the population remains low (16, 135). Additionally, any neutralizing responses against the vector would be directed against the VSV G protein, which has been removed from the vaccine construct,

potentially allowing its re-use with a different glycoprotein of interest (183). Concerns have been raised about the safety of the platform; especially the use of a replication-competent virus in immunosuppressed patients, such as those treated with immunosuppressive drugs or infected with HIV. However, studies with rhesus macaques infected with simian-human immunodeficiency virus (SHIV) showed no adverse effects following immunization with a replication-competent VSV expressing the Ebola virus glycoprotein (VSV Δ G/ZEBOVGP). In addition, the vaccine was still able to protect 66% of the highly immunocompromised animals against lethal Ebola virus challenge (57). The vaccine dose of replication-competent vaccines is also expected to be much lower (approximately 3 logs) and thus less toxic compared with, for example, the replication-incompetent Ad5 platform, based on recent studies which compared both platforms as Ebola virus vaccines (59, 72, 87, 208).

This study shows that the VSV Δ G/ANDVGPC vaccine fully protects hamsters from lethal ANDV infection with a single dose when administered 28 days prior to challenge. This protection is specific to the incorporated glycoprotein, as control animals immunized with VSV Δ G/ZEBOVGP all showed signs of disease and succumbed to infection between days 8 and 11. In addition to fully protecting the hamsters from disease, the vaccine also appears to prevent ANDV replication from occurring, as examined by qRT-PCR of ANDV RNA and seroconversion against the N protein (not included in the vaccine), suggesting that the vaccine is capable of producing a sterile immunity. In contrast, all control animals showed high levels of ANDV replication prior to death.

Reports have shown that ANDV is lethal when administered to hamsters through a variety of different routes including subcutaneous, intranasal, intramuscular and intragastric (79). The i.p route of injection was chosen for this study for both the immunization with the VSV vectors as well as the lethal ANDV challenge for a number of reasons, including the ease of administration with a consistent dose and the shorter time to death with a lower LD₅₀. Although the i.p route of injection may not resemble that of a natural infection, hamsters injected through any of the routes described above display similar disease symptoms, with only the time of death significantly varying between them.

Overall, the results seem to indicate that an adaptive immune response directed against the ANDV glycoproteins is developed from immunization with the VSVΔG/ANDVGPC vector and is sufficiently strong enough to almost completely prevent ANDV replication in an infected individual as well as preventing all signs of disease.

4.4.2 Immune Response

Although other studies have attempted to determine the mechanisms of protection against HPS disease, the results remain unclear. DNA vaccines encoding the ANDV M-segment cDNA were only partially protective in the hamster model (29); however, immunization of NHPs or rabbits with the vaccine generated high levels of neutralizing antibodies against the ANDV glycoproteins. These antibodies, when passively transferred to the hamsters, fully protected them from lethal ANDV challenge

(79). This suggests a possible important role for neutralizing antibodies as a mechanism of protection. A series of constructs based on the recombinant human Ad5 platform were also evaluated as a potential hantavirus vaccine. Hamsters were immunized with Ad5 expressing the ANDV N, G_N or G_C proteins, which were all shown to be fully protective against lethal ANDV challenge (186). The combination of the G_N and G_C vectors given together was also shown to give an almost sterile immunity, with little or no ANDV replication, suggesting that the combination of the two glycoproteins together may be an important aspect in protection. Despite fully protecting the hamsters from disease, either no or only low levels of neutralizing antibodies were detected. The immunization of BALB/c mice with the constructs showed a strong CD8⁺ cytotoxic lymphocyte response, suggesting that an adaptive cellular immune response may also play an important role in protection.

This study shows that the VSVΔG/ANDVGPC vaccine is capable of generating a strong neutralizing antibody response against the ANDV glycoproteins. Serum collected from hamsters prior to ANDV challenge was able to neutralize both VSVΔG/ANDVGPC, as well as native ANDV, in either a PRNT₈₀ or FRNT₈₀ assay, respectively, at high titres. However, serum collected from surviving hamsters 45 days post-challenge showed a slight drop in overall neutralizing titres. Although the sterile immunity induced by the vaccine can be viewed as desirable, ANDV shows little or no replication, meaning it cannot act as a booster towards the immune response. The significance of this drop is unknown, as the level of neutralizing response required for

protection over a longer time period has not yet been examined, and therefore would need to be confirmed by future long-term protection studies.

Unfortunately, there are currently very few immunological reagents available to evaluate the Syrian hamster cellular immune responses. Although the Syrian hamster is used as a disease model for over 22 biological agents, there continues to be very little commercial interest in producing these reagents (226). Most existing reagents and kits for other rodent species show little or no cross-reactivity with hamster cytokines and chemokines. Non-species specific methods of measuring proliferation were attempted, including CFSE and BrdU labelling. Unfortunately, these assays showed a high degree of variability with hamster splenocytes, and the lack of antibodies to label which subset of the cells were proliferating limited the usefulness of the assay. A recent publication describing a number of T cell and B cell antibodies that cross-react with hamster immune cells will hopefully allow further investigation into the cellular responses in the future (70).

Overall, it appears that the strong neutralizing response produced by the VSVΔG/ANDVGPC vaccine is important for protection; however, the possible supporting role of a cellular immune response still remains to be fully characterized. The differences seen in this and previous studies may be due more to the vector used for the vaccine platform (replication competent vs. replication incompetent), and the primary mechanism by which they stimulate the immune response.

4.5 Time to Protection and Post-Exposure Vaccine Efficacy

4.5.1 Time to Protection Efficacy

As the previous experiments evaluated the efficacy of the VSV Δ G/ANDVGPC vaccine when administered to the hamsters at 28 days prior to challenge, additional experiments were carried out in order to determine the efficacy of the vaccine when challenged at 14, 7 or 3 days post-immunization. It was shown that hamsters receiving the VSV Δ G/ANDVGPC vaccine at any of those days prior to lethal ANDV challenge were fully protected from disease, with control animals receiving DMEM immunization all showing signs of disease and dying between days 9 and 10. Interestingly, hamsters receiving the VSV Δ G/ZEBOVGP negative control vaccine did not survive at day 14, but showed survivors when challenged at days 7 and 3 post-immunization. This is the first time that a VSV construct containing an unrelated immunogen has provided protection against a heterologous virus challenge. The most likely explanation is that VSV is able to mediate a strong non-specific innate immune response (182, 183). Hantaviruses have been shown to be sensitive to innate responses, in particular interferons, prior to an established infection, but become insensitive to treatment with interferons following an established infection (206). The fact that more hamsters survived at day 3 (83%) compared to day 7 (50%) vaccination also supports the idea of a strong innate immune response, which is typically strongest shortly after immunization/infection.

However, these results suggest that VSV Δ G/ANDVGPC remains the superior vaccine with 100% protection at all time points tested. While the adaptive immune

response is most likely not the primary means of protection at the 7 and 3 day time points, the development of an ANDV specific response such as non-neutralizing antibodies may also be occurring and contributing to the protection seen.

4.5.2 Post-Exposure Efficacy

Previous investigations have shown that recombinant VSV expressing either the Ebola or Marburg virus glycoprotein administered post-exposure provided full or partial protection from lethal challenge in both the rodent and NHP animal models (38, 58, 60). Therefore, the VSV Δ G/ANDVGPC and VSV Δ G/ZEBOVGP vaccines were evaluated for their effectiveness as treatments following lethal ANDV infection in the hamster. Hamsters received one of the vaccine constructs, or DMEM as a negative control at 1, 3 and 5 days post-exposure. VSV Δ G/ANDVGPC showed a 90% survival rate in the hamsters immunized 1 day post-challenge; however, no animals survived when receiving the treatment after 3 days. Similar to the time to protection study, the VSV Δ G/ZEBOVGP vaccine also elicited protection in the hamsters, despite containing an unrelated immunogen. In this case, the VSV Δ G/ZEBOVGP actually proved to be the superior post-exposure treatment option, with 100% protection of hamsters immunized at 1 day post-challenge, and 67% surviving after 3 days. None of the hamsters receiving treatment at 5 days post-challenge or DMEM at any of the time points survived lethal challenge. These results again suggest the important role of the innate immune system in offering protection against challenge from either vaccine. The innate immune response is thought to be at least partially essential in the success of the VSV platform in its use

for the post-exposure treatment of filovirus infections, keeping virus loads at levels that allow the adaptive immune response, which otherwise would be developed too late, to clear the virus (38). However, the non-specificity of the protection from the different VSV vaccines differs from what was seen against filovirus challenge in the NHP model, where a homologous VSV vaccine was required in order to achieve successful post-exposure protection (38, 58, 60). As an alternative theory, one could argue that the recombinant VSV vaccine might interfere with and thus control ANDV replication (viral interference) allowing only subclinical or mild infections. A similar concept has been developed for other vaccines given simultaneously with challenge virus resulting in subclinical infection that allows the development of a protective humoral immune response, as was seen with the VSV Δ G/ANDVGPC vaccine (162). It is unclear why the VSV Δ G/ZEBOVGP provides better protection when given post-exposure, but there are a few possible explanations. VSV Δ G/ZEBOVGP was shown to have faster growth kinetics when compared to VSV Δ G/ANDVGPC, reaching its peak titre in a shorter time frame. This would allow a stronger stimulation of the innate immune response by VSV Δ G/ZEBOVGP simply based on a greater number of virus particles across the same time frame. More importantly, however, may be the difference in tropism between the different glycoproteins. The ZEBOV glycoproteins have a tropism for cells involved in early innate immune response, including macrophage, monocytes and dendritic cells (187). In contrast, although ANDV has been shown to be capable of infecting these cell types, it has a clear preference for endothelial cells (54, 168, 174, 211). Therefore, it

may simply be a case of the VSV Δ G/ZEBOVGP vaccine being targeted to the most appropriate cells for mounting a stronger innate immune response.

These post-exposure treatment results are very promising, and for the first time suggest that a VSV construct carrying the ZEBOV glycoproteins may be capable of protecting against a virus that is highly susceptible to innate immune responses. However, the exact mechanism of stimulation remains to be characterized once the tools and reagents to do so become available. This supports the idea of using VSV Δ G/ZEBOVGP as the backbone for further vaccine development with the concept of introducing combined strong innate and adaptive immune responses.

4.5.3 Time to Protection – Adaptive Immune Response

In the previous study, the immunization of hamsters with the VSV Δ G/ANDVGPC vaccine 28 days before challenge produced a sterile immunity, with little or no ANDV replication occurring in these animals. Seroconversion against the N protein was measured 45 days after challenge from all surviving animals across the 3 time points. The results indicate that immunization with VSV Δ G/ANDVGPC at 7 or 3 days, like 28 days, can produce a sterile immunity with the prevention of ANDV replication. However, high levels of seroconversion were detected in the hamsters immunized 14 days before challenge, despite the survival of all animals. This is an interesting result, and seems to indicate that there may be a period of time between immunization and virus challenge where protection is less optimal. A specific, adaptive response takes time to develop, and non-specific innate immune responses are not

typically long-lasting. Therefore, it would appear that the 14 day time point is too early for inducing a complete humoral or cellular immune response, but too long ago for a sustained innate response to have an effect. This would appear to be supported by the fact that there were no survivors in the VSV Δ G/ZEBOVGP negative control immunized group at this time point. No specific immune response against the ANDV glycoproteins can be achieved from this vector, and the innate immune response is unable to provide protection this far before challenge.

As it appears that a neutralizing antibody response was important for the VSV Δ G/ANDVGPC vaccine administered at 28, but not 7 or 3 days before challenge, the neutralizing antibody titres against the ANDV glycoproteins were determined for all 3 time points in serum samples collected immediately before challenge. As expected, no antibodies were detected at either 7 or 3 days; however, titres start to appear at 14 days post-immunization, with the highest levels achieved at 28 days post-immunization. No neutralizing antibodies against the ANDV glycoproteins were detected from the VSV Δ G/ZEBOVGP immunized animals. In serum samples collected from surviving hamsters at 45 days post-challenge, the neutralizing responses appeared to be very similar, with a few minor discrepancies. The slightly lower titres seen in the day 28 group may be due to the longer period of time (73 days) between immunization and sample collection compared with the day 7 (52 days) or day 3 (49 days) animals. This would need to be confirmed by the collection of samples at similar time points post-immunization. All of these animals have sterile immunity against ANDV, and therefore challenge with ANDV would do little to boost the overall neutralizing antibody levels.

In contrast, the day 14 hamsters show a slightly elevated level of neutralizing antibodies when compared to the other groups. This may be due to the non-sterile immunity produced in these animals, with the replication of ANDV causing a stimulation of the immune system acting as a boosting effect towards total antibody levels. At this point, it is unclear what levels of neutralizing antibodies would be protective against a future infection, and could be answered by the proposed long-term protection studies.

Overall, these results support the theory that the adaptive response is important for protection at 28 and 14 days, but does not play a significant role at 7 or 3 days before challenge. The lower neutralizing titres seen at 14 days support the idea that the adaptive response is strong enough to prevent lethal infection at this point, but unable to prevent ANDV replication from occurring.

4.5.4 Time to Protection – Innate Immune Response

Although the results from this study seem to indicate a difference in the mechanism of protection depending on the timing between immunization and challenge, the role of the innate immune response against the different vaccine vectors needed to be confirmed. As previously mentioned, very few hamster-specific reagents exist to measure these responses and kits designed for other rodent species show very limited or no cross-reactivity. Fortunately, another member of the lab recently validated and published a qRT-PCR assay for the detection and quantification of hamster cytokine responses at the mRNA level (226). To validate these assays, a suitable housekeeping gene known as RPL18 was chosen in order to normalize the responses, and the C_T

Discussion

values were compared between hamsters receiving LPS or VSV wt compared with DMEM control hamsters. Although mRNA transcript levels are known to not always correlate with expressed protein levels, the up-regulation of certain cytokines in spleen, lung and liver samples was correlated to pathological changes observed in these tissues during VSV infection (50, 226). To monitor the innate immune response seen in hamsters following immunization with the VSV vaccines, 4 genes were chosen; Mx-2, IRF-1, STAT-1 and IFN- γ . These 4 genes represent a subset of the overall panel that affect different host innate immune response pathways, and showed a response when the hamsters were infected with VSV wt, suggesting that they would most likely also be affected by the VSV vaccine constructs. Lung and liver samples were collected from hamsters immunized with VSV Δ G/ANDVGPC, VSV Δ G/ZEBOVGP or DMEM at 1, 3, 7, 14 and 28 days post-immunization. The RNA was extracted from these tissues and analyzed by qRT-PCR using cytokine specific primers/probe. The hamsters immunized with the VSV Δ G/ZEBOVGP vaccine showed a quicker and much more robust response compared with the animals immunized with VSV Δ G/ANDVGPC. These levels peaked at the first day measured, and returned close to normal levels past 7 days. The results of these assays confirm that different components of the innate immune response are stimulated by the VSV constructs almost immediately after immunization. This response typically lasts for close to a week before returning to normal levels. Attempts were made to analyze the effects of the vaccines on cytokine levels when used as a post-exposure treatment; however, the results were difficult to interpret due to the co-infection with ANDV. Future experiments will need to first focus on characterizing the hamster

Discussion

cytokine response seen from ANDV infection so that differences with the VSV treatment can be more clearly recognized.

In summation, the relatively high up-regulation of cytokines involved in the innate response seen from VSV Δ G/ZEBOVGP compared to VSV Δ G/ANDVGPC can help explain the results seen in the surviving hamsters that received the vaccine at 7 or 3 days prior to challenge, and its superior role in post-exposure protection.

5.0 Conclusions

The results of this study have shown two main things. First, this study describes the first successful production of an ANDV minigenome system; the first such system described for a New World hantavirus (manuscript submitted). The results obtained with the ANDV minigenome suggest that the development of a full length infectious clone system should be possible, but the key to achieving the correct biological conditions still remains unknown. Unfortunately, I was not able to address my hypothesis, as I was unable to successfully create an infectious clone system despite a long period of optimizations. However, work towards this goal should continue as it would represent an important milestone in hantavirus research, and allow a great expansion in the current understanding of the field.

Second, the data from the vaccine studies suggest the great potential of using VSV reverse genetics to create vaccine candidates that are effective in both hantavirus vaccination and post-exposure treatment. My hypothesis was supported in that the VSV Δ G/ANDVGPC vaccine expressing the ANDV glycoproteins on the surface of the VSV particles was able to fully protect Syrian hamsters from lethal ANDV challenge with a single dose when administered at 28, 14, 7 or 3 days before challenge. With the exception of the day 14 immunized hamsters, the vaccine produced a sterile immunity that did not allow ANDV replication to occur. A neutralizing antibody response was postulated as the most likely mechanism of protection with hamsters immunized at 14 or 28 days before challenge, with the innate immune response playing a primary role when immunized 7 or 3 days before challenge. The VSV Δ G/ANDVGPC was also shown to

Conclusions

be 90% protective as a post-exposure treatment when given 1 day post-exposure, where the innate immune system is also thought to play a significant role. Unexpectedly, the VSV Δ G/ZEBOVGP was able to also stimulate the innate immune response to such a degree to offer full or partial protection against disease when administered shortly before or after lethal ANDV challenge. VSV Δ G/ZEBOVGP was shown to be able to up-regulate hamster cytokines involved in innate pathways more quickly and robustly than VSV Δ G/ANDVGPC. This may be due to a difference in viral growth kinetics or tropism, but the exact mechanisms remain unclear. Therefore, the inclusion of the ZEBOV GP may potentially have an overall enhancement effect on the vaccine, due to its increased stimulation of the innate immune response in a shorter period of time, but this remains to be tested. Overall, this study has greatly advanced the field's understanding behind the requirements for protection from hantaviral disease, the understanding of the Syrian hamster model and the important roles of all aspects of the immune response, and was recently accepted for publication (17).

In terms of future directions with the recombinant VSV-based vaccines, a few questions still need to be addressed. First, the roles of the cellular and innate immune responses need to be thoroughly evaluated to confirm a number of proposed theories and gaps existing in my conclusions. Unfortunately, the tools needed to address these questions were unavailable throughout my studies and are only now starting to be developed. Hopefully the continued use and characterization of the Syrian hamster model will convince commercial research & development companies of the need to develop these much needed reagents. Second, long-term protection studies need to be

Conclusions

carried out in order to evaluate the length and amount of protection gained from immunization with the vaccine. A decrease in the neutralizing titres was observed in the animals at the endpoint of the study; therefore, the minimal titres necessary for protection against lethal disease should be determined, in addition to the potential need for a second boosting dose. Finally, the rescued VSV expressing both the ANDV and ZEBOV glycoproteins (VSV Δ G/ANDVGPC-ZEBOVGP) may be an important tool that to date remains only partially characterized. Although not described in this study, it has been shown to fully protect hamsters from both lethal ANDV and lethal mouse-adapted ZEBOV infection when immunized 28 days before challenge, and shows the potential of a vaccine containing immunogens from two completely unrelated virus families (214). Additionally, it will allow the testing of whether the inclusion of a secondary protein causing a strong stimulation of the immune system will have an overall enhancement on the levels of post-exposure protection. Finally, it may also be important in answering questions related to post-exposure treatment that may be due to differences in viral growth kinetics and cell tropism and/or differences in the induction of innate immune responses.

6.0 References

1. **Alfadhli, A., E. Steel, L. Finlay, H. P. Bächinger, and E. Barklis.** 2002. Hantavirus nucleocapsid protein coiled-coil domains. *J Biol Chem* **277**:27103-27108.
2. **Alff, P. J., I. N. Gavrillovskaya, E. Gorbunova, K. Endriss, Y. Chong, E. Geimonen, N. Sen, N. C. Reich, and E. R. Mackow.** 2006. The pathogenic NY-1 hantavirus G1 cytoplasmic tail inhibits RIG-I- and TBK-1-directed interferon responses. *J Virol* **80**:9676-9686.
3. **Alff, P. J., N. Sen, E. Gorbunova, I. N. Gavrillovskaya, and E. R. Mackow.** 2008. The NY-1 hantavirus Gn cytoplasmic tail coprecipitates TRAF3 and inhibits cellular interferon responses by disrupting TBK1-TRAF3 complex formation. *J Virol* **82**:9115-9122.
4. **Anonymous.** 1997. Hantavirus Pulmonary Syndrome -- Chile 1997. *MMWR: Morbidity and Mortality Weekly Report* **46**:949-951.
5. **Arikawa, J., A. L. Schmaljohn, J. M. Dalrymple, and C. S. Schmaljohn.** 1989. Characterization of Hantaan virus envelope glycoprotein antigenic determinants defined by monoclonal antibodies. *J Gen Virol* **70 (Pt 3)**:615-624.
6. **Basler, C. F., X. Wang, E. Mühlberger, V. Volchkov, J. Paragas, H. D. Klenk, A. García-Sastre, and P. Palese.** 2000. The Ebola virus VP35 protein functions as a type I IFN antagonist. *Proc Natl Acad Sci U S A* **97**:12289-12294.
7. **Bharadwaj, M., C. R. Lyons, I. A. Wortman, and B. Hjelle.** 1999. Intramuscular inoculation of Sin Nombre hantavirus cDNAs induces cellular and humoral immune responses in BALB/c mice. *Vaccine* **17**:2836-2843.
8. **Bharadwaj, M., K. Mirowsky, C. Ye, J. Botten, B. Masten, J. Yee, C. R. Lyons, and B. Hjelle.** 2002. Genetic vaccines protect against Sin Nombre hantavirus challenge in the deer mouse (*Peromyscus maniculatus*). *J Gen Virol* **83**:1745-1751.
9. **Bi, Z., P. B. Formenty, and C. E. Roth.** 2008. Hantavirus infection: a review and global update. *J Infect Dev Ctries* **2**:3-23.
10. **Blakqori, G., G. Kochs, O. Haller, and F. Weber.** 2003. Functional L polymerase of La Crosse virus allows in vivo reconstitution of recombinant nucleocapsids. *J Gen Virol* **84**:1207-1214.

References

11. **Blaney, J. E., C. Wirblich, A. B. Papaneri, R. F. Johnson, C. J. Myers, T. L. Juelich, M. R. Holbrook, A. N. Freiberg, J. G. Bernbaum, P. B. Jahrling, J. Paragas, and M. J. Schnell.** 2011. Inactivated or Live-Attenuated Bivalent Vaccines That Confer Protection against Rabies and Ebola Viruses. *J Virol* **85**:10605-10616.
12. **Blignaut, B., N. Visser, J. Theron, E. Rieder, and F. F. Maree.** 2011. Custom-engineered chimeric foot-and-mouth disease vaccine elicits protective immune responses in pigs. *J Gen Virol* **92**:849-859.
13. **Botten, J., K. Mirowsky, C. Ye, K. Gottlieb, M. Saavedra, L. Ponce, and B. Hjelle.** 2002. Shedding and intracage transmission of Sin Nombre hantavirus in the deer mouse (*Peromyscus maniculatus*) model. *J Virol* **76**:7587-7594.
14. **Brennan, B., S. R. Welch, A. McLees, and R. M. Elliott.** 2011. Creation of a recombinant rift valley Fever virus with a two-segmented genome. *J Virol* **85**:10310-10318.
15. **Bridgen, A., and R. M. Elliott.** 1996. Rescue of a segmented negative-strand RNA virus entirely from cloned complementary DNAs. *Proc Natl Acad Sci U S A* **93**:15400-15404.
16. **Brody, J. A., G. F. Fischer, and P. H. Peralta.** 1967. Vesicular stomatitis virus in Panama. Human serologic patterns in a cattle raising area. *Am J Epidemiol* **86**:158-161.
17. **Brown, K. S., D. Safronetz, A. Marzi, H. Ebihara, and H. Feldmann.** 2011. Vesicular Stomatitis Virus-Based Vaccine Protects Hamsters against Lethal Challenge with Andes Virus. *J Virol* **85**:12781-12791.
18. **Campen, M. J., M. L. Milazzo, C. F. Fulhorst, C. J. Obot Akata, and F. Koster.** 2006. Characterization of shock in a hamster model of hantavirus infection. *Virology* **356**:45-49.
19. **Caramello, P., F. Canta, L. Bonino, C. Moiraghi, F. Navone, F. Lipani, R. Balbiano, A. M. Caputo, and V. Gai.** 2002. Puumala virus pulmonary syndrome in a Romanian immigrant. *J Travel Med* **9**:326-329.
20. **Carey, D. E., R. Reuben, K. N. Panicker, R. E. Shope, and R. M. Myers.** 1971. Thottapalayam virus: a presumptive arbovirus isolated from a shrew in India. *Indian J Med Res* **59**:1758-1760.
21. **Carroll, D. S., J. N. Mills, J. M. Montgomery, D. G. Bausch, P. J. Blair, J. P. Burans, V. Felices, A. Gianella, N. Iihoshi, S. T. Nichol, J. G. Olson, D. S. Rogers, M. Salazar, and T. G. Ksiazek.** 2005. Hantavirus pulmonary syndrome

References

- in Central Bolivia: relationships between reservoir hosts, habitats, and viral genotypes. *Am J Trop Med Hyg* **72**:42-46.
22. **Casals, J., B. E. Henderson, H. Hoogstraal, K. M. Johnson, and A. Shelokov.** 1970. A review of Soviet viral hemorrhagic fevers, 1969. *J Infect Dis* **122**:437-453.
 23. **Childs, J. E., T. G. Ksiazek, C. F. Spiropoulou, J. W. Krebs, S. Morzunov, G. O. Maupin, K. L. Gage, P. E. Rollin, J. Sarisky, R. E. Enscore, and et al.** 1994. Serologic and genetic identification of *Peromyscus maniculatus* as the primary rodent reservoir for a new hantavirus in the southwestern United States. *J Infect Dis* **169**:1271-1280.
 24. **Cho, H. W., and C. R. Howard.** 1999. Antibody responses in humans to an inactivated hantavirus vaccine (Hantavax). *Vaccine* **17**:2569-2575.
 25. **Chu, Y. K., G. B. Jennings, and C. S. Schmaljohn.** 1995. A vaccinia virus-vectored Hantaan virus vaccine protects hamsters from challenge with Hantaan and Seoul viruses but not Puumala virus. *J Virol* **69**:6417-6423.
 26. **Cobleigh, M. A., L. Buonocore, S. L. Uprichard, J. K. Rose, and M. D. Robek.** 2010. A vesicular stomatitis virus-based hepatitis B virus vaccine vector provides protection against challenge in a single dose. *J Virol* **84**:7513-7522.
 27. **Conzelmann, K. K., and G. Meyers.** 1996. Genetic engineering of animal RNA viruses. *Trends Microbiol* **4**:386-393.
 28. **Conzelmann, K. K., and M. Schnell.** 1994. Rescue of synthetic genomic RNA analogs of rabies virus by plasmid-encoded proteins. *J Virol* **68**:713-719.
 29. **Custer, D. M., E. Thompson, C. S. Schmaljohn, T. G. Ksiazek, and J. W. Hooper.** 2003. Active and passive vaccination against hantavirus pulmonary syndrome with Andes virus M genome segment-based DNA vaccine. *J Virol* **77**:9894-9905.
 30. **de Carvalho Nicacio, C., M. Gonzalez Della Valle, P. Padula, E. Björling, A. Plyusnin, and A. Lundkvist.** 2002. Cross-protection against challenge with Puumala virus after immunization with nucleocapsid proteins from different hantaviruses. *J Virol* **76**:6669-6677.
 31. **Dohmae, K., and Y. Nishimune.** 1995. Protection against hantavirus infection by dam's immunity transferred vertically to neonates. *Arch Virol* **140**:165-172.
 32. **Dong, G. M., L. Han, Q. An, W. X. Liu, Y. Kong, and L. H. Yang.** 2005. Immunization effect of purified bivalent vaccine to haemorrhagic fever with renal

- syndrome manufactured from primary cultured hamster kidney cells. *Chin Med J (Engl)* **118**:766-768.
33. **Easterbrook, J. D., and S. L. Klein.** 2008. Immunological mechanisms mediating hantavirus persistence in rodent reservoirs. *PLoS Pathog* **4**:e1000172.
 34. **Elgh, F., A. Lundkvist, O. A. Alexeyev, H. Stenlund, T. Avsic-Zupanc, B. Hjelle, H. W. Lee, K. J. Smith, R. Vainionpää, D. Wiger, G. Wadell, and P. Juto.** 1997. Serological diagnosis of hantavirus infections by an enzyme-linked immunosorbent assay based on detection of immunoglobulin G and M responses to recombinant nucleocapsid proteins of five viral serotypes. *J Clin Microbiol* **35**:1122-1130.
 35. **Ennis, F. A., J. Cruz, C. F. Spiropoulou, D. Waite, C. J. Peters, S. T. Nichol, H. Kariwa, and F. T. Koster.** 1997. Hantavirus pulmonary syndrome: CD8+ and CD4+ cytotoxic T lymphocytes to epitopes on Sin Nombre virus nucleocapsid protein isolated during acute illness. *Virology* **238**:380-390.
 36. **Enria, D. A., A. M. Briggiler, N. Pini, and S. Levis.** 2001. Clinical manifestations of New World hantaviruses. *Curr Top Microbiol Immunol* **256**:117-134.
 37. **Fedorchenko, I. L., B. Z. Sirotin, and E. N. Rozhkovskaia.** 1990. [Vascular permeability, microcirculation and biologically active substances in patients with hemorrhagic fever with renal syndrome]. *Ter Arkh* **62**:71-74.
 38. **Feldmann, H., S. M. Jones, K. M. Daddario-DiCaprio, J. B. Geisbert, U. Stroher, A. Grolla, M. Bray, E. A. Fritz, L. Fernando, F. Feldmann, L. E. Hensley, and T. W. Geisbert.** 2007. Effective post-exposure treatment of Ebola infection. *PLoS Pathog* **3**:e2.
 39. **Feldmann, H., A. Sanchez, S. Morzunov, C. F. Spiropoulou, P. E. Rollin, T. G. Ksiazek, C. J. Peters, and S. T. Nichol.** 1993. Utilization of autopsy RNA for the synthesis of the nucleocapsid antigen of a newly recognized virus associated with hantavirus pulmonary syndrome. *Virus Res* **30**:351-367.
 40. **Ferrer, J. F., C. B. Jonsson, E. Esteban, D. Galligan, M. A. Basombrio, M. Peralta-Ramos, M. Bharadwaj, N. Torrez-Martinez, J. Callahan, A. Segovia, and B. Hjelle.** 1998. High prevalence of hantavirus infection in Indian communities of the Paraguayan and Argentinean Gran Chaco. *Am J Trop Med Hyg* **59**:438-444.
 41. **Flatz, L., A. Bergthaler, J. C. de la Torre, and D. D. Pinschewer.** 2006. Recovery of an arenavirus entirely from RNA polymerase I/II-driven cDNA. *Proc Natl Acad Sci U S A* **103**:4663-4668.

References

42. **Flick, K., J. W. Hooper, C. S. Schmaljohn, R. F. Pettersson, H. Feldmann, and R. Flick.** 2003. Rescue of Hantaan virus minigenomes. *Virology* **306**:219-224.
43. **Flick, R., F. Elgh, and R. F. Pettersson.** 2002. Mutational analysis of the Uukuniemi virus (Bunyaviridae family) promoter reveals two elements of functional importance. *J Virol* **76**:10849-10860.
44. **Flick, R., K. Flick, H. Feldmann, and F. Elgh.** 2003. Reverse genetics for crimean-congo hemorrhagic fever virus. *J Virol* **77**:5997-6006.
45. **Flick, R., and R. F. Pettersson.** 2001. Reverse genetics system for Uukuniemi virus (Bunyaviridae): RNA polymerase I-catalyzed expression of chimeric viral RNAs. *J Virol* **75**:1643-1655.
46. **Foecking, M. K., and H. Hofstetter.** 1986. Powerful and versatile enhancer-promoter unit for mammalian expression vectors. *Gene* **45**:101-105.
47. **French, G. R., R. S. Foulke, O. A. Brand, G. A. Eddy, H. W. Lee, and P. W. Lee.** 1981. Korean hemorrhagic fever: propagation of the etiologic agent in a cell line of human origin. *Science* **211**:1046-1048.
48. **Fuerst, T. R., E. G. Nilis, F. W. Studier, and B. Moss.** 1986. Eukaryotic transient-expression system based on recombinant vaccinia virus that synthesizes bacteriophage T7 RNA polymerase. *Proc Natl Acad Sci U S A* **83**:8122-8126.
49. **Fultz, P. N., J. A. Shaddock, C. Y. Kang, and J. W. Streilein.** 1981. Genetic analysis of resistance to lethal infections of vesicular stomatitis virus in Syrian hamsters. *Infect Immun* **32**:1007-1013.
50. **Fultz, P. N., J. A. Shaddock, C. Y. Kang, and J. W. Streilein.** 1981. Involvement of cells of hematopoietic origin in genetically determined resistance of Syrian hamsters to vesicular stomatitis virus. *Infect Immun* **34**:540-549.
51. **Garbutt, M., R. Liebscher, V. Wahl-Jensen, S. Jones, P. Moller, R. Wagner, V. Volchkov, H. D. Klenk, H. Feldmann, and U. Stroher.** 2004. Properties of replication-competent vesicular stomatitis virus vectors expressing glycoproteins of filoviruses and arenaviruses. *J Virol* **78**:5458-5465.
52. **Garcin, D., M. Lezzi, M. Dobbs, R. M. Elliott, C. Schmaljohn, C. Y. Kang, and D. Kolakofsky.** 1995. The 5' ends of Hantaan virus (Bunyaviridae) RNAs suggest a prime-and-realign mechanism for the initiation of RNA synthesis. *J Virol* **69**:5754-5762.

References

53. **Garry, C. E., and R. F. Garry.** 2004. Proteomics computational analyses suggest that the carboxyl terminal glycoproteins of Bunyaviruses are class II viral fusion protein (beta-penitrenes). *Theor Biol Med Model* **1**:10.
54. **Gavrilovskaya, I. N., E. J. Brown, M. H. Ginsberg, and E. R. Mackow.** 1999. Cellular entry of hantaviruses which cause hemorrhagic fever with renal syndrome is mediated by beta3 integrins. *J Virol* **73**:3951-3959.
55. **Geimonen, E., I. Fernandez, I. N. Gavrilovskaya, and E. R. Mackow.** 2003. Tyrosine residues direct the ubiquitination and degradation of the NY-1 hantavirus G1 cytoplasmic tail. *J Virol* **77**:10760-10868.
56. **Geimonen, E., S. Neff, T. Raymond, S. S. Kocer, I. N. Gavrilovskaya, and E. R. Mackow.** 2002. Pathogenic and nonpathogenic hantaviruses differentially regulate endothelial cell responses. *Proc Natl Acad Sci U S A* **99**:13837-13842.
57. **Geisbert, T. W., K. M. Daddario-Dicaprio, M. G. Lewis, J. B. Geisbert, A. Grolla, A. Leung, J. Paragas, L. Matthias, M. A. Smith, S. M. Jones, L. E. Hensley, H. Feldmann, and P. B. Jahrling.** 2008. Vesicular stomatitis virus-based ebola vaccine is well-tolerated and protects immunocompromised nonhuman primates. *PLoS Pathog* **4**:e1000225.
58. **Geisbert, T. W., K. M. Daddario-DiCaprio, K. J. Williams, J. B. Geisbert, A. Leung, F. Feldmann, L. E. Hensley, H. Feldmann, and S. M. Jones.** 2008. Recombinant vesicular stomatitis virus vector mediates postexposure protection against Sudan Ebola hemorrhagic fever in nonhuman primates. *J Virol* **82**:5664-5668.
59. **Geisbert, T. W., J. B. Geisbert, A. Leung, K. M. Daddario-DiCaprio, L. E. Hensley, A. Grolla, and H. Feldmann.** 2009. Single-injection vaccine protects nonhuman primates against infection with marburg virus and three species of ebola virus. *J Virol* **83**:7296-7304.
60. **Geisbert, T. W., L. E. Hensley, J. B. Geisbert, A. Leung, J. C. Johnson, A. Grolla, and H. Feldmann.** 2010. Postexposure treatment of Marburg virus infection. *Emerg Infect Dis* **16**:1119-1122.
61. **Geldmacher, A., M. Schmalzer, D. H. Krüger, and R. Ulrich.** 2004. Yeast-expressed hantavirus Dobrava nucleocapsid protein induces a strong, long-lasting, and highly cross-reactive immune response in mice. *Viral Immunol* **17**:115-122.
62. **Geldmacher, A., D. Skrastina, G. Borisova, I. Petrovskis, D. H. Krüger, P. Pumpens, and R. Ulrich.** 2005. A hantavirus nucleocapsid protein segment exposed on hepatitis B virus core particles is highly immunogenic in mice when

- applied without adjuvants or in the presence of pre-existing anti-core antibodies. *Vaccine* **23**:3973-3983.
63. **Geldmacher, A., D. Skrastina, I. Petrovskis, G. Borisova, J. A. Berriman, A. M. Roseman, R. A. Crowther, J. Fischer, S. Musema, H. R. Gelderblom, A. Lundkvist, R. Renhofa, V. Ose, D. H. Krüger, P. Pumpens, and R. Ulrich.** 2004. An amino-terminal segment of hantavirus nucleocapsid protein presented on hepatitis B virus core particles induces a strong and highly cross-reactive antibody response in mice. *Virology* **323**:108-119.
 64. **Gluzman, Y.** 1981. SV40-transformed simian cells support the replication of early SV40 mutants. *Cell* **23**:175-182.
 65. **Graham, F. L., J. Smiley, W. C. Russell, and R. Nairn.** 1977. Characteristics of a human cell line transformed by DNA from human adenovirus type 5. *J Gen Virol* **36**:59-74.
 66. **Groseth, A., H. Feldmann, S. Theriault, G. Mehmetoglu, and R. Flick.** 2005. RNA polymerase I-driven minigenome system for Ebola viruses. *J Virol* **79**:4425-4433.
 67. **Haglund, K., J. Forman, H. G. Krausslich, and J. K. Rose.** 2000. Expression of human immunodeficiency virus type 1 Gag protein precursor and envelope proteins from a vesicular stomatitis virus recombinant: high-level production of virus-like particles containing HIV envelope. *Virology* **268**:112-121.
 68. **Halfmann, P., H. Ebihara, A. Marzi, Y. Hatta, S. Watanabe, M. Suresh, G. Neumann, H. Feldmann, and Y. Kawaoka.** 2009. Replication-deficient ebolavirus as a vaccine candidate. *J Virol* **83**:3810-3815.
 69. **Halpin, K., B. Bankamp, B. H. Harcourt, W. J. Bellini, and P. A. Rota.** 2004. Nipah virus conforms to the rule of six in a minigenome replication assay. *J Gen Virol* **85**:701-707.
 70. **Hammerbeck, C. D., and J. W. Hooper.** 2011. T Cells Are Not Required for Pathogenesis in the Syrian Hamster Model of Hantavirus Pulmonary Syndrome. *J Virol*.
 71. **Heinzel, S. S., P. J. Krysan, M. P. Calos, and R. B. DuBridge.** 1988. Use of simian virus 40 replication to amplify Epstein-Barr virus shuttle vectors in human cells. *J Virol* **62**:3738-3746.
 72. **Hensley, L. E., S. Mulangu, C. Asiedu, J. Johnson, A. N. Honko, D. Stanley, G. Fabozzi, S. T. Nichol, T. G. Ksiazek, P. E. Rollin, V. Wahl-Jensen, M. Bailey, P. B. Jahrling, M. Roederer, R. A. Koup, and N. J. Sullivan.** 2010.

References

- Demonstration of cross-protective vaccine immunity against an emerging pathogenic Ebolavirus Species. *PLoS Pathog* **6**:e1000904.
73. **Hewlett, M. J., R. F. Pettersson, and D. Baltimore.** 1977. Circular forms of Uukuniemi virion RNA: an electron microscopic study. *J Virol* **21**:1085-1093.
74. **Hjelle, B., D. Goade, N. Torrez-Martinez, M. Lang-Williams, J. Kim, R. L. Harris, and J. A. Rawlings.** 1996. Hantavirus pulmonary syndrome, renal insufficiency, and myositis associated with infection by Bayou hantavirus. *Clin Infect Dis* **23**:495-500.
75. **Hjelle, B., S. A. Jenison, D. E. Goade, W. B. Green, R. M. Feddersen, and A. A. Scott.** 1995. Hantaviruses: clinical, microbiologic, and epidemiologic aspects. *Crit Rev Clin Lab Sci* **32**:469-508.
76. **Hoffmann, E., G. Neumann, Y. Kawaoka, G. Hobom, and R. G. Webster.** 2000. A DNA transfection system for generation of influenza A virus from eight plasmids. *Proc Natl Acad Sci U S A* **97**:6108-6113.
77. **Hooper, J. W., D. M. Custer, J. Smith, and V. Wahl-Jensen.** 2006. Hantaan/Andes virus DNA vaccine elicits a broadly cross-reactive neutralizing antibody response in nonhuman primates. *Virology* **347**:208-216.
78. **Hooper, J. W., D. M. Custer, E. Thompson, and C. S. Schmaljohn.** 2001. DNA vaccination with the Hantaan virus M gene protects Hamsters against three of four HFRS hantaviruses and elicits a high-titer neutralizing antibody response in Rhesus monkeys. *J Virol* **75**:8469-8477.
79. **Hooper, J. W., A. M. Ferro, and V. Wahl-Jensen.** 2008. Immune serum produced by DNA vaccination protects hamsters against lethal respiratory challenge with Andes virus. *J Virol* **82**:1332-1338.
80. **Hooper, J. W., K. I. Kamrud, F. Elgh, D. Custer, and C. S. Schmaljohn.** 1999. DNA vaccination with hantavirus M segment elicits neutralizing antibodies and protects against seoul virus infection. *Virology* **255**:269-278.
81. **Hooper, J. W., T. Larsen, D. M. Custer, and C. S. Schmaljohn.** 2001. A lethal disease model for hantavirus pulmonary syndrome. *Virology* **289**:6-14.
82. **Hutchinson, K. L., C. J. Peters, and S. T. Nichol.** 1996. Sin Nombre virus mRNA synthesis. *Virology* **224**:139-149.
83. **Ikegami, T., C. J. Peters, and S. Makino.** 2005. Rift valley fever virus nonstructural protein NSs promotes viral RNA replication and transcription in a minigenome system. *J Virol* **79**:5606-5615.

References

84. **Iyer, A. V., B. Pahar, M. J. Boudreaux, N. Wakamatsu, A. F. Roy, V. N. Chouljenko, A. Baghian, C. Apetrei, P. A. Marx, and K. G. Kousoulas.** 2009. Recombinant vesicular stomatitis virus-based west Nile vaccine elicits strong humoral and cellular immune responses and protects mice against lethal challenge with the virulent west Nile virus strain LSU-AR01. *Vaccine* **27**:893-903.
85. **Jin, M., J. Park, S. Lee, B. Park, J. Shin, K. J. Song, T. I. Ahn, S. Y. Hwang, B. Y. Ahn, and K. Ahn.** 2002. Hantaan virus enters cells by clathrin-dependent receptor-mediated endocytosis. *Virology* **294**:60-69.
86. **Jokinen, E. J., Y. Collan, and J. Lähdevirta.** 1977. Renal immune complexes in epidemic nephropathy. *Lancet* **1**:1012-1013.
87. **Jones, S. M., H. Feldmann, U. Stroher, J. B. Geisbert, L. Fernando, A. Grolla, H. D. Klenk, N. J. Sullivan, V. E. Volchkov, E. A. Fritz, K. M. Daddario, L. E. Hensley, P. B. Jahrling, and T. W. Geisbert.** 2005. Live attenuated recombinant vaccine protects nonhuman primates against Ebola and Marburg viruses. *Nat Med* **11**:786-790.
88. **Jonsson, C. B., L. T. Figueiredo, and O. Vapalahti.** 2010. A global perspective on hantavirus ecology, epidemiology, and disease. *Clin Microbiol Rev* **23**:412-441.
89. **Jonsson, C. B., J. Hooper, and G. Mertz.** 2008. Treatment of hantavirus pulmonary syndrome. *Antiviral Res* **78**:162-169.
90. **Jääskeläinen, K. M., P. Kaukinen, E. S. Minskaya, A. Plyusnina, O. Vapalahti, R. M. Elliott, F. Weber, A. Vaheri, and A. Plyusnin.** 2007. Tula and Puumala hantavirus NSs ORFs are functional and the products inhibit activation of the interferon-beta promoter. *J Med Virol* **79**:1527-1536.
91. **Kanerva, M., J. Mustonen, and A. Vaheri.** 1998. Pathogenesis of puumala and other hantavirus infections. *Rev Med Virol* **8**:67-86.
92. **Kariwa, H., H. Tanabe, T. Mizutani, Y. Kon, K. Lokugamage, N. Lokugamage, M. A. Iwasa, T. Hagiya, K. Araki, K. Yoshimatsu, J. Arikawa, and I. Takashima.** 2003. Synthesis of Seoul virus RNA and structural proteins in cultured cells. *Arch Virol* **148**:1671-1685.
93. **Kato, A., Y. Sakai, T. Shioda, T. Kondo, M. Nakanishi, and Y. Nagai.** 1996. Initiation of Sendai virus multiplication from transfected cDNA or RNA with negative or positive sense. *Genes Cells* **1**:569-579.
94. **Khaiboullina, S. F., S. P. Morzunov, and S. C. St Jeor.** 2005. Hantaviruses: molecular biology, evolution and pathogenesis. *Curr Mol Med* **5**:773-790.

References

95. **Khaiboullina, S. F., A. A. Rizvanov, V. M. Deyde, and S. C. St Jeor.** 2005. Andes virus stimulates interferon-inducible MxA protein expression in endothelial cells. *J Med Virol* **75**:267-275.
96. **Khan, A. S., T. G. Ksiazek, and C. J. Peters.** 1996. Hantavirus pulmonary syndrome. *Lancet* **347**:739-741.
97. **Kim, Y. S., C. Ahn, J. S. Han, S. Kim, J. S. Lee, and P. W. Lee.** 1995. Hemorrhagic fever with renal syndrome caused by the Seoul virus. *Nephron* **71**:419-427.
98. **Klempa, B., E. Fichet-Calvet, E. Lecompte, B. Auste, V. Aniskin, H. Meisel, P. Barrière, L. Koivogui, J. ter Meulen, and D. H. Krüger.** 2007. Novel hantavirus sequences in Shrew, Guinea. *Emerg Infect Dis* **13**:520-522.
99. **Klempa, B., E. Fichet-Calvet, E. Lecompte, B. Auste, V. Aniskin, H. Meisel, C. Denys, L. Koivogui, J. ter Meulen, and D. H. Krüger.** 2006. Hantavirus in African wood mouse, Guinea. *Emerg Infect Dis* **12**:838-840.
100. **Kochs, G., A. García-Sastre, and L. Martínez-Sobrido.** 2007. Multiple anti-interferon actions of the influenza A virus NS1 protein. *J Virol* **81**:7011-7021.
101. **Kohl, A., E. F. Dunn, A. C. Lowen, and R. M. Elliott.** 2004. Complementarity, sequence and structural elements within the 3' and 5' non-coding regions of the Bunyamwera orthobunyavirus S segment determine promoter strength. *J Gen Virol* **85**:3269-3278.
102. **Koma, T., K. Yoshimatsu, N. Pini, D. Safronetz, M. Taruishi, S. Levis, R. Endo, K. Shimizu, S. P. Yasuda, H. Ebihara, H. Feldmann, D. Enria, and J. Arikawa.** 2010. Truncated hantavirus nucleocapsid proteins for serotyping Sin Nombre, Andes, and Laguna Negra hantavirus infections in humans and rodents. *J Clin Microbiol* **48**:1635-1642.
103. **Kopecky, S. A., M. C. Willingham, and D. S. Lyles.** 2001. Matrix protein and another viral component contribute to induction of apoptosis in cells infected with vesicular stomatitis virus. *J Virol* **75**:12169-12181.
104. **Kraus, A. A., M. J. Raftery, T. Giese, R. Ulrich, R. Zawatzky, S. Hippenstiel, N. Suttorp, D. H. Krüger, and G. Schönrich.** 2004. Differential antiviral response of endothelial cells after infection with pathogenic and nonpathogenic hantaviruses. *J Virol* **78**:6143-6150.
105. **Krautkrämer, E., and M. Zeier.** 2008. Hantavirus causing hemorrhagic fever with renal syndrome enters from the apical surface and requires decay-accelerating factor (DAF/CD55). *J Virol* **82**:4257-4264.

References

106. **Kretzschmar, E., L. Buonocore, M. J. Schnell, and J. K. Rose.** 1997. High-efficiency incorporation of functional influenza virus glycoproteins into recombinant vesicular stomatitis viruses. *J Virol* **71**:5982-5989.
107. **Ksiazek, T. G., C. J. Peters, P. E. Rollin, S. Zaki, S. Nichol, C. Spiropoulou, S. Morzunov, H. Feldmann, A. Sanchez, and A. S. Khan.** 1995. Identification of a new North American hantavirus that causes acute pulmonary insufficiency. *Am J Trop Med Hyg* **52**:117-123.
108. **Kukkonen, S. K., A. Vaheri, and A. Plyusnin.** 2005. L protein, the RNA-dependent RNA polymerase of hantaviruses. *Arch Virol* **150**:533-556.
109. **Kukkonen, S. K., A. Vaheri, and A. Plyusnin.** 2004. Tula hantavirus L protein is a 250 kDa perinuclear membrane-associated protein. *J Gen Virol* **85**:1181-1189.
110. **Lamb, R. A., and D. P. Griffith.** 2007. Paramyxoviridae : The Viruses and Their Replication, p. 1449-1496. *In* D. M. Knipe and P. A. Howley (ed.), *Field's Virology*, 5 ed. Lippincott Williams & Wilkins, Philadelphia, PA.
111. **Lawson, N. D., E. A. Stillman, M. A. Whitt, and J. K. Rose.** 1995. Recombinant vesicular stomatitis viruses from DNA. *Proc Natl Acad Sci U S A* **92**:4477-4481.
112. **Lazaro, M. E., G. E. Cantoni, L. M. Calanni, A. J. Resa, E. R. Herrero, M. A. Iacono, D. A. Enria, and S. M. Gonzalez Cappa.** 2007. Clusters of hantavirus infection, southern Argentina. *Emerg Infect Dis* **13**:104-110.
113. **LeDuc, J. W., G. A. Smith, J. E. Childs, F. P. Pinheiro, J. I. Maiztegui, B. Niklasson, A. Antoniadis, D. M. Robinson, M. Khin, and K. F. Shortridge.** 1986. Global survey of antibody to Hantaan-related viruses among peridomestic rodents. *Bull World Health Organ* **64**:139-144.
114. **Lee, B. H., K. Yoshimatsu, K. Araki, M. Okumura, I. Nakamura, and J. Arikawa.** 2006. A pseudotype vesicular stomatitis virus containing Hantaan virus envelope glycoproteins G1 and G2 as an alternative to hantavirus vaccine in mice. *Vaccine* **24**:2928-2934.
115. **Lee, H. W.** 1982. Hemorrhagic fever with renal syndrome (HFRS). *Scand J Infect Dis Suppl* **36**:82-85.
116. **Lee, H. W.** 1989. Hemorrhagic fever with renal syndrome in Korea. *Rev Infect Dis* **11 Suppl 4**:S864-876.

References

117. **Lee, H. W., G. R. French, P. W. Lee, L. J. Baek, K. Tsuchiya, and R. S. Foulke.** 1981. Observations on natural and laboratory infection of rodents with the etiologic agent of Korean hemorrhagic fever. *Am J Trop Med Hyg* **30**:477-482.
118. **Lee, H. W., and P. W. Lee.** 1976. Korean hemorrhagic fever. I. Demonstration of causative antigen and antibodies. *Korean Journal of Internal Medicine* **19**:371-394.
119. **Lee, H. W., P. W. Lee, L. J. Baek, C. K. Song, and I. W. Seong.** 1981. Intraspecific transmission of Hantaan virus, etiologic agent of Korean hemorrhagic fever, in the rodent *Apodemus agrarius*. *Am J Trop Med Hyg* **30**:1106-1112.
120. **Lee, H. W., P. W. Lee, and K. M. Johnson.** 1978. Isolation of the etiologic agent of Korean Hemorrhagic fever. *J Infect Dis* **137**:298-308.
121. **Lee, H. W., P. W. Lee, J. Lähdevirta, and M. Brummer-Korventkontio.** 1979. Aetiological relation between Korean haemorrhagic fever and nephropathia epidemica. *Lancet* **1**:186-187.
122. **Lee, H. W., P. W. Lee, M. Tamura, T. Tamura, and Y. Okuno.** 1979. Etiological relation between Korean hemorrhagic fever and epidemic hemorrhagic fever in Japan. *Biken J* **22**:41-45.
123. **Lee, K. J., I. S. Novella, M. N. Teng, M. B. Oldstone, and J. C. de La Torre.** 2000. NP and L proteins of lymphocytic choriomeningitis virus (LCMV) are sufficient for efficient transcription and replication of LCMV genomic RNA analogs. *J Virol* **74**:3470-3477.
124. **Lee, P. W., D. C. Gajdusek, C. J. Gibbs, and Z. Y. Xu.** 1980. Aetiological relation between Korean haemorrhagic fever with renal syndrome in People's Republic of China. *Lancet* **1**:819-820.
125. **Levine, J. R., J. Prescott, K. S. Brown, S. M. Best, H. Ebihara, and H. Feldmann.** 2010. Antagonism of type I interferon responses by new world hantaviruses. *J Virol* **84**:11790-11801.
126. **Levis, S., S. P. Morzunov, J. E. Rowe, D. Enria, N. Pini, G. Calderon, M. Sabattini, and S. C. St Jeor.** 1998. Genetic diversity and epidemiology of hantaviruses in Argentina. *J Infect Dis* **177**:529-538.
127. **Levis, S., J. E. Rowe, S. Morzunov, D. A. Enria, and S. St Jeor.** 1997. New hantaviruses causing hantavirus pulmonary syndrome in central Argentina. *Lancet* **349**:998-999.

References

128. **Lewis, R. M., H. W. Lee, A. F. See, D. B. Parrish, J. S. Moon, D. J. Kim, and T. M. Cosgriff.** 1991. Changes in populations of immune effector cells during the course of haemorrhagic fever with renal syndrome. *Trans R Soc Trop Med Hyg* **85**:282-286.
129. **Livak, K. J., and T. D. Schmittgen.** 2001. Analysis of relative gene expression data using real-time quantitative PCR and the 2^{(-Delta Delta C(T))} Method. *Methods* **25**:402-408.
130. **Lopez, N., R. Muller, C. Prehaud, and M. Bouloy.** 1995. The L protein of Rift Valley fever virus can rescue viral ribonucleoproteins and transcribe synthetic genome-like RNA molecules. *J Virol* **69**:3972-3979.
131. **Lopez, N., P. Padula, C. Rossi, M. E. Lazaro, and M. T. Franze-Fernandez.** 1996. Genetic identification of a new hantavirus causing severe pulmonary syndrome in Argentina. *Virology* **220**:223-226.
132. **Lowen, A. C., and R. M. Elliott.** 2005. Mutational analyses of the nonconserved sequences in the Bunyamwera Orthobunyavirus S segment untranslated regions. *J Virol* **79**:12861-12870.
133. **Lowin, B., M. Hahne, C. Mattmann, and J. Tschopp.** 1994. Cytolytic T-cell cytotoxicity is mediated through perforin and Fas lytic pathways. *Nature* **370**:650-652.
134. **Luytjes, W., M. Krystal, M. Enami, J. D. Parvin, and P. Palese.** 1989. Amplification, expression, and packaging of foreign gene by influenza virus. *Cell* **59**:1107-1113.
135. **Lyles, D. S., and C. E. Rupprecht.** 2007. Rhabdoviridae, p. 1364-1409. *In* D. M. Knipe and P. M. Howley (ed.), *Field's Virology*, 5th ed. Lippincott Williams & Wilkins, Philadelphia, PA.
136. **Löber, C., B. Anheier, S. Lindow, H. D. Klenk, and H. Feldmann.** 2001. The Hantaan virus glycoprotein precursor is cleaved at the conserved pentapeptide WAASA. *Virology* **289**:224-229.
137. **Maeda, K., K. West, T. Toyosaki-Maeda, A. L. Rothman, F. A. Ennis, and M. Terajima.** 2004. Identification and analysis for cross-reactivity among hantaviruses of H-2b-restricted cytotoxic T-lymphocyte epitopes in Sin Nombre virus nucleocapsid protein. *J Gen Virol* **85**:1909-1919.
138. **Maes, P., J. Clement, and M. Van Ranst.** 2009. Recent approaches in hantavirus vaccine development. *Expert Rev Vaccines* **8**:67-76.

References

139. **Martin, A., P. Staeheli, and U. Schneider.** 2006. RNA polymerase II-controlled expression of antigenomic RNA enhances the rescue efficacies of two different members of the Mononegavirales independently of the site of viral genome replication. *J Virol* **80**:5708-5715.
140. **Martinez, I., L. L. Rodriguez, C. Jimenez, S. J. Pauszek, and G. W. Wertz.** 2003. Vesicular stomatitis virus glycoprotein is a determinant of pathogenesis in swine, a natural host. *J Virol* **77**:8039-8047.
141. **Martinez, V. P., C. Bellomo, J. San Juan, D. Pinna, R. Forlenza, M. Elder, and P. J. Padula.** 2005. Person-to-person transmission of Andes virus. *Emerg Infect Dis* **11**:1848-1853.
142. **Martinez, V. P., C. M. Bellomo, M. L. Cacace, P. Suarez, L. Bogni, and P. J. Padula.** 2010. Hantavirus pulmonary syndrome in Argentina, 1995-2008. *Emerg Infect Dis* **16**:1853-1860.
143. **Matsuo, E., C. C. Celma, M. Boyce, C. Viarouge, C. Sailleau, E. Dubois, E. Bréard, R. Thiéry, S. Zientara, and P. Roy.** 2011. Generation of Replication-Defective Virus-Based Vaccines That Confer Full Protection in Sheep against Virulent Bluetongue Virus Challenge. *J Virol* **85**:10213-10221.
144. **McClain, D. J., P. L. Summers, S. A. Harrison, A. L. Schmaljohn, and C. S. Schmaljohn.** 2000. Clinical evaluation of a vaccinia-vectored Hantaan virus vaccine. *J Med Virol* **60**:77-85.
145. **McElroy, A. K., J. M. Smith, J. W. Hooper, and C. S. Schmaljohn.** 2004. Andes virus M genome segment is not sufficient to confer the virulence associated with Andes virus in Syrian hamsters. *Virology* **326**:130-139.
146. **Mertz, G. J., L. Miedzinski, D. Goade, A. T. Pavia, B. Hjelle, C. O. Hansbarger, H. Levy, F. T. Koster, K. Baum, A. Lindemulder, W. Wang, L. Riser, H. Fernandez, and R. J. Whitley.** 2004. Placebo-controlled, double-blind trial of intravenous ribavirin for the treatment of hantavirus cardiopulmonary syndrome in North America. *Clin Infect Dis* **39**:1307-1313.
147. **Meyer, B. J., and C. Schmaljohn.** 2000. Accumulation of terminally deleted RNAs may play a role in Seoul virus persistence. *J Virol* **74**:1321-1331.
148. **Meyer, H., G. Sutter, and A. Mayr.** 1991. Mapping of deletions in the genome of the highly attenuated vaccinia virus MVA and their influence on virulence. *J Gen Virol* **72** (Pt 5):1031-1038.

References

149. **Mir, M. A., W. A. Duran, B. L. Hjelle, C. Ye, and A. T. Panganiban.** 2008. Storage of cellular 5' mRNA caps in P bodies for viral cap-snatching. *Proc Natl Acad Sci U S A* **105**:19294-19299.
150. **Mir, M. A., and A. T. Panganiban.** 2008. A protein that replaces the entire cellular eIF4F complex. *EMBO J* **27**:3129-3139.
151. **Mir, M. A., and A. T. Panganiban.** 2006. Characterization of the RNA chaperone activity of hantavirus nucleocapsid protein. *J Virol* **80**:6276-6285.
152. **Mir, M. A., and A. T. Panganiban.** 2010. The triplet repeats of the Sin Nombre hantavirus 5' untranslated region are sufficient in cis for nucleocapsid-mediated translation initiation. *J Virol* **84**:8937-8944.
153. **Mühlberger, E., M. Weik, V. E. Volchkov, H. D. Klenk, and S. Becker.** 1999. Comparison of the transcription and replication strategies of marburg virus and Ebola virus by using artificial replication systems. *J Virol* **73**:2333-2342.
154. **Netski, D., B. H. Thran, and S. C. St Jeor.** 1999. Sin Nombre virus pathogenesis in *Peromyscus maniculatus*. *J Virol* **73**:585-591.
155. **Neumann, G., T. Watanabe, H. Ito, S. Watanabe, H. Goto, P. Gao, M. Hughes, D. R. Perez, R. Donis, E. Hoffmann, G. Hobom, and Y. Kawaoka.** 1999. Generation of influenza A viruses entirely from cloned cDNAs. *Proc Natl Acad Sci U S A* **96**:9345-9350.
156. **Neumann, G., M. A. Whitt, and Y. Kawaoka.** 2002. A decade after the generation of a negative-sense RNA virus from cloned cDNA - what have we learned? *J Gen Virol* **83**:2635-2662.
157. **Nichol, S. T.** 1999. Genetic analysis of hantaviruses and their host relationships, p. 99-109. *In* J. F. Saluzzo and B. Dodet (ed.), *Factors in the emergence and control of rodent-borne viral diseases*. Elsevier, Paris.
158. **Nichol, S. T., R. M. Elliot, R. Goldbach, A. Plyusnin, B. J. Beaty, C. S. Schmaljohn, and R. B. Tesh.** 2005. Bunyaviridae, p. 695-716. *In* C. M. Fauquet, M. A. Mayo, J. Maniloff, U. Desselberger, and L. A. Ball (ed.), *Virus Taxonomy: VIIIth Report of the International Committee on Taxonomy of Viruses*. Academic Press, San Diego, CA.
159. **Nichol, S. T., C. F. Spiropoulou, S. Morzunov, P. E. Rollin, T. G. Ksiazek, H. Feldmann, A. Sanchez, J. Childs, S. Zaki, and C. J. Peters.** 1993. Genetic identification of a hantavirus associated with an outbreak of acute respiratory illness. *Science* **262**:914-917.

References

160. **Niklasson, B., J. Leduc, K. Nyström, and L. Nyman.** 1987. Nephropathia epidemica: incidence of clinical cases and antibody prevalence in an endemic area of Sweden. *Epidemiol Infect* **99**:559-562.
161. **Niwa, H., K. Yamamura, and J. Miyazaki.** 1991. Efficient selection for high-expression transfectants with a novel eukaryotic vector. *Gene* **108**:193-199.
162. **Noble, S., L. McLain, and N. J. Dimmock.** 2004. Interfering vaccine: a novel antiviral that converts a potentially virulent infection into one that is subclinical and immunizing. *Vaccine* **22**:3018-3025.
163. **Ogino, M., H. Ebihara, B. H. Lee, K. Araki, A. Lundkvist, Y. Kawaoka, K. Yoshimatsu, and J. Arikawa.** 2003. Use of vesicular stomatitis virus pseudotypes bearing hantaan or seoul virus envelope proteins in a rapid and safe neutralization test. *Clin Diagn Lab Immunol* **10**:154-160.
164. **Ogino, M., K. Yoshimatsu, H. Ebihara, K. Araki, B. H. Lee, M. Okumura, and J. Arikawa.** 2004. Cell fusion activities of Hantaan virus envelope glycoproteins. *J Virol* **78**:10776-10782.
165. **Padula, P. J., A. Edelstein, S. D. Miguel, N. M. Lopez, C. M. Rossi, and R. D. Rabinovich.** 1998. Hantavirus pulmonary syndrome outbreak in Argentina: molecular evidence for person-to-person transmission of Andes virus. *Virology* **241**:323-330.
166. **Padula, P. J., A. J. Sanchez, A. Edelstein, and S. T. Nichol.** 2002. Complete nucleotide sequence of the M RNA segment of Andes virus and analysis of the variability of the termini of the virus S, M and L RNA segments. *J Gen Virol* **83**:2117-2122.
167. **Papa, A., A. M. Johnson, P. C. Stockton, M. D. Bowen, C. F. Spiropoulou, S. Alexiou-Daniel, T. G. Ksiazek, S. T. Nichol, and A. Antoniadis.** 1998. Retrospective serological and genetic study of the distribution of hantaviruses in Greece. *J Med Virol* **55**:321-327.
168. **Pensiero, M. N., J. B. Sharefkin, C. W. Dieffenbach, and J. Hay.** 1992. Hantaan virus infection of human endothelial cells. *J Virol* **66**:5929-5936.
169. **Penttinen, K., J. Lähdevirta, R. Kekomäki, B. Ziola, A. Salmi, A. Hautanen, P. Lindström, A. Vaheri, M. Brummer-Korvenkontio, and O. Wager.** 1981. Circulating immune complexes, immunoconglutinins, and rheumatoid factors in nephropathia epidemica. *J Infect Dis* **143**:15-21.

References

170. **Perrotta, A. T., and M. D. Been.** 1990. The self-cleaving domain from the genomic RNA of hepatitis delta virus: sequence requirements and the effects of denaturant. *Nucleic Acids Res* **18**:6821-6827.
171. **Prehaud, C., N. Lopez, M. J. Blok, V. Obry, and M. Bouloy.** 1997. Analysis of the 3' terminal sequence recognized by the Rift Valley fever virus transcription complex in its ambisense S segment. *Virology* **227**:189-197.
172. **Racaniello, V. R., and D. Baltimore.** 1981. Cloned poliovirus complementary DNA is infectious in mammalian cells. *Science* **214**:916-919.
173. **Radecke, F., P. Spielhofer, H. Schneider, K. Kaelin, M. Huber, C. Dötsch, G. Christiansen, and M. A. Billeter.** 1995. Rescue of measles viruses from cloned DNA. *EMBO J* **14**:5773-5784.
174. **Raftery, M. J., A. A. Kraus, R. Ulrich, D. H. Krüger, and G. Schönrich.** 2002. Hantavirus infection of dendritic cells. *J Virol* **76**:10724-10733.
175. **Ramanathan, H. N., D. H. Chung, S. J. Plane, E. Sztul, Y. K. Chu, M. C. Gutteri, M. McDowell, G. Ali, and C. B. Jonsson.** 2007. Dynein-dependent transport of the hantaan virus nucleocapsid protein to the endoplasmic reticulum-Golgi intermediate compartment. *J Virol* **81**:8634-8647.
176. **Rasmuson, J., C. Andersson, E. Norrman, M. Haney, M. Evander, and C. Ahlm.** 2011. Time to revise the paradigm of hantavirus syndromes? Hantavirus pulmonary syndrome caused by European hantavirus. *Eur J Clin Microbiol Infect Dis* **30**:685-690.
177. **Ravkov, E. V., and R. W. Compans.** 2001. Hantavirus nucleocapsid protein is expressed as a membrane-associated protein in the perinuclear region. *J Virol* **75**:1808-1815.
178. **Ravkov, E. V., S. T. Nichol, and R. W. Compans.** 1997. Polarized entry and release in epithelial cells of Black Creek Canal virus, a New World hantavirus. *J Virol* **71**:1147-1154.
179. **Ray, N., J. Whidby, S. Stewart, J. W. Hooper, and A. Bertolotti-Ciarlet.** 2010. Study of Andes virus entry and neutralization using a pseudovirion system. *J Virol Methods* **163**:416-423.
180. **Reed, L. J., and H. Muench.** 1938. A simple method of estimating fifty per cent endpoints. *American Journal of Epidemiology* **27**:493-497.
181. **Reid, S. P., L. W. Leung, A. L. Hartman, O. Martinez, M. L. Shaw, C. Carbonnelle, V. E. Volchkov, S. T. Nichol, and C. F. Basler.** 2006. Ebola virus

References

- VP24 binds karyopherin alpha1 and blocks STAT1 nuclear accumulation. *J Virol* **80**:5156-5167.
182. **Roberts, A., L. Buonocore, R. Price, J. Forman, and J. K. Rose.** 1999. Attenuated vesicular stomatitis viruses as vaccine vectors. *J Virol* **73**:3723-3732.
183. **Roberts, A., E. Kretzschmar, A. S. Perkins, J. Forman, R. Price, L. Buonocore, Y. Kawaoka, and J. K. Rose.** 1998. Vaccination with a recombinant vesicular stomatitis virus expressing an influenza virus hemagglutinin provides complete protection from influenza virus challenge. *J Virol* **72**:4704-4711.
184. **Rusnak, J. M., W. R. Byrne, K. N. Chung, P. H. Gibbs, T. T. Kim, E. F. Boudreau, T. Cosgriff, P. Pittman, K. Y. Kim, M. S. Erlichman, D. F. Rezvani, and J. W. Huggins.** 2009. Experience with intravenous ribavirin in the treatment of hemorrhagic fever with renal syndrome in Korea. *Antiviral Res* **81**:68-76.
185. **Ruusala, A., R. Persson, C. S. Schmaljohn, and R. F. Pettersson.** 1992. Coexpression of the membrane glycoproteins G1 and G2 of Hantaan virus is required for targeting to the Golgi complex. *Virology* **186**:53-64.
186. **Safronetz, D., N. R. Hegde, H. Ebihara, M. Denton, G. P. Kobinger, S. St Jeor, H. Feldmann, and D. C. Johnson.** 2009. Adenovirus vectors expressing hantavirus proteins protect hamsters against lethal challenge with andes virus. *J Virol* **83**:7285-7295.
187. **Sanchez, A., T. W. Geisbert, and H. Feldmann.** 2007. Filoviridae, p. 1409-1448. *In* D. M. Knipe and P. M. Howley (ed.), *Field's Virology*, 5th ed. Lippincott Williams & Wilkins, Philadelphia, PA.
188. **Schmaljohn, C.** 2009. Vaccines for hantaviruses. *Vaccine* **27 Suppl 4**:D61-64.
189. **Schmaljohn, C. S., and J. M. Dalrymple.** 1983. Analysis of Hantaan virus RNA: evidence for a new genus of bunyaviridae. *Virology* **131**:482-491.
190. **Schmaljohn, C. S., S. E. Hasty, and J. M. Dalrymple.** 1992. Preparation of candidate vaccinia-vectored vaccines for haemorrhagic fever with renal syndrome. *Vaccine* **10**:10-13.
191. **Schmaljohn, C. S., S. E. Hasty, S. A. Harrison, and J. M. Dalrymple.** 1983. Characterization of Hantaan virions, the prototype virus of hemorrhagic fever with renal syndrome. *J Infect Dis* **148**:1005-1012.

192. **Schmaljohn, C. S., S. E. Hasty, L. Rasmussen, and J. M. Dalrymple.** 1986. Hantaan virus replication: effects of monensin, tunicamycin and endoglycosidases on the structural glycoproteins. *J Gen Virol* **67 (Pt 4):**707-717.
193. **Schmaljohn, C. S., and S. T. Nichol.** 2007. Bunyaviridae, p. 1742-1789. *In* D. M. Knipe, Howley, P.A. (ed.), *Fields Virology*, 5 ed. Lippincott Williams & Wilkins, Philadelphia, PA.
194. **Schneider, U., M. Schwemmle, and P. Staeheli.** 2005. Genome trimming: a unique strategy for replication control employed by Borna disease virus. *Proc Natl Acad Sci U S A* **102:**3441-3446.
195. **Schnell, M. J., L. Buonocore, E. Kretzschmar, E. Johnson, and J. K. Rose.** 1996. Foreign glycoproteins expressed from recombinant vesicular stomatitis viruses are incorporated efficiently into virus particles. *Proc Natl Acad Sci U S A* **93:**11359-11365.
196. **Schnell, M. J., L. Buonocore, M. A. Whitt, and J. K. Rose.** 1996. The minimal conserved transcription stop-start signal promotes stable expression of a foreign gene in vesicular stomatitis virus. *J Virol* **70:**2318-2323.
197. **Schnell, M. J., T. Mebatsion, and K. K. Conzelmann.** 1994. Infectious rabies viruses from cloned cDNA. *EMBO J* **13:**4195-4203.
198. **Schonrich, G., A. Rang, N. Lutteke, M. J. Raftery, N. Charbonnel, and R. G. Ulrich.** 2008. Hantavirus-induced immunity in rodent reservoirs and humans. *Immunol Rev* **225:**163-189.
199. **Schwartz, J. A., L. Buonocore, A. L. Suguitan, Jr., A. Silaghi, D. Kobasa, G. Kobinger, H. Feldmann, K. Subbarao, and J. K. Rose.** 2010. Potent vesicular stomatitis virus-based avian influenza vaccines provide long-term sterilizing immunity against heterologous challenge. *J Virol* **84:**4611-4618.
200. **Severson, W. E., X. Xu, and C. B. Jonsson.** 2001. cis-Acting signals in encapsidation of Hantaan virus S-segment viral genomic RNA by its N protein. *J Virol* **75:**2646-2652.
201. **Shi, X., and R. M. Elliott.** 2002. Golgi localization of Hantaan virus glycoproteins requires coexpression of G1 and G2. *Virology* **300:**31-38.
202. **SMADEL, J. E.** 1953. Epidemic hemorrhagic fever. *Am J Public Health Nations Health* **43:**1327-1330.
203. **Sohn, Y. M., H. O. Rho, M. S. Park, J. S. Kim, and P. L. Summers.** 2001. Primary humoral immune responses to formalin inactivated hemorrhagic fever

References

- with renal syndrome vaccine (Hantavax): consideration of active immunization in South Korea. *Yonsei Med J* **42**:278-284.
204. **Spiropoulou, C. F., C. G. Albariño, T. G. Ksiazek, and P. E. Rollin.** 2007. Andes and Prospect Hill hantaviruses differ in early induction of interferon although both can downregulate interferon signaling. *J Virol* **81**:2769-2776.
205. **Spiropoulou, C. F., S. Morzunov, H. Feldmann, A. Sanchez, C. J. Peters, and S. T. Nichol.** 1994. Genome structure and variability of a virus causing hantavirus pulmonary syndrome. *Virology* **200**:715-723.
206. **Stoltz, M., C. Ahlm, A. Lundkvist, and J. Klingström.** 2007. Lambda interferon (IFN-lambda) in serum is decreased in hantavirus-infected patients, and in vitro-established infection is insensitive to treatment with all IFNs and inhibits IFN-gamma-induced nitric oxide production. *J Virol* **81**:8685-8691.
207. **Sugiyama, K., S. Morikawa, Y. Matsuura, E. A. Tkachenko, C. Morita, T. Komatsu, Y. Akao, and T. Kitamura.** 1987. Four serotypes of haemorrhagic fever with renal syndrome viruses identified by polyclonal and monoclonal antibodies. *J Gen Virol* **68 (Pt 4)**:979-987.
208. **Sullivan, N. J., T. W. Geisbert, J. B. Geisbert, D. J. Shedlock, L. Xu, L. Lamoreaux, J. H. Custers, P. M. Popernack, Z. Y. Yang, M. G. Pau, M. Roederer, R. A. Koup, J. Goudsmit, P. B. Jahrling, and G. J. Nabel.** 2006. Immune protection of nonhuman primates against Ebola virus with single low-dose adenovirus vectors encoding modified GPs. *PLoS Med* **3**:e177.
209. **Sutter, G., M. Ohlmann, and V. Erfle.** 1995. Non-replicating vaccinia vector efficiently expresses bacteriophage T7 RNA polymerase. *FEBS Lett* **371**:9-12.
210. **Svedmyr, A., H. W. Lee, A. Berglund, B. Hoorn, K. Nyström, and D. C. Gajdusek.** 1979. Epidemic nephropathy in Scandinavia is related to Korean haemorrhagic fever. *Lancet* **1**:100.
211. **Temonen, M., O. Vapalahti, H. Holthöfer, M. Brummer-Korvenkontio, A. Vaheri, and H. Lankinen.** 1993. Susceptibility of human cells to Puumala virus infection. *J Gen Virol* **74 (Pt 3)**:515-518.
212. **Tischler, N. D., A. Gonzalez, T. Perez-Acle, M. Roseblatt, and P. D. Valenzuela.** 2005. Hantavirus Gc glycoprotein: evidence for a class II fusion protein. *J Gen Virol* **86**:2937-2947.
213. **Toro, J., J. D. Vega, A. S. Khan, J. N. Mills, P. Padula, W. Terry, Z. Yadon, R. Valderrama, B. A. Ellis, C. Pavletic, R. Cerda, S. Zaki, W. J. Shieh, R. Meyer, M. Tapia, C. Mansilla, M. Baro, J. A. Vergara, M. Concha, G.**

- Calderon, D. Enria, C. J. Peters, and T. G. Ksiazek.** 1998. An outbreak of hantavirus pulmonary syndrome, Chile, 1997. *Emerg Infect Dis* **4**:687-694.
214. **Tsuda, Y., D. Safronetz, K. Brown, R. LaCasse, A. Marzi, H. Ebihara, and H. Feldmann.** 2011. Protective efficacy of a bivalent recombinant vesicular stomatitis virus vaccine in the Syrian hamster model of lethal Ebola virus infection. *J Infect Dis* **204 Suppl 3**:S1090-1097.
215. **Volchkov, V. E., V. A. Volchkova, E. Muhlberger, L. V. Kolesnikova, M. Weik, O. Dolnik, and H. D. Klenk.** 2001. Recovery of infectious Ebola virus from complementary DNA: RNA editing of the GP gene and viral cytotoxicity. *Science* **291**:1965-1969.
216. **Wahl-Jensen, V., J. Chapman, L. Asher, R. Fisher, M. Zimmerman, T. Larsen, and J. W. Hooper.** 2007. Temporal analysis of Andes virus and Sin Nombre virus infections of Syrian hamsters. *J Virol* **81**:7449-7462.
217. **Walpita, P., and R. Flick.** 2005. Reverse genetics of negative-stranded RNA viruses: a global perspective. *FEMS Microbiol Lett* **244**:9-18.
218. **Weber, F., E. F. Dunn, A. Bridgen, and R. M. Elliott.** 2001. The Bunyamwera virus nonstructural protein NSs inhibits viral RNA synthesis in a minireplicon system. *Virology* **281**:67-74.
219. **Whelan, S. P., L. A. Ball, J. N. Barr, and G. T. Wertz.** 1995. Efficient recovery of infectious vesicular stomatitis virus entirely from cDNA clones. *Proc Natl Acad Sci U S A* **92**:8388-8392.
220. **White, J. D., F. G. Shirey, G. R. French, J. W. Huggins, O. M. Brand, and H. W. Lee.** 1982. Hantaan virus, aetiological agent of Korean haemorrhagic fever, has Bunyaviridae-like morphology. *Lancet* **1**:768-771.
221. **Wyatt, L. S., B. Moss, and S. Rozenblatt.** 1995. Replication-deficient vaccinia virus encoding bacteriophage T7 RNA polymerase for transient gene expression in mammalian cells. *Virology* **210**:202-205.
222. **Yang, Z. Q., T. M. Zhang, M. V. Zhang, Z. M. Zheng, Z. J. Hu, C. F. Qu, J. M. Xiang, J. W. Huggins, T. M. Cosgriff, and J. I. Smith.** 1991. Interruption study of viremia of patients with hemorrhagic fever with renal syndrome in the febrile phase. *Chin Med J (Engl)* **104**:149-153.
223. **Yoneda, M., V. Guillaume, F. Ikeda, Y. Sakuma, H. Sato, T. F. Wild, and C. Kai.** 2006. Establishment of a Nipah virus rescue system. *Proc Natl Acad Sci U S A* **103**:16508-16513.

References

224. **Zaki, S. R., P. W. Greer, L. M. Coffield, C. S. Goldsmith, K. B. Nolte, K. Foucar, R. M. Feddersen, R. E. Zumwalt, G. L. Miller, and A. S. Khan.** 1995. Hantavirus pulmonary syndrome. Pathogenesis of an emerging infectious disease. *Am J Pathol* **146**:552-579.
225. **Zhang, Y., X. H. Li, H. Jiang, C. X. Huang, P. Z. Wang, D. L. Mou, L. Sun, Z. Xu, X. Wei, and X. F. Bai.** 2008. Expression of L protein of Hantaan virus 84FLi strain and its application for recovery of minigenomes. *APMIS* **116**:1089-1096.
226. **Zivcec, M., D. Safronetz, E. Haddock, H. Feldmann, and H. Ebihara.** 2011. Validation of assays to monitor immune responses in the Syrian golden hamster (*Mesocricetus auratus*). *J Immunol Methods* **368**:24-35.
227. **Zobel, A., G. Neumann, and G. Hobom.** 1993. RNA polymerase I catalysed transcription of insert viral cDNA. *Nucleic Acids Res* **21**:3607-3614.

7.0 Appendices

Appendix 1 – Buffer Recipes

LB Broth(+AMP/KAN)

10g tryptone
5g yeast extract
10g NaCl
Adjust volume with ddH₂O to 1000ml
Filter sterilize

Antibiotic selection:

Add 100µg/ml Ampicillin (AMP)
Add 35µg/ml Kanamycin (KAN)

TSS Buffer

85ml LB Broth
10g Polyethylene glycol
5ml DMSO
1g MgCl₂
Add ddH₂O to 100ml
Filter sterilize

SOC Media

20g Bacto tryptone
5g Bacto yeast extract
2ml 5M NaCl
2.5ml M KCl
10ml 1M MgCl₂
10ml 1M MgSO₄
20ml 1M Glucose
900ml water
Adjust volume with ddH₂O to 1000ml

4X SDS Gel Loading Buffer

20ml 1M Tris-HCL (pH 7.5)
40ml 10% SDS
35ml Glycerol
0.5g Bromophenol Blue
Adjust volume to 100 ml with ddH₂O
Add 2-mercaptoethanol (BME) to a final concentration of 10% before use

SDS PAGE Gel Recipes (10mL)

10% (w/w) Resolving Gel

4.9ml ddH₂O
2.5ml 40% Acrylamide
2.5ml 1.5M Tris-HCL pH 8.8
100µl 10% SDS
50µl 10% Ammonium Persulfate
10µl TEMED

12% (w/w) Resolving Gel

4.3ml ddH₂O
3.0ml 40% Acrylamide
2.5ml 1.5M Tris-HCL pH 8.8
100µl 10% SDS
50µl 10% Ammonium Persulfate
10µl TEMED

4% (w/w) Stacking Gel

6.4ml ddH₂O
1.0ml 40% Acrylamide
2.5ml 0.5M Tris-HCL pH 6.8
100µl 10% SDS
50µl 10% Ammonium Persulfate
10µl TEMED

Wet Transfer Buffer

2.9g Tris-Base
1.47g Glycine
2ml 10% SDS
100ml Methanol
Adjust volume to 500ml with ddH₂O

Stripping buffer

125ml 1M Tris-HCL (pH 6.7)
40ml 10% SDS solution
Adjust volume to 200ml
Before using add 0.7% BME

Crude Miniprep Buffers

Qiagen DNA Prep Buffer P1 (Resuspension Buffer)

Appendix 1

50 mM Tris·Cl, pH 8.0
10 mM EDTA
100 µg/ml RNase A
Store at 4°C after addition of RNase A

Qiagen DNA Prep Buffer P2 (Lysis Buffer)

200 mM NaOH
1% SDS (w/v)
Store at 15–25°C

Qiagen DNA Prep Buffer P3 (Neutralization Buffer)

3.0 M potassium acetate pH 5.5
Store at 15-25°C or 4°C

6x DNA Gel Loading buffer

30% Glycerol (dissolved in water)
0.25% Bromophenol Blue

Crystal Violet Stain

200ml 100% EtOH
100ml 40% Formaldehyde
2.5g Crystal violet
Add ddH₂O to 1000ml

Appendix 2 – List of Primary and Secondary Antibodies

Primary Antibodies

Antibody	Company	Clone	Source	Method	Dilution
Anti- ANDV N	Austral Biologicals	BZ1 1A8/F6	Mouse	IFA WB	1:500 1:10,000
Anti-ANDV G _N	Austral Biologicals	CX1 6B9/F5	Mouse	IFA WB	1:200 1:8,000
Anti-ANDV G _C	Austral Biologicals	AX1 2H4/F6	Mouse	IFA WB	1:200 1:6,000
Anti-VSV G	Sigma	P5D4	Mouse	WB	1:2,500
Anti-FLAG	Sigma	M2	Mouse	IFA	1:200
Anti-ZEBOV GP	In-house		Mouse	WB	1:10,000
Anti-ANDV N	In-house		Hamster	FRNT	1:1000

Secondary Antibodies

Antibody	Company	Clone	Source	Method	Dilution
Anti-Mouse IgG Alexa Fluor 488	Invitrogen	---	Goat	IFA	1:1000
Anti-Mouse IgG HRP	Sigma	---	Goat	WB	1:10,000
Anti-Hamster IgG HRP	KPL	---	Goat	ELISA FRNT	1:1000 1:1000

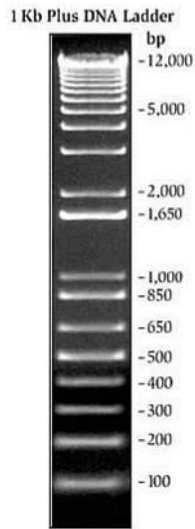
Minigenome			
MsegNCR1 F	Clone M Segment NCRs into	CCGACGGTGGATCCGGTACCGTCTCCGGTCTAGTGTAGTACTCCGCAAGAAAGCAAAAAATTAAG	RT-PCR
MsegNCR1 R	p.ATXMC53	ACCGTCTGACTCCCTCCCTAGGGTGTACAAAGCATCTCTACTAAC	RT-PCR
MsegNCR2 F		AACAGAACCTCACATCAACAACAACAAGCTTGAATGGATCGAC	RT-PCR
MsegNCR2 R		ATAAGAAATCGGGCGCGGATCCGCTCAACCCCTAGTGTAGTGTCCGCGAGCAAAAAGCCTCGGTAAG	RT-PCR
Isolate NCR F	Remove ORF portions	GGAAITTCGATAGATGAAGACTAGACCTACCTCCATTAATGATCAT	PCR
Isolate NCR R		GGAAITTCGTAAGTGAAGACTATTTAACTCACTCTTTAAITTTTGGCTTC	PCR
CAT F	Insert Reporter Genes	ACATGAAGACTATAAAATGGAGAAAATAAACTACTGGATATACCACC	PCR
CAT R		ACATGAAGACTAATGCTTACCGCCCGCCCTGCCACTCATCGAGTA	PCR
GFP F		ACATGAAGACTATAAAATGGAGAAAAGGGGGAGGAGCTTTCACCGGGTGTGC	PCR
GFP R		ACATGAAGACTAATGCTTACCGCTCCAGCTCCGCGAGAGTATCCCGGGG	PCR
LUC F		ACATCGTCTCTAAATGGAAAGCAACCAAAAACATAAGAAAGGC	PCR
LUC R		ACATCGTCTCTATGCTTACCGGGGATCTTCCGGCCCTTTTGGC	PCR
Insert I7 F	Insert into RNA Polymerase	TACGGGAATTCGAGTCACTGCTGCTCTCCGGTCCGCAATGGCATCTCCACTCCCTCGGG	PCR
Insert I7 R	Plasmids	TACGGGAATTCGAGGATCGTCTCTCTATAGTGTAGTGTCTTACTAGTCCGCTC	PCR
Insert Pol II F		GCATCGTCTCCGGTCTAGTGTATGCTCCGCGCAAGCAAAAAGCCT	PCR
Insert Pol II R		GCATCGTCTCCGCTAGTGTAGTACTCCGCAAGAAAGCAAAA	PCR
Insert Pol I F		AGATGTTACCCGCTCAGGGTGTAGTGTAGTGTCCGCAAGAAAGCAAAA	PCR
Insert Pol I R		AGATGCTATCCGCTCTCATTTTGTAGTGTATGCTCCGCGCAAGCAAAAAGCCT	PCR
pCAG-CAT F	Positive Controls	ACATGTTACCATGGAGAAAATAAACTACTGGATATACCACC	PCR
pCAG-CAT R		TCGAGCTAGCTTATTAAGCCCGCCCTGCCACTCATCGAGTA	PCR
pCAG-LUC F		ACATGTTACCATGGAGAAAAGGGGGAGGAGCTTTCACCGGGTGTGC	PCR
pCAG-LUC R		ACATGTTACCATGGAGAAAAGGGGGAGGAGCTTTCACCGGGTGTGC	PCR
pCAG-GFP F		ACATGTTACCATGGAGAAAAGGGGGAGGAGCTTTCACCGGGTGTGC	PCR
pCAG-GFP R		ACATGTTACCATGGAGAAAAGGGGGAGGAGCTTTCACCGGGTGTGC	PCR
Hamster Cytokine			
IFN- γ F	Hamster Cytokine Primer and Probe Sets	GGCCATCCAGAGGAGCATAG	qRT-PCR
IFN- γ R		TTTTCCTCATGCTGTGTGAA	qRT-PCR
IFN- γ Probe		6FAM-CACCATCAAGGCAGACCTGTTGCTAACTT-BBQ	qRT-PCR
STAT-1 F		GCCAAAGTGTCTCTTTC	qRT-PCR
STAT-1 R		GCTATATGGTCAATCCAGCTGAGA	qRT-PCR
STAT-1 Probe		6FAM-ACCATCCGTTTCCATGACCTCC-BBQ	qRT-PCR
IRF-1 F		GGCATAACAATGCTCTCAGG	qRT-PCR
IRF-1 R		GCTATGCTTTGCCATGTCAA	qRT-PCR
IRF-1 Probe		6FAM-CACAATGAGCCAGACCTTGTCA-BBQ	qRT-PCR
Mx-2 F		CCAGTAATGGACATGGC	qRT-PCR
Mx-2 R		CATCAACGACCTTGTCTCAGTA	qRT-PCR
Mx-2 Probe		6FAM-TGTCCACAGATCAGGTTGTCA-BBQ	qRT-PCR
RPL-18 F	Internal Reference Gene	GTTTATGATGCGCACTAACCG	qRT-PCR
RPL-18 R	Primers and Probe	TGTTCTCTCCGGCCAGGAA	qRT-PCR
RPL18 Probe		YAK-TCTGTCCCTCTCCGGGATGTC-BBQ	qRT-PCR

Appendix 3

Segment Sequencing			
AndS11F	Sequencing S Segment Forward Primers	TAGTAGAGACTCCTTGAGA	Sequencing
AndS21F		AGGATGATTCCTCTTGAA	Sequencing
AndS1041F		CCTCAGGACATGCGTAATA	Sequencing
AndS1511F		ATTGATTTGGCACTAAGGGA	Sequencing
AndS1871R	Sequencing S Segment Reverse Primers	TAGTAGATGCTCCTTGAAA	Sequencing
AndS1370R		AGCCCGAAAGTCTTCTTC	Sequencing
AndS20R		TAGACATGAAGGCTCTGAG	Sequencing
AndS310R		GATGATCATCAGGCTCAAGC	Sequencing
AndM1F	Sequencing M Segment Forward Primers	TAGTAGAGACTCCTCGAAGA	Sequencing
AndM531F		TTGTATGGCTAGTGTGTTA	Sequencing
AndM1031F		CTTATCTACACTAGTCAGA	Sequencing
AndM1521F		TCTATCAACATTCGCTTTG	Sequencing
AndM2041F		GCTCATGGTGTGGTGAGAT	Sequencing
AndM2561F		TGGGCACAGTTCAAAACTT	Sequencing
AndM3081F		GGCATGTGACTAGCTATGT	Sequencing
AndM3501F		ACATTTATGCACTTCTTCAT	Sequencing
AndM2671R	Sequencing M Segment Reverse Primers	TAGTAGATGCTCCTCGAAGA	Sequencing
AndM3400R		TCACAACAAGCACTACAACA	Sequencing
AndM2880R		CCATTCAAGCTTGTGTTG	Sequencing
AndM2320R		CAAAGAAGCACTTAGATGTC	Sequencing
AndM1280R		ACAAGACATGTGGAGAACT	Sequencing
AndM760R		TCTTGTGCAAACTCTTCA	Sequencing
AndM280R		TCTTCTGGCCATAGATGTT	Sequencing
AndL1F	Sequencing L Segment Forward Primers	TAGTAGAGACTCCTCGGATA	Sequencing
AndL511F		TTGCAATTAAACAACAGATGA	Sequencing
AndL1011F		CCAGAAACACCACTACAGAT	Sequencing
AndL1511F		GCTGCGCGTCTTAATATTT	Sequencing
AndL2001F		TCACTGGATGATACCTTTA	Sequencing
AndL2501F		TTTCAGTCAACACCCAAATA	Sequencing
AndL3511F		AATATATGATGGCTTATCAG	Sequencing
AndL4011F		CACCTAAGAAAGACACAGTA	Sequencing
AndL4511F		GACCGATTGGGTGAGTTTAG	Sequencing
AndL5011F		TGTTAGAAAGAGGACCAGG	Sequencing
AndL5501F		AGACATTTGATGGATGGGTA	Sequencing
AndL5991F		GCTTGTACGAACACAGCCAA	Sequencing
AndL6562R	Sequencing L Segment Reverse Primers	ATAGCACTGGATGATTTGA	Sequencing
AndL6270R		TAGTAGATGCTCCTCGGAAA	Sequencing
AndL5760R		CAAGGGTGTGAACTGAAA	Sequencing
AndL5260R		TGGCAGCAGTAAAGCCTTTC	Sequencing
AndL4760R		CTTGCACAATCTAAACCAA	Sequencing
AndL4260R		CACAATAACAACCGTGACC	Sequencing
AndL3760R		TACGGAAACGAAATCTAAT	Sequencing
AndL3260R		CCATACAACTCTCAACTTT	Sequencing
AndL2760R		TAATGAGACAGGAGCCAA	Sequencing
AndL2260R		TTAITTCTAATCGCACCTTA	Sequencing
AndL1760R		AITTTAGCCTCTCTGGTAA	Sequencing
AndL1260R		AAAAGCTATGTTCAAAGCCA	Sequencing
AndL760R		CCACATTTATGCTATCTATG	Sequencing
AndL260R		TTGTCAATCCGGTTCACA	Sequencing
AndL260R		CTCCATGCCCTTGTATATAT	Sequencing

Appendix 4 – DNA and Protein Ladders

1 Kb Plus DNA Ladder (Invitrogen)



SeeBlue Plus2 Protein Molecular Weight Ladder

Protein	Approximate Molecular Weights (kDa)				
	Tris-Glycine	Tricine	NuPAGE [®] MES	NuPAGE [®] MOFS	NuPAGE [®] Tris-Acetate
Myosin	250	210	188	191	210
Phosphorylase	148	105	98	97	111
BSA	98	78	62	64	71
Glutamic Dehydrogenase	64	55	49	51	55
Alcohol Dehydrogenase	50	45	38	39	41
Carbonic Anhydrase	36	34	28	28	n/a
Myoglobin Red	22	17	17	19	n/a
Lysozyme	16	16	14	14	n/a
Aprotinin	6	7	6	n/a	n/a
Insulin, B Chain	4	4	3	n/a	n/a

NuPAGE[®] Novex Bis-Tris 4-12% Gel

©1999-2002 Invitrogen Corporation. All rights reserved.

IM-1008F 072602

Appendix 5 – Minigenome Rescue ConditionsPlasmids used for Protein Expression / Minigenomes:

Expression Plasmids	Promoter	WB	IFA	MG
pCAGGS-N	CAG	+	+	+
gWIZ-N	CMV	+	+	+
pT7-N	T7	+	+	+
pKS336-N	HEF-1 α	+	+	+
pCAGGS-L	CAG	-	-	+
gWIZ-L	CMV	-	-	+
pT7-L	T7	-	-	+
pKS336-L	HEF-1 α	-	+	+
pCAGGS-GPC	CAG	+	+	+
pT7-M-CAT	T7	-----	-----	+
pRF240-M-CAT	Pol I	-----	-----	+

LEGEND

+ = successful expression/use

- = unsuccessful expression/use

----- = not applicable

WB = Western Blot; IFA = Immunofluorescent assay; MG = Minigenome Rescue; CAG = Chicken β -actin; CMV = Cytomegalovirus immediate early; T7 = T7 bacteriophage; HEF-1 α = human elongation factor-1 α ; Pol I = Human RNA polymerase I

Cell Lines Tested for Minigenome Rescue:

1. COS-7 (most reliable expression)
2. BHK-21 / BSR-T7
3. VeroE6 / Vero
4. 293T / 293
5. HuH7
6. A549